

GPO PRICE \$ _____
CFSTI PRICE(S) \$ _____

Hard copy (HC) 3.00
Microfiche (MF) 1.65

ff 653 July 65

SUMMARY REPORT
MHD BOUNDARY LAYERS INVOLVING
NON-EQUILIBRIUM IONIZATION

Principal Investigator: A. Sherman

Consultant: E. Reshotko

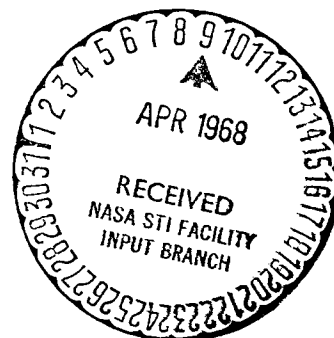
prepared for

NATIONAL AERONAUTICS AND SPACE ADMINISTRATION

February 24, 1968

CONTRACT NASw-1586

FACILITY FORM 602	<u>168-23191</u>	_____
	(ACCESSION NUMBER)	(THRU)
	<u>124</u>	_____
	(PAGES)	(CODE)
	<u>CF-94537</u>	<u>25</u>
	(NASA CR OR TMX OR AD NUMBER)	(CATEGORY)



GENERAL ELECTRIC COMPANY
Missile and Space Division
Space Sciences Laboratory
P.O. Box 8555, Philadelphia, Pa. 19101

SUMMARY REPORT
MHD BOUNDARY LAYERS INVOLVING
NON-EQUILIBRIUM IONIZATION

Principal Investigator: A. Sherman

Consultant: E. Reshotko

prepared for

NATIONAL AERONAUTICS AND SPACE ADMINISTRATION

February 24, 1968

CONTRACT NASw-1586

GENERAL ELECTRIC COMPANY
Missile and Space Division
Space Sciences Laboratory
P.O. Box 8555, Philadelphia, Pa. 19101

ABSTRACT

The present report describes theoretical research carried out under NASA contract NASw-1586 during the twelve months ending January 24, 1968. Studies have been made of the boundary layer in a plasma in which the electron and heavy particle temperatures may be different. The problem is formulated from the viewpoint of multi-fluid magnetohydrodynamics (MHD). It differs from earlier treatments in that the complete electron energy equation is retained so that one must consider the plasma sheath in order to establish a boundary condition at the wall on the electron temperature. In our initial studies a two-dimensional, laminar, steady flow is assumed. We also assume infinitely fast ionization and recombination rates so that the electron density can be calculated from the Saha equation at the electron temperature. Actual calculations have been carried out along a channel wall which is partly insulator and partly thermionically emitting electrode. For the initial studies, restricted to a non-emitting insulator, we used the method of local similarity to solve our equations. All later studies have used a finite difference scheme and the exact equations. Results obtained demonstrate that the electron temperature can differ significantly from the heavy particle temperature and is very dependent on the magnetic field, thermionic emission and current level.

TABLE OF CONTENTS

<u>Section</u>	<u>Page</u>
I. Introduction	1
II. Boundary Layer Equations for Two Temperature Plasma	3
1. Characteristic quantities	3
2. Assumptions	4
3. Basic equations	4
4. Boundary conditions	10
III. Solution Procedures for Non-Similar Boundary Layers	13
1. Equations in transformed plane	13
2. Finite difference form of equations	16
3. Determination of external conditions	23
4. Initial profiles - local similarity	25
IV. Examples and Discussion	26
1. General description of example	26
2. Locally similar solution on insulator wall with $B = 0$	28
3. Boundary layer over finite electrode segment with $B \neq 0$	29
V. Suggestions for further work	40
References	41
Appendices	

I. INTRODUCTION

Several attempts have been made to analyze the magnetohydrodynamic boundary layer occurring in the internal flow of a compressible plasma, in order to determine skin friction, heat transfer, and potential differences between wall and external stream for both electrode and insulator surfaces. The first such attempt was by Kerrebrock^{1,2}. He considered the equilibrium electrode boundary layer in a magnetohydrodynamic accelerator having constant external static temperature and cooled electrodes. He argued that in the immediate vicinity of the electrode the conductivity would be low because of the cooling. This would lead to considerable Joule heating of the gas near the wall resulting in large temperature gradients and high heat transfer rates. Kerrebrock's calculations bore out these expectations. It was felt that these results were not realistic because the electrons would not be in equilibrium with the heavy species. Accordingly, Oates³ made a rough estimate of boundary layer behavior considering the electrons to be at an elevated temperature. He found that the increased conductivity near the wall over that found on the basis of equilibrium theory greatly reduced the Joule heating. He found that transport of enthalpy to the walls by electrons was enhanced because of the increased electron temperature. He further pointed out that when the electron transport of enthalpy is significant, there is a considerably larger heat flux to the anode than to the cathode. In Oates' analysis, the electron temperature was determined on the basis of a simple energy balance rather than the complete electron energy equation, and as a result no "sheath" analysis was carried out.

In the above described analyses the Hall effect, ion slip, and electron pressure gradient effects were neglected in the Ohm's Law. Finally, the solutions were obtained by the approximate method of local similarity, and did not allow for such things as finite segmentation of the electrodes.

For the insulator boundary layer an analysis has been carried out by Hale² who also used the assumption of local similarity, but did include the Hall effect. Hale, however, considered the non-equilibrium effect by assuming

a conductivity relationship $\sigma = \sigma(j)$ rather than by accounting for the behavior of electron temperature. This again obviated the need for an examination of the "sheath". Nonetheless, this study did demonstrate the possibility of enhanced heat flux due to nonequilibrium ionization, as well as temperature and velocity overshoots.

The present study has as its objective a more refined treatment of the nonequilibrium boundary layer development through the use of multifluid magnetohydrodynamics. A set of conservation equations is written for each constituent of the working fluid. These equations are in turn reduced and combined to achieve a usable set of equations for a two temperature plasma - one where the electrons may be at a temperature that is significantly different from that of the heavy particles. The formulation is somewhat like those of the two temperature treatments of Camac and Kemp⁴ and Dix⁵ except that their problems were generally nonflowing and noncurrent carrying, whereas Joule heating and Lorentz forces are essential features of generators and accelerators.

The first portion of this report formulates the equations to be used in treating this problem and their boundary conditions. In the second part we formulate the numerical techniques necessary for their solution. Here both the finite difference and local similarity approaches are developed. Finally, some solutions for problems of interest are presented and discussed. The influence of the sheath, magnetic field, thermionic emission, etc. are all illustrated by the solutions obtained.

II. BOUNDARY LAYER EQUATIONS FOR TWO TEMPERATURE PLASMA

1. Characteristic Quantities

To better define the physical character of the ionized gas being studied, it is useful to establish typical magnitudes of the quantities of interest. Most pertinent are the characteristic lengths since we wish to formulate a boundary layer study.

Gas stagnation temperature	2000°K
Gas static temperature	400-2000°K
Wall temperature	1500°K
Electron temperature	1700-10,000°K
Gas particle density	10^{19} cm^{-3}
Electron density	10^{15} cm^{-3}
Electron-electron cross section	$5 \times 10^{-13} \text{ cm}^2$
Electron-neutral cross section	10^{-16} cm^2
Magnetic field strength	20,000 gauss
Electron debye length	$2 \times 10^{-5} \text{ cm}$
Electron-electron mean free path	$.2 \times 10^{-2} \text{ cm}$
Electron-neutral mean free path	10^{-3} cm
Neutral-neutral mean free path	10^{-4} cm
Ion-neutral mean free path	$10^{-3} - 10^{-2} \text{ cm}$
Ion-ion mean free path	$.2 \times 10^{-2} \text{ cm}$
Electron-ion mean free path	$.5 \times 10^{-2} \text{ cm}$
Boundary layer thickness	0.1-1.0 cm
Electron gyro-radius	$1.5 \times 10^{-4} \text{ cm}$
Ion gyro-radius	10^{-2} cm

We note that the electron Debye length is much smaller than all mean free paths and also smaller than the electron gyro-radius. We will therefore assume a collision free sheath free of magnetic effects. Again, the boundary layer thickness is larger than all mean free paths and gyro-radii, so we are justified in pursuing a continuum-type approach the fluid flow problem. The above estimates, of course, must be continually reviewed as the solution is carried out.

2. Assumptions

The formulation of our problem will be for a two temperature plasma under the following simplifying assumptions:

1. Steady flow $\frac{\partial}{\partial t} = 0$
2. Laminar flow
3. No induced magnetic fields $R_m \cong 0$
4. Plasma consists only of electrons, atoms (carrier and seed), and singly ionized seed ions
5. Plasma composition determined by Saha equation evaluated at the electron temperature
6. No continuum radiation losses
7. Collision free plasma sheath
8. Only thermionic emission
9. Neglect pressure differences normal to wall.

The general geometry of the two types of channels which will be of interest are shown in Figure 1. The boundary layer on any of the four walls can be studied.

3. Basic Equations

For the two dimensional boundary layer, and the geometries of Figure 1, the basic equations can be written as follows.

Mass Conservation:

$$\frac{\partial}{\partial x}(\rho u) + \frac{\partial}{\partial y}(\rho v) = 0 \quad (1)$$

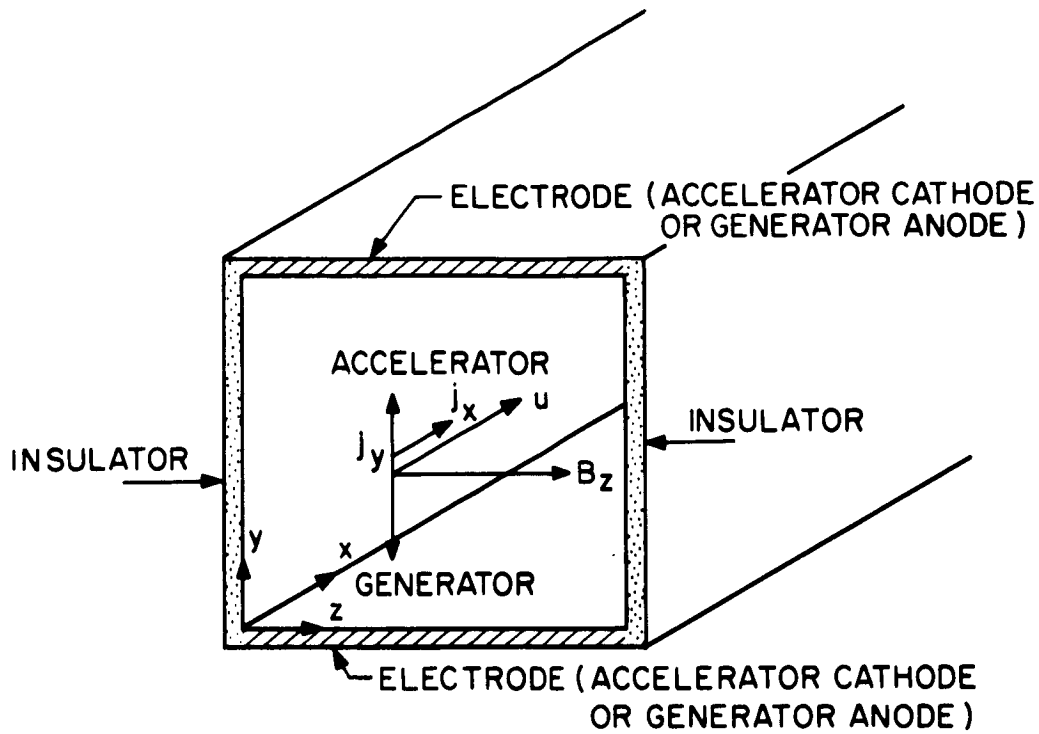
Momentum Equation:

Longitudinal --

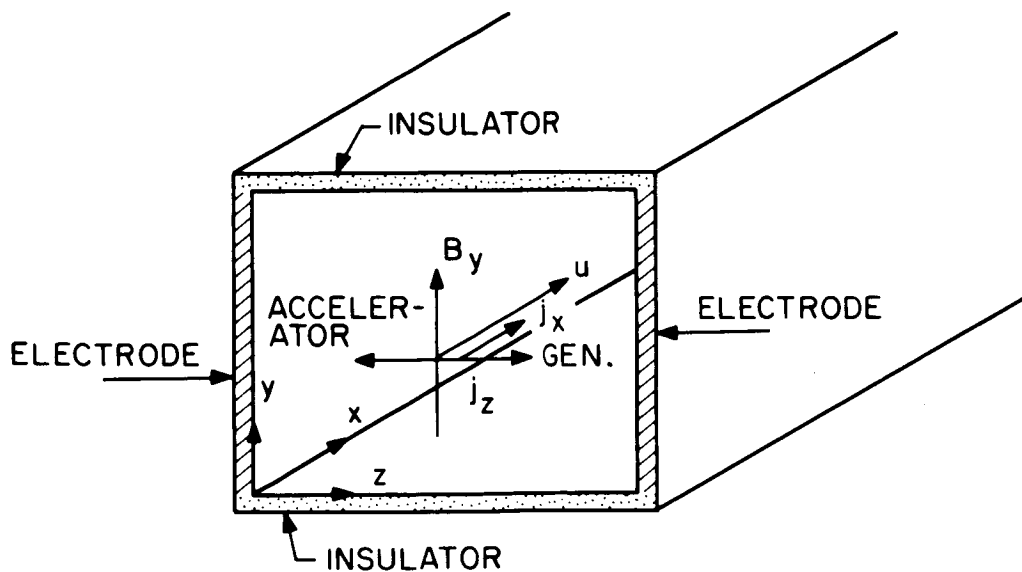
$$\rho u \frac{\partial u}{\partial x} + \rho v \frac{\partial u}{\partial y} = -\frac{\partial p}{\partial x} + \frac{\partial}{\partial y} \left(\mu \frac{\partial u}{\partial y} \right) + \begin{cases} j_y B_z \text{ (electrode)} \\ -j_z B_y \text{ (insulator)} \end{cases} \quad (2a)$$

Spanwise (Insulator wall only) --

$$\rho u \frac{\partial w}{\partial x} + \rho v \frac{\partial w}{\partial y} = \frac{\partial}{\partial y} \left(\mu \frac{\partial w}{\partial y} \right) + j_x B_y \quad (2b)$$



(A) GEOMETRY FOR ELECTRODE BOUNDARY LAYER



(B) GEOMETRY FOR INSULATOR BOUNDARY LAYER

N 207-024

Figure 1. Geometries of electrode and insulator boundary layers in channel flow devices

Conservation of Energy (Static enthalpy form):

$$\begin{aligned} \rho u \frac{\partial h^*}{\partial x} + \rho v \frac{\partial h^*}{\partial y} &= u \frac{\partial p}{\partial x} - \frac{\partial}{\partial y} (q_y) \\ &+ j_x E_x + \left\{ \begin{aligned} &\mu \left(\frac{\partial u}{\partial y} \right)^2 + j_y (E_y - u B_z) \text{ (electrode)} \\ &\mu \left[\left(\frac{\partial u}{\partial y} \right)^2 + \left(\frac{\partial w}{\partial y} \right)^2 \right] + j_z (E_z + u B_y) \text{ (insulator)} \end{aligned} \right\} \end{aligned} \quad (3)$$

Conservation of Electron Energy:

$$\begin{aligned} \frac{3}{2} k n_e \frac{\partial T_e}{\partial x} + \frac{3}{2} k u T_e \frac{\partial n_e}{\partial x} + \frac{3}{2} k v n_e \frac{\partial T_e}{\partial y} + \frac{3}{2} k v T_e \frac{\partial n_e}{\partial y} \\ + n_e \left[\frac{5}{2} k T_e + I \right] \left(\frac{\partial u}{\partial x} + \frac{\partial v}{\partial y} \right) - \frac{\partial}{\partial y} \left[K_e \frac{\partial T_e}{\partial y} + \frac{5}{2} \frac{k}{e} T_e j_{e_y} \right] \\ = E_x j_{e_x} + \left\{ \begin{aligned} &j_{e_y} (E_y - u B_z) \text{ (electrode)} \\ &j_{e_z} (E_z + u B_y) \text{ (insulator)} \end{aligned} \right\} \\ + 3 \rho_e k (T - T_e) \Sigma \frac{\nu_{es}}{m_s} - I u \frac{\partial n_e}{\partial x} - I v \frac{\partial n_e}{\partial y} \end{aligned} \quad (4)$$

These latter two relations can be rewritten, making use of the Saha relation, as shown in Appendix A and B. The results are given below for an electrode wall alone. The modification needed to study an insulator boundary layer is quite straight forward.

Overall Energy Conservation:

$$\begin{aligned} \rho u \frac{\partial h}{\partial x} + \rho v \frac{\partial h}{\partial y} &= - \rho_\infty u_\infty \frac{du_\infty}{dx} u + \mu \left(\frac{\partial u}{\partial y} \right)^2 + \frac{\partial}{\partial y} \left(\Sigma K_i \frac{\partial T}{\partial y} + \frac{5kT_e}{2e} j_{e_y} \right) \\ &+ j_x E_x + j_y E_y - I \left[u S_1 \frac{\partial T_e}{\partial x} - u S_2 \frac{\partial h}{\partial x} + u S_3 j_y B_z - u S_3 \rho_\infty u_\infty \frac{du_\infty}{dx} \right. \\ &\left. + v S_1 \frac{\partial T_e}{\partial y} - v S_2 \frac{\partial h}{\partial y} - n_e \left(\frac{u}{p} j_y B_z - \frac{u}{p} \rho_\infty u_\infty \frac{du_\infty}{dx} - \frac{u}{h} \frac{\partial h}{\partial x} - \frac{v}{h} \frac{\partial h}{\partial y} \right) \right] \end{aligned} \quad (5)$$

Electron Energy Conservation:

$$\begin{aligned}
& \frac{3}{2} k n_e \frac{\partial T_e}{\partial x} + \frac{3}{2} k v n_e \frac{\partial T_e}{\partial y} + \left(\frac{3}{2} k T_e + I \right) u \left\{ S_1 \frac{\partial T_e}{\partial x} - S_2 \frac{\partial h}{\partial x} \right. \\
& \quad \left. + S_3 \left(j_{y_e} B_z - \rho_e u_e \frac{du_e}{dx} \right) \right\} + \left(\frac{3}{2} k T_e + I \right) v \left\{ S_1 \frac{\partial T_e}{\partial y} - S_2 \frac{\partial h}{\partial y} \right\} \\
& \quad + n_e \left[\frac{5}{2} k T_e + I \right] \left\{ \rho u \frac{\partial \rho^{-1}}{\partial x} + \rho v \frac{\partial \rho^{-1}}{\partial y} \right\} - \frac{\partial}{\partial y} \left(K_e \frac{\partial T_e}{\partial y} + \frac{5}{2} \frac{k}{e} T_e j_{e_y} \right) \\
& = E_x j_{e_x} + (E_y - u B_z) j_{e_y} + 3 \rho_e k (T - T_e) \sum_s \frac{\nu_{es}}{m_s}
\end{aligned} \tag{6}$$

To complete the formulation of our problem, we must conserve current and satisfy Maxwell's equations. Thus,

Current Conservation:

$$\nabla \cdot \underline{j} = 0 \tag{7}$$

Electric Field Relation:

$$\nabla \times \underline{E} = 0 \tag{8}$$

Finally, the individual species momentum is conserved by satisfying a generalized Ohm's law.

Generalized Ohm's Law:

$$J_x = \frac{\sigma}{(1 + \beta_e \beta_i)^2 + \beta_e^2} \left[(1 + \beta_e \beta_i) E_x - \beta_e (E_y - u B_z) \right] \tag{9}$$

$$J_y = \frac{\sigma}{(1 + \beta_e \beta_i)^2 + \beta_e^2} \left[(1 + \beta_e \beta_i) (E_y - u B_z) + \beta_e E_x \right] \tag{10}$$

where the electron inertia and electron pressure gradients have been neglected.

Next, we observe that if we try to satisfy Eq's. (7) and (8) explicitly we have for the two-dimensional problem the following relations:

$$\frac{\partial j_x}{\partial x} + \frac{\partial j_y}{\partial y} = 0 \tag{7a}$$

and

$$\frac{\partial E_x}{\partial y} = \frac{\partial E_y}{\partial x} \quad (8a)$$

along with Eq's. (9) and (10). Now, even if we assumed the flow field, gas conditions and electron temperature known, the above four equations lead to a nonlinear "elliptic" partial differential equation for the current stream function. If this equation must then be solved as part of the system, one cannot solve a boundary layer problem which is "parabolic" in character. Furthermore, the effects of finite electrical resistivity of the plasma are such that the significant variations in current density and electric field are not restricted to a narrow layer in the neighborhood of the wall.

Accordingly, since we still wish to treat a boundary layer type of problem we must abandon hope of satisfying (7a) and (8a) exactly and look for a procedure whereby they can be satisfied approximately. Such a procedure is available if we assume that the boundary layer thickness is small compared to the electrode or insulator segment lengths on the electrode wall.

In the analysis of the inviscid problem⁶, one obtains $j_y(x)$ along the electrode and $E_x(x)$ along the insulator. The boundary layer problem can then be handled by making the following assumptions:

1. Over an electrode segment $j_y = j_{y\infty}(x)$, $E_x = 0$ for all y 's.
2. Over an insulator segment $j_y = 0$, $E_x = E_{x\infty}(x)$ for all y 's.

With these assumptions Eq's. (7a) and (8a) are satisfied approximately and one must then only satisfy the Ohm's law at every point within the boundary layer.

Working with Eq's. (9) and (10) we can obtain expressions for $j_x E_x$, $j_y E_y$, j_{ex} , and j_{ey} as is shown in Appendix C. Substituting these into Eq's. (5) and (6) yield the following results:

Overall Energy Conservation:

$$\begin{aligned}
\rho u \frac{\partial h}{\partial x} + \rho v \frac{\partial h}{\partial y} = & - \left(\rho_{\infty} u_{\infty} \frac{du_{\infty}}{dx} \right) u + \mu \left(\frac{\partial u}{\partial y} \right)^2 \\
& + \frac{\partial}{\partial y} \left[\sum_i K_i \frac{\partial T}{\partial y} + \frac{5kT_e}{2e} \left(\alpha_1 j_{y_{\infty}} + \alpha_2 E_{x_{\infty}} \right) \right] \\
& + \frac{\sigma}{1+\beta_e \beta_i} E_{x_{\infty}}^2 + \frac{j_{y_{\infty}}^2}{\sigma} \left[\frac{(1+\beta_e \beta_i)^2 + \beta_e^2}{1+\beta_e \beta_i} \right] + u B_z j_{y_{\infty}} \\
& - I \left[u S_1 \frac{\partial T_e}{\partial x} - u S_2 \frac{\partial h}{\partial x} + u S_3 j_{y_{\infty}} B_z - u S_3 \rho_{\infty} u_{\infty} \frac{du_{\infty}}{dx} \right. \\
& + v S_1 \frac{\partial T_e}{\partial y} - v S_2 \frac{\partial h}{\partial y} - n_e \left(\frac{u}{p} j_{y_{\infty}} B_z - \frac{u}{p} \rho_{\infty} u_{\infty} \frac{du_{\infty}}{dx} \right. \\
& \left. \left. - \frac{u}{h} \frac{\partial h}{\partial x} - \frac{v}{h} \frac{\partial h}{\partial y} \right) \right] \quad (11)
\end{aligned}$$

Electron Energy Conservation:

$$\begin{aligned}
\frac{3}{2} k n_e \frac{\partial T_e}{\partial x} + \frac{3}{2} k v n_e \frac{\partial T_e}{\partial y} + \left(\frac{3}{2} k T_e + I \right) x \\
u \left\{ S_1 \frac{\partial T_e}{\partial x} - S_2 \frac{\partial h}{\partial x} + S_3 j_{y_{\infty}} B_z - S_3 \rho_{\infty} u_{\infty} \frac{du_{\infty}}{dx} \right\} \\
+ \left(\frac{3}{2} k T_e + I \right) v \left\{ S_1 \frac{\partial T_e}{\partial y} - S_2 \frac{\partial h}{\partial y} \right\} + n_e \left[\frac{5}{2} k T_e + I \right] \left\{ \rho u \frac{\partial \rho^{-1}}{\partial x} \right. \\
\left. + \rho v \frac{\partial \rho^{-1}}{\partial y} \right\} - \frac{\partial}{\partial y} \left[K_e \frac{\partial T_e}{\partial y} + \frac{5}{2} \frac{k}{e} T_e \left(\alpha_1 j_{y_{\infty}} + \alpha_2 E_{x_{\infty}} \right) \right] \\
= \left[\frac{(1+\beta_e \beta_i)^2 + \beta_e^2}{(1+\beta_e \beta_i)^2} \right] \frac{j_{y_{\infty}}^2}{\sigma} + \frac{\sigma}{(1+\beta_e \beta_i)^2} E_{x_{\infty}}^2 \\
+ 3 m_e n_e k (T - T_e) \sum_s \frac{\nu_{es}}{m_s} \quad (12)
\end{aligned}$$

4. Boundary Conditions

To complete the formulation, we must specify boundary conditions. At the outer edge of the boundary layer we have from the results of channel flow calculations

$$\begin{aligned}u(\infty) &= u_{\infty}(x) \\p(\infty) &= p_{\infty}(x) \\T(\infty) &= T_{\infty}(x) \\T_e(\infty) &= T_{e\infty}(x)\end{aligned}$$

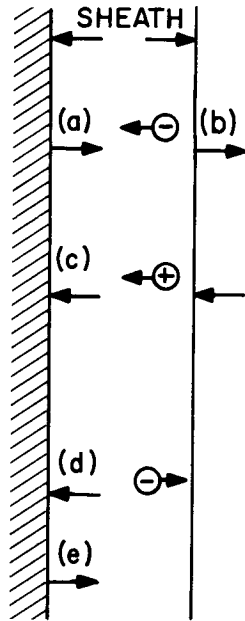
Along the wall we have

$$\begin{aligned}u(0) &= v(0) = 0 \\T(0) &= T_w(x) \text{ or } q(0) = q_w(x)\end{aligned}$$

To establish the inner boundary condition on the electron temperature T_e , we must consider the nature of the plasma sheath. The sheath will be considered collision-free and free of magnetic effects. The validity of such a treatment depends on the Debye length being much smaller than both the electron cyclotron radius and the electron mean free path. Such conditions obtain in the external channel flow but it is not clear that the desired length ordering is appropriate at the wall. In fact, it can be shown that if in the external stream the electron gyro radius is say ten times the Debye length, then just a 25% reduction in electron temperature will equalize the two lengths. Such a reduction may well occur in the boundary layer. Nevertheless, let us now consider the ideal sheath.

Consider the surface at $y = 0$ (Fig. 2). The net current density in the positive y direction is that due to electron arrival at the wall minus the sum of the current densities due to ion arrival at the wall and electron emission from the wall⁴. For the present problem where the only ions present are seed ions, the net current density normal to the wall can be expressed as

$$(j_y)_w = \frac{n_e \langle V_e \rangle}{4} e - \frac{e \Delta \phi}{k T_{ew}} - n_i e V_i - i_w \quad (13)$$



- (a) current density due to electron arrival at wall

$$\frac{n_e e \langle V \rangle_e}{4} e^{-\frac{e \Delta \phi}{k T_e}}$$

- (b) current density due to electron arrival at outer edge of sheath

$$\frac{n_e e \langle V \rangle_e}{4}$$

- (c) current density due to ions entering sheath (all these ions reach the wall since they are accelerated by the sheath drop)

$$n_i e V_i$$

- (d) electron emission current density i_w

- (e) net current density j_y

Figure 2. Contributions to current density at wall

where n_e , n_i refer to the number densities at the edge of the sheath ($n_e = n_i$ for singly ionized ions), where

$$\langle V_e \rangle = \sqrt{\frac{8kT_{ew}}{\pi m_e}}$$

$$V_i \geq \sqrt{\frac{kT_{ew}}{m_i}}$$

T_{ew} being the electron temperature at the sheath edge, and where the emission current density i_w is dependent on the surface temperature and work function of the surface. This gives one relation between the electron temperature at the sheath edge T_{ew} and the sheath drop, $\Delta\phi$.*

A second relation is obtained from continuity of electron energy flux at the sheath interface between continuum and molecular descriptions⁴.

Thus,

$$K_e \left(\frac{\partial T_e}{\partial y} \right)_w + \frac{5}{2} \frac{j_e}{e} kT_{ew} = \left(2kT_{ew} + e |\Delta\phi| \right) \frac{n_e \langle V_e \rangle}{e} e^{-\frac{e\Delta\phi}{kT_{ew}}} - i_w \frac{\mathcal{E}}{e} \quad (14)$$

where \mathcal{E} is the average energy of a thermionically emitted electron as it crosses the sheath interface, and will be taken equal to $(2kT_w + e\Delta\phi)$. Between the two relations (13) and (14) we have the sheath drop $\Delta\phi$ and the mixed inner boundary condition on T_e .

* The anode sheath drop is slightly less than the difference between plasma and floating potentials while the cathode sheath drop exceeds the aforementioned potential difference.

III. SOLUTION PROCEDURES FOR NON-SIMILAR BOUNDARY LAYERS

1. Equations in Transformed Plane

The boundary layer equations so far presented are a set of nonlinear partial differential equations dependent on two space variables. It has been common at this point to seek a similarity transformation that would reduce the dependence to just one independent variable. Such a transformation has in fact been carried out. While complete similarity is not attainable, by suitable approximations a form of local similarity (the longitudinal distance appears as a parameter but not in differentiations) can be obtained. While clearly inadequate for the regions of finite segmentation, the local similarity procedure allows solution of the boundary layer equations from a stagnation point or from a leading edge up to the region of segmentation. The solution may then be continued by a finite difference procedure in the plane of the transformed variables with the longitudinal step size determined by electrode length and spacing.

The new independent variables are those of the Levy-Lees transformation.

$$\xi(x) = \int_0^x (\rho\mu)_r u_\infty dx$$

$$\eta(x, y) = \frac{u_\infty}{\sqrt{2\xi}} \int_0^y \rho dy$$

so that

$$\frac{\partial}{\partial x} = (\rho\mu)_r u_\infty \frac{\partial}{\partial \xi} + \eta_x \frac{\partial}{\partial \eta}$$

$$\frac{\partial}{\partial y} = \frac{\rho u_\infty}{\sqrt{2\xi}} \frac{\partial}{\partial \eta}$$

and where

$$V \equiv \frac{2\xi}{(\rho\mu)_r u_\infty} \left(f' \eta_x + \frac{\rho v}{\sqrt{2\xi}} \right)$$

Equations (1), (2), (11), and (12) become

Continuity:

$$2\xi \frac{\partial f'}{\partial \xi} + \frac{\partial V}{\partial \eta} + f' = 0 \quad (15)$$

Momentum:

$$2\xi f' \frac{\partial f}{\partial \xi} + V \frac{\partial f'}{\partial \eta} = \frac{2\xi}{u_\infty} \frac{du_\infty}{d\xi} [g - f'^2] + \frac{\partial}{\partial \eta} \left(\lambda \frac{\partial f'}{\partial \eta} \right) \quad (16)$$

Energy:

$$\begin{aligned} 2\xi f' \frac{\partial g}{\partial \xi} + V \frac{\partial g}{\partial \eta} + \frac{2\xi f' g}{h_\infty} \frac{dh_\infty}{d\xi} = & - \frac{2\xi u_\infty}{h_\infty} \frac{du_\infty}{d\xi} (1 - IS_3) f' g \\ & + \frac{u_\infty^2}{h_\infty} \lambda \left(\frac{\partial f'}{\partial \eta} \right)^2 + \frac{\partial}{\partial \eta} \left[\frac{\lambda}{P_R} \frac{\partial g}{\partial \eta} \right] + \frac{T_{e_\infty}}{T_\infty} \frac{\partial}{\partial \eta} \left[\lambda \frac{\partial \theta}{\partial \eta} \right] \\ & + \frac{5}{2} \frac{\sqrt{2\xi} kT_{e_\infty} \alpha_1 j_{y_\infty}}{(\rho\mu)_r u_\infty C_p T_{e_\infty}} \frac{\partial \theta}{\partial \eta} + \frac{5}{2} \frac{\sqrt{2\xi} kT_{e_\infty} \alpha_2 E_{x_\infty}}{(\rho\mu)_r u_\infty C_p T_{e_\infty}} \frac{\partial \theta}{\partial \eta} \\ & + \frac{5}{2} \frac{\sqrt{2\xi} kT_{e_\infty} \alpha'_1 j_{y_\infty}}{(\rho\mu)_r u_\infty C_p T_{e_\infty}} \theta + \frac{5}{2} \frac{\sqrt{2\xi} kT_{e_\infty} \alpha'_2 E_{x_\infty}}{(\rho\mu)_r u_\infty C_p T_{e_\infty}} \theta \\ & + \frac{2\xi}{C_p T_\infty} \frac{1}{(\rho\mu)_r \rho_\infty u_\infty^2} \left[\frac{\sigma E_{x_\infty}^2}{1 + \beta_e \beta_i} + \frac{j_{y_\infty}^2}{\sigma} \frac{(1 + \beta_e \beta_i)^2 + \beta_e^2}{1 + \beta_e \beta_i} \right] g \\ & + \frac{2\xi B_z j_{y_\infty} f' g}{(\rho\mu)_r C_p T_\infty \rho_\infty u_\infty} (1 - IS_3) - \frac{IS_1 T_{e_\infty} (2\xi)}{C_p T_\infty \rho_\infty} g f' \frac{\partial \theta}{\partial \xi} \\ & - \frac{IS_1 T_{e_\infty} V}{\rho_\infty C_p T_\infty} g \frac{\partial \theta}{\partial \eta} - \frac{IS_1 (2\xi) \frac{dT_{e_\infty}}{d\xi}}{\rho_\infty C_p T_\infty} g f' \theta + \frac{IS_2 (2\xi)}{\rho_\infty} g f' \frac{\partial g}{\partial \xi} \\ & + \frac{IS_2 V}{\rho_\infty} g \frac{\partial g}{\partial \eta} + \frac{IS_2 (2\xi)}{\rho_\infty T_\infty} \left(\frac{dT_\infty}{d\xi} \right) g^2 f' - \frac{2\xi \ln_e}{C_p T_\infty \rho_\infty} f' \frac{\partial g}{\partial \xi} \end{aligned}$$

(17)

(continued on next page)

$$\begin{aligned}
& - \frac{I_{n_e}}{C_p T_\infty \rho_\infty} V \frac{\partial g}{\partial \eta} - \frac{I_{n_e}(2\xi)}{C_p T_\infty^2 \rho_\infty} \frac{dT_e}{d\xi} f' g + \frac{I_{n_e} j_{y_\infty}(2\xi) B_z}{p(\rho\mu)_r \rho_\infty C_p T_\infty u_\infty} g f' \\
& - \frac{I_{u_\infty} n_e(2\xi)}{p C_p T_\infty} \frac{du_\infty}{d\xi} g f'
\end{aligned} \tag{17}$$

cont'd)

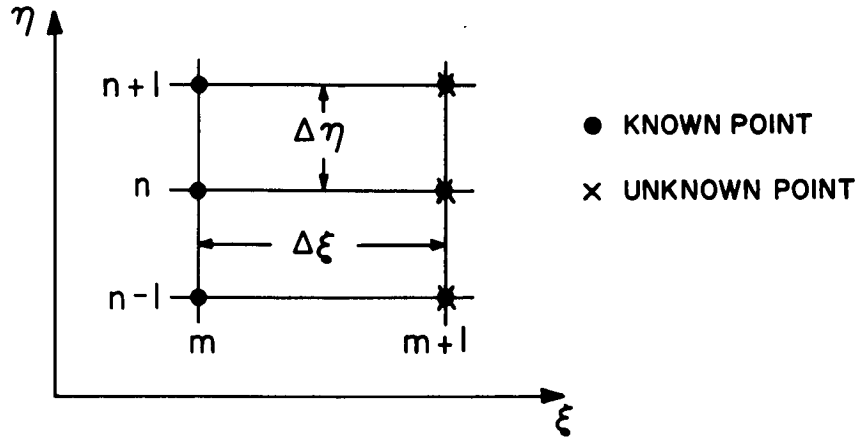
Electron Energy:

$$\begin{aligned}
& \left(\frac{3}{2} k n_e + \left[\frac{3}{2} k T_{e_\infty} \theta + I \right] S_1 \right) \left(\frac{(\rho\mu)_r T_{e_\infty} u_\infty}{2\xi} \right) \left[2\xi f' \frac{\partial \theta}{\partial \xi} + V \frac{\partial \theta}{\partial \eta} \right. \\
& \quad \left. + 2\xi \frac{f' \theta}{T_{e_\infty}} \frac{dT_{e_\infty}}{d\xi} \right] - S_2 \left[\frac{3}{2} k T_{e_\infty} \theta + I \right] \left(\frac{(\rho\mu)_r h_\infty u_\infty^2}{2\xi} \right) \left[2\xi f' \frac{\partial g}{\partial \xi} \right. \\
& \quad \left. + V \frac{\partial g}{\partial \eta} + 2\xi \frac{f' g}{T_\infty} \frac{dT_\infty}{d\xi} \right] - \left(\frac{3}{2} k T_{e_\infty} \theta + I \right) S_3 \rho_\infty u_\infty^3 \frac{du_\infty}{d\xi} (\rho\mu)_r f' \\
& \quad + \left(\frac{3}{2} k T_{e_\infty} \theta + I \right) S_3 j_{y_\infty} B_z u_\infty f' - \frac{\rho_\infty u_\infty^2 C_p (\rho\mu)_r T_{e_\infty}}{2\xi g} \frac{\partial}{\partial \eta} \left(\lambda \frac{\partial \theta}{\partial \eta} \right) \\
& \quad - \frac{\rho_\infty u_\infty}{g \sqrt{2\xi}} \frac{5}{2} \frac{k}{e} T_{e_\infty} j_{y_\infty} \frac{\partial}{\partial \eta} (\theta \alpha_1) - \frac{\rho_\infty u_\infty}{g \sqrt{2\xi}} \frac{5}{2} \frac{k}{e} T_{e_\infty} E_{x_\infty} \frac{\partial}{\partial \eta} (\theta \alpha_2) \\
& \quad + n_e \left[\frac{5}{2} k T_{e_\infty} \theta + I \right] \left[\frac{(\rho\mu)_r u_\infty^2}{2\xi g} \right] \left[2\xi f' \frac{\partial g}{\partial \xi} + V \frac{\partial g}{\partial \eta} - \frac{2\xi f' g}{\rho_\infty} \frac{d\rho_\infty}{d\xi} \right] \\
& \quad = E_{x_\infty}^2 \frac{\sigma}{(1+\beta_{e_i})^2} + \frac{j_{y_\infty}^2}{\sigma} \frac{[(1+\beta_{e_i})^2 + \beta_e^2]}{(1+\beta_{e_i})^2} \\
& \quad + 3m_e n_e k T_{e_\infty} \left(g \frac{T_\infty}{T_{e_\infty}} - \theta \right) \sum_s \frac{\nu_s}{m_s}
\end{aligned} \tag{18}$$

2. Finite Difference Form of Equations

Of the many finite-difference schemes that can be employed to solve the boundary layer equations, the implicit procedure of Blottner (references 7 and 8) is adopted for the present study. Implicit procedures are less likely to have stability difficulties as encountered with explicit schemes and the truncation error is of higher order than in the explicit schemes.

The flow field is divided into a grid or mesh as indicated in the following sketch:



It is assumed that all the dependent quantities are known at the grid points in the m^{th} column but unknown in the $(m+1)^{\text{th}}$ column. In the implicit scheme, the various derivatives are replaced by linear difference quotients and the partial differential equations are evaluated at $(m + \frac{1}{2}, n)$. For example, consider the functions $M(\xi, \eta)$ and $N(\xi, \eta)$. The difference quotients at this point $(m + \frac{1}{2}, n)$ are

$$\frac{\partial M}{\partial \xi} = \frac{M_{m+1, n} - M_{m, n}}{\Delta \xi}$$

$$\frac{\partial M}{\partial \eta} = \frac{(M_{\eta}) + (M_{m+1, n+1} - M_{m+1, n-1}) / 2 \Delta \eta}{2}$$

$$\text{where } M_{\eta} = \frac{(M_{m,n+1} - M_{m,n-1})}{2 \Delta \eta}$$

$$\frac{\partial^2 M}{\partial \eta^2} = \frac{M_{\eta\eta} + (M_{m+1,n+1} - 2 M_{m+1,n} + M_{m+1,n-1}) / (\Delta \eta)^2}{2}$$

$$\text{where } M_{\eta\eta} = \frac{M_{m,n+1} - 2 M_{m,n} + M_{m,n-1}}{(\Delta \eta)^2}$$

$$\left(\frac{\partial M}{\partial \eta} \right)^2 = M_{\eta} \frac{(M_{m+1,n+1} - M_{m+1,n-1})}{2 \Delta \eta}$$

$$\frac{\partial M}{\partial \eta} \frac{\partial N}{\partial \eta} = \frac{1}{4 \Delta \eta} \left[M_{\eta} (N_{m+1,n+1} - N_{m+1,n-1}) + N_{\eta} (M_{m+1,n+1} - M_{m+1,n-1}) \right]$$

Product terms are written

$$M^2 = M_{m,n} M_{m+1,n}$$

$$MN = \frac{1}{2} \left[M_{m,n} N_{m+1,n} + M_{m+1,n} N_{m,n} \right]$$

In all of the above equations, terms of order $(\Delta \xi)^2$ and $(\Delta \eta)^2$ have been neglected. To preserve the linearity of the difference equations, terms of the following form are approximated as

$$N \frac{\partial M}{\partial \xi} = \left[N_{m,n} + \frac{1}{2} \left(\frac{\partial N}{\partial \xi} \right)_{m,n} \Delta \xi + \dots \right] \left[\frac{M_{m+1,n} - M_{m,n} + \dots}{\Delta \xi} \right]$$

$$\cong \frac{N_{m,n} (M_{m+1,n} - M_{m,n})}{\Delta \xi}$$

When the difference quotients and terms of the above equations are substituted in the boundary layer equations (16) to (18), the resulting linear difference equations are written

$$A_n W_{n+1} + B_n W_n + C_n W_{n-1} = D_n \quad (19)$$

whose quantities are the matrices

$$W_n = \begin{bmatrix} f'_{m+1,n} \\ g_{m+1,n} \\ \theta_{m+1,n} \end{bmatrix}$$

$$A_n = \begin{bmatrix} A_{11} & 0 & 0 \\ A_{21} & A_{22} & A_{23} \\ 0 & 0 & A_{33} \end{bmatrix}, B_n = \begin{bmatrix} B_{11} & B_{12} & 0 \\ B_{21} & B_{22} & B_{23} \\ B_{31} & B_{32} & B_{33} \end{bmatrix}, C_n = \begin{bmatrix} C_{11} & 0 & 0 \\ C_{21} & C_{22} & C_{23} \\ 0 & 0 & C_{33} \end{bmatrix}$$

$$D_n = \begin{bmatrix} D_1 \\ D_2 \\ D_3 \end{bmatrix}$$

The top, middle and bottom lines of the matrix equation (19) are respectively the momentum, energy and electron energy equations. The continuity equation is invoked to calculate V knowing the values of $f'_{m+1,n+1}$, $f'_{m+1,n}$ and $f'_{m+1,n-1}$.

The elements of the matrices A_n , B_n , C_n and D_n are given in Appendix D.

At the wall we want a linear B.C. to fit in with our linear system of finite difference equations. Thus,

$$w_1 = Hw_2 + Fw_3 + h \quad w = \begin{Bmatrix} f' \\ g \\ \theta \end{Bmatrix}_{m+1, n} \quad (19a)$$

We note that $f' = 0$ at the wall ($n=1$). Also, $T_{\text{wall}} = \text{const.}$ so $g_1 = T_w/T_\infty(\xi) = g_w(\xi)$. For θ we have problems. We have two equations to work with, each containing θ and $\Delta\varphi$, and have to eliminate $\Delta\varphi$ between them. So

$$j_{y_\infty} + i_w = \frac{n_{e_w} e \langle V_e \rangle}{4} e^{\frac{-e|\Delta\varphi|}{kT_{e_\infty}\theta_w}} - n_{e_w} e \sqrt{\frac{kT_{e_\infty}\theta_w}{m_c}}$$

and

$$K_e T_{e_\infty} \left(\frac{\partial \theta}{\partial y} \right)_w + \frac{5}{2} \left(j_{e_y} \right)_w \frac{k}{e} T_{e_\infty} \theta_w = \left(2kT_{e_\infty} \theta_w + e |\Delta\varphi| \right) \times$$

$$\times \frac{n_{e_w} \langle V_e \rangle}{4} e^{\frac{-e|\Delta\varphi|}{kT_{e_\infty}\theta_w}} - \frac{i_w}{e} \left(2kT_{e_\infty} g_w + e \Delta\varphi \right)$$

alternately,

$$j_{y_\infty} + i_w = \frac{\frac{\lambda C_p (\rho\mu)_r u_{e_\infty}}{k\sqrt{2\xi}} \left(\frac{\partial \theta}{\partial \eta} \right)_w + i_w \left(\frac{2T_\infty}{T_{e_\infty}} g_w + \frac{e\Delta\varphi}{kT_{e_\infty}} \right) + \frac{5}{2} \left(j_{e_y} \right)_w \theta_w}{2\theta_w + \frac{e|\Delta\varphi|}{kT_{e_\infty}}} - n_{e_w} e \sqrt{\frac{kT_{e_\infty}\theta_w}{m_c}}$$

Next write

$$\left(\frac{\partial \theta}{\partial \eta} \right)_w = \frac{-3\theta_1 + 4\theta_2 - \theta_3}{2\Delta\eta}$$

Then we have

$$j_{y_\infty} + i_w = \frac{\frac{\lambda C_p (\rho \mu)_r u_\infty}{k \sqrt{2\xi}} \left[\frac{-3\theta_1 + 4\theta_2 - \theta_3}{2\Delta\eta} \right] + \frac{5}{2} \left(j_{e_y} \right)_w \theta_1 + i_w \left(\frac{2T_\infty}{T_{e_\infty}} g_w + \frac{e\Delta\varphi}{kT_{e_\infty}} \right)}{2\theta_1 + \frac{e|\Delta\varphi|}{kT_{e_\infty}}} - n_{e_w} e \sqrt{\frac{kT_{e_\infty} \theta_1}{m_c}}$$

or

$$\begin{aligned} \left(j_{y_\infty} + i_w \right) \left(2\theta_1 + \frac{e|\Delta\varphi|}{kT_{e_\infty}} \right) &= \frac{\lambda C_p (\rho \mu)_r u_\infty}{k \sqrt{2\xi}} \frac{(-3\theta_1 + 4\theta_2 - \theta_3)}{2\Delta\eta} + \frac{5}{2} \left(j_{e_y} \right)_w \theta_1 \\ &+ i_w \left(\frac{2T_\infty}{T_{e_\infty}} g_w + \frac{e\Delta\varphi}{kT_{e_\infty}} \right) - n_{e_w} e \sqrt{\frac{kT_{e_\infty} \theta_1}{m_c}} \left[2\theta_1 + \frac{e|\Delta\varphi|}{kT_{e_\infty}} \right] \end{aligned}$$

We find $|\Delta\varphi|$ from the 1st of our original two equations

$$\begin{aligned} e \frac{e|\Delta\varphi|}{kT_{e_\infty} \theta_1} &= \left[\left(j_{y_\infty} + i_w \right) + n_{e_w} e \sqrt{\frac{kT_{e_\infty} \theta_1}{m_c}} \right] \frac{4}{n_{e_w}} \sqrt{\frac{\pi m_c}{8kT_{e_\infty} \theta_1}} \\ &= \left[\frac{\left(j_{y_\infty} + i_w \right)}{n_{e_w}} \sqrt{\frac{2\pi m_e}{kT_{e_\infty} \theta_1}} + \sqrt{\frac{2\pi m_e}{m_c}} \right] = a^{-1} \end{aligned}$$

$$\frac{e|\Delta\varphi|}{kT_{e_\infty} \theta_1} = -\ln a^{-1} = \ln a \quad \text{or} \quad \frac{e|\Delta\varphi|}{kT_{e_\infty}} = \theta_1 \ln a$$

so,

$$\theta_1 \left\{ j_{y_\infty} (2 + \ln a) + 2i_w + \frac{3\lambda C_p (\rho\mu)_r u_\infty e}{2k \sqrt{2\xi} \Delta\eta} - \frac{5}{2} \left(j_{e_y} \right)_w + en_{e_w} \sqrt{\frac{kT_{e_\infty} \theta_1}{m_s}} (2 + \ln a) \right\} = \left(\frac{2\lambda C_p (\rho\mu)_r u_\infty e}{k \sqrt{2\xi} \Delta\eta} \right) \theta_2 - \left(\frac{\lambda C_p (\rho\mu)_r u_\infty e}{2k \sqrt{2\xi} \Delta\eta} \right) \theta_3 + i_w \left(\frac{2T_\infty}{T_{e_\infty}} \right) g_w$$

This is highly non-linear in θ_1 . Since we wish to deal with a linear system treat θ_1 in $\sqrt{\quad}$ and "a" terms as $\theta_{m,1}$ while $\theta_1, \theta_2, \theta_3$ in linear terms are $\theta_{m+1,1}$ etc. Actually, we must express our boundary condition at $m + 1/2, n$. So,

$$\frac{\theta_{m+1,1} + \theta_{m,1}}{2} = B_2 \left[\frac{\theta_{m+1,2} + \theta_{m,2}}{2} \right] + B_3 \left[\frac{\theta_{m+1,3} + \theta_{m,3}}{3} \right] + C$$

where

$$B_2 = \frac{\frac{2\lambda_1 C_p (\rho\mu)_r u_\infty e}{k \sqrt{2\xi} (\Delta\eta)}}{[2 + \ln a] \left[j_{y_\infty} + en_{e_w} \sqrt{\frac{kT_{e_\infty} \theta_1}{m_s}} \right] + \frac{3\lambda_1 C_p (\rho\mu)_r u_\infty e}{2k \sqrt{2\xi} \Delta\eta} - \frac{5}{2} \left(j_{e_y} \right)_w + 2i_w}$$

$$= \frac{2\lambda_1 C_p (\rho\mu)_r u_\infty e}{k \sqrt{2\xi} (\Delta\eta)} \Big/ R \quad (20)$$

$$B_3 = -\frac{1}{4} B_2 \quad (21)$$

$$C = \frac{2T_\infty g_w}{T_{e_\infty}} i_w / R \quad (22)$$

and where

$$a = \left[\frac{(j_{y_\infty} + i_w)}{en_{e_w}} \sqrt{\frac{2\pi m_e}{kT_{e_\infty} \theta_1}} + \sqrt{\frac{2\pi m_e}{m_s}} \right]^{-1}$$

$$n_{e_w} = n_e(g_1, \theta_1); \quad (j_{e_y})_w = j_{e_y}(g_1, \theta_1)$$

$$\lambda_1 = \lambda(g_1, \theta_1)$$

Also all ξ dependent quantities, j_{y_∞} , u_∞ , T_{e_∞} , are evaluated at $m + 1/2$ location. Now θ_1 will be treated as an iterable quantity. That is, for first calculation take $\theta_{m,1}$, and for subsequent iterations take $\frac{\theta_{m,1} + \theta_{m+1,1}}{2}$.

Finally,

$$\theta_{m+1,1} = B_2 \theta_{m+1,2} + B_3 \theta_{m+1,3} + \left[B_2 \theta_{m,2} + B_3 \theta_{m,3} - \theta_{m,1} + C \right]$$

or

$$\theta_{m+1,1} = B_2 \theta_{m+1,2} + B_3 \theta_{m+1,3} + B_4$$

Then

$$H = \begin{bmatrix} 0 & 0 & 0 \\ 0 & 0 & 0 \\ 0 & 0 & B_2 \end{bmatrix} \quad F = \begin{bmatrix} 0 & 0 & 0 \\ 0 & 0 & 0 \\ 0 & 0 & B_3 \end{bmatrix}$$

$$h = \begin{Bmatrix} 0 \\ g_1 \\ B_4 \end{Bmatrix} \quad (23)$$

where $g_1 = T_w / T_{\infty m+1}$

and $T_w = \text{constant}$, $T_{\infty m+1}$ corresponds to $T_\infty(\xi)$ evaluated when ξ corresponds to $m + 1$ location.

3. Determination of External Conditions

Analyses of complete MHD generator channels are generally one-dimensional. The variations of flow and electric quantities predicted from such analyses are usually continuous since they ignore the details of any finite electrode structure. Such calculations may be considered to represent what goes on in the core of the generator channel but do not necessarily provide outer "inviscid" conditions for a boundary layer analysis.

Consider for example the problem of determining exterior conditions for J_y and E_x along a segmented electrode wall (Figure 3). The uppermost sketch in Figure 3 depicts the results of one dimensional flow calculations for a non-equilibrium generator. Numerous such calculations for constant-area, segmented-electrode Faraday generators using noble carrier gases and alkali seed gases have been carried out by Highway and Nichols (reference 10). The portion of the continuous current distribution assigned to a given electrode pair must now be distributed. The current streamlines within the cell boundaries for a given pair of electrodes are estimated from the results of Hurwitz, Kilb and Sutton (reference 8) as recently modified for non-equilibrium conductivity ($\sigma = \sigma |J|$) by Sherman¹¹. Over an electrode $J_{y\infty}(x)$ is according to the solid curve shown while $E_{x\infty}(x) = 0$. Over the insulator portion between adjacent electrode segments $J_{y\infty}(x) = 0$ and $E_{x\infty}(x)$ is given by the dotted curve.

It is implied by this kind of argument that the characteristic thickness for accommodation of electrical quantities to the discrete electrode structure is large compared to the viscous and thermal boundary layer thicknesses. It must be realized that the relative scale of these phenomena is inverse to some power of the appropriate magnetic Prandtl number. Since for the expected working fluids $Pr_m \ll 1$, it is felt that a procedure as described by Figure 3 is justified for the electrical quantities.

In the absence of better information, the external velocity and enthalpy distribution were taken to be the same as at channel centerline (one-dimensional).

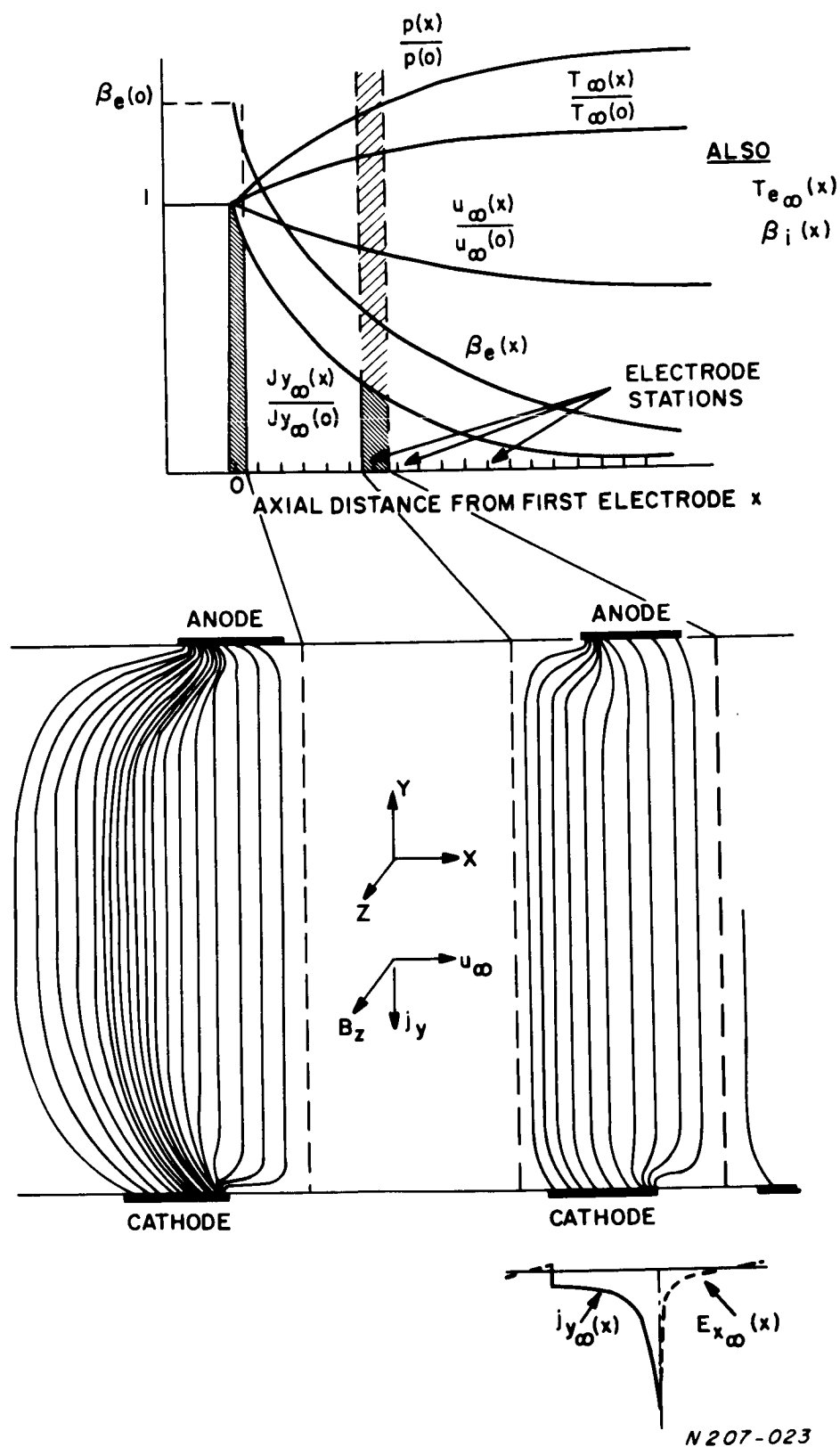


Figure 3. Determination of outer boundary conditions on J_y and E_x .

4. Initial Profile - Local Similarity

The calculation can proceed by finite differences over a finitely segmented electrode wall. However, an initial profile will always be needed. If the boundary layer development is assumed to begin from a sharp leading edge the profiles at $\xi = 0$ will be similar. If we assume, on the other hand, that it develops from a nozzle then an initial profile can be obtained by assuming local similarity. That is, $\frac{\partial}{\partial \xi} = 0$ and $\xi =$ parameter so that we only have to integrate over η .

In the final section of this report we will describe some locally similar solutions as well as a finite difference solution starting at a leading edge. The former is convenient as the calculation is simplified so that many different cases can be studied.

IV. EXAMPLES AND DISCUSSION

1. General Description of Example

The channel flow which we have taken as a basis for our initial boundary layer calculations has been developed by Les Nichols and is his case #001351 dated Nov. 16, 1966. He chose the following conditions for the channel flow.

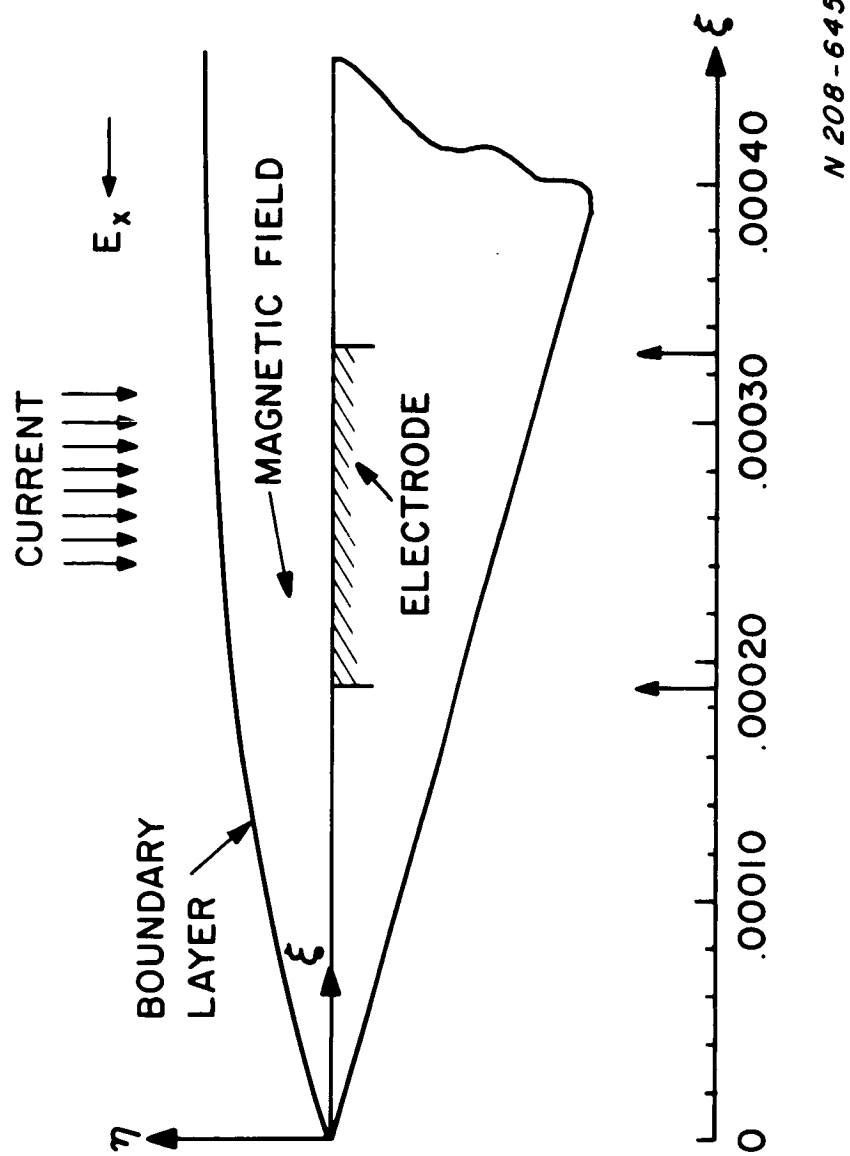
$$\begin{array}{lll} K = 0.700 & \text{Seed} = 0.01 & p^{\circ} = 2 \times 10^5 \frac{\text{newtons}}{\text{m}^2} \\ T^{\circ} = 2000^{\circ}\text{K} & M = 0.500 & B = 10,000 \text{ gauss} \\ \text{Argon + Cesium} & & \end{array}$$

The ξ variation of velocity, gas temperature, pressure, and density can be taken from his calculation. However, for the subsonic case the ξ variations over the first and second electrode pairs are slight, so we have assumed them to be zero. Thus,

$$\begin{array}{l} u_{\infty} = 395.61 \text{ meters/second} \\ T_{\infty} = 1920^{\circ}\text{K} \\ p = 164,000 \text{ newtons/m}^2 \\ \rho_{\infty} = 0.5 \text{ Kg/m}^3 \end{array}$$

In addition we have taken $\ell = g^{-1/4}$ and $P_R = 2/3$. For the generator considered by Nichols the first electrode would be approximately 34 inches from the nozzle throat. This would correspond to a value of $\xi = .01$, and the locally similar solutions have been carried out at this location. The finite difference solutions, on the other hand, have been started from a sharp leading edge at $\xi = 0$. The geometry and dimensions are shown in Figure 4.

For the electrical quantities and T_e we cannot use the channel flow values directly as they assume an infinitely fine segmentation whereas we are calculating a boundary layer with finite segments. Estimates obtained from several analytical calculations show that $T_{e_{\infty}}$ will vary by only several degrees over an electrode for the case cited above. Therefore, for these



N 208-645

Figure 4. Boundary layer grown from sharp leading edge

initial calculations we have assumed $T_{e\infty}$ constant as well.

Finally, we have allowed $j_{y\infty}$ and $E_{x\infty}$ to have the following average values at the channel centerline.

$$j_{y\infty} = -75 \text{ amps/m}^2$$
$$E_{x\infty} = 200 \text{ volts/meter}$$

These values are actually not representative of any specific channel design but rather were chosen to illustrate the phenomena caused by currents and axial electric fields. Using these, ξ distributions were assumed using constant property channel flow solutions including Hall effects as a guide. These, as well as the B field and thermionic emission distributions chosen are shown in Section IV 3.

2. Locally Similar Solutions on Insulator Wall with $B = 0$

Before attempting the more difficult problem of a finite electrode in an insulator wall, we have obtained locally similar solutions when $B = 0$ on an insulator alone. Such solutions, aside from their obvious usefulness, can also be used as starting profiles for the more complete finite difference solutions.

Our basic equations reduced to local similarity form are shown in Eq.'s (17), (18), (19), and (20) of Appendix E. They have been solved by numerical integration (Runge-Kutta) using an iteration scheme on the unknown wall values of θ , g' , and f'' . The principal difficulty was the large value of θ' at the wall which demanded a very fine interval for integration. A computer program was written to carry out this solution and is shown in Appendix F.

Solutions obtained for various wall temperatures and ξ locations are shown in Appendix E. It was particularly interesting to find the electron temperature to differ so widely from the gas and wall temperatures even though in the free stream they were assumed equal. Since there was no current flowing or electric or magnetic fields applied, the conclusion one must draw is that the gradients within the boundary layer and wall sheath boundary condition are the causes.

3. Boundary Layer Over Finite Electrode Segment with $B \neq 0$

In order to carry out the finite difference solution we had to establish a method for the solution of Eq's. (19) along with the appropriate boundary conditions. They are in a form identical to Blottner's so that his calculation procedure can be followed⁸. Due to the special form of the equations an algorithm exists which makes digital solution quite efficient. The vectors W_n and W_{n+1} may be related by

$$W_n = E_n W_{n+1} + e_n \quad W_n = \begin{Bmatrix} f' \\ g \\ \theta \end{Bmatrix} \quad (24)$$

where

$$E_2 = \frac{-(A_2 + C_2 F)}{B_2 + C_2 H}$$

$$e_2 = \frac{D_2 - C_2 h}{B_2 + C_2 H}$$

and

$$\left. \begin{aligned} E_n &= \frac{-A_n}{B_n + C_n E_{n-1}} \\ e_n &= \frac{D_n - C_n e_{n-1}}{B_n + C_n E_{n-1}} \end{aligned} \right\} \quad 3 \leq n \leq N-1 \quad (25)$$

where we must remember that E_n is a 3×3 matrix and e_n is a three component vector.

Knowing the iterated solution W_n at ξ_m , the solution at ξ_{m+1} is obtained as follows:

- Evaluate the quantities B_2 , B_3 and C (Equations 20-22) using values of the number densities and θ_n from the prior step ($\eta = 0$, $\xi = \xi_m$).
- Knowing H , F , and h (Equation 23) evaluate E_2 and e_2 after first evaluating the components of A_2 , B_2 , C_2 and D_2 from Appendix D.
- Continue outward through the boundary layer evaluating E_n and e_n at each step $3 \leq n \leq N-1$.

- d) As the outer edge of the boundary layer is not at a definite location, the matrix E_n and the vector e_n are computed until f' , g , and θ become fairly constant. The conditions from equation (24) are

$$1 - E_{i1} - E_{i2} - E_{i3} - e_i < \epsilon_i \quad i = 1, 2, 3 \quad (26)$$

where the ϵ_i are small quantities to be determined from experience.

- e) Once the values of E_n and e_n are calculated throughout the boundary layer, the computation then shifts to the determination of W_n starting at the outer edge with all W_N values equal to one. The calculation is simply accomplished using eq. (24). It is continued in this manner to the evaluation of W_2 ; then W_1 is determined from Eq. (19a).

- f) With $f'_{m,n}$ and $f'_{m+1,n}$ known, the transformed normal velocity parameter V is determined from the continuity equation (15).

The derivatives of the continuity equation are evaluated at the point $(m + \frac{1}{2}, n - \frac{1}{2})$. Then Eq. (15) reduces to

$$V_{m+1/2,n} = V_{m+1/2,n-1} - \Delta\eta \left(\frac{\xi}{\Delta\xi} + \frac{1}{4} \right) (f'_{m+1,n} + f'_{m+1,n-1}) \\ + \Delta\eta \left(\frac{\xi}{\Delta\xi} - \frac{1}{4} \right) (f'_{m,n} + f'_{m,n-1})$$

- g) To iterate, steps (a) through (f) are repeated evaluating A, B, C, D, E matrices and D, e vectors using values of all quantities (excluding f' , g , and θ) that appear in these expressions evaluated at $m + \frac{1}{2}, n$. That is, we work with average values at (m, n) and $(m+1, n)$. For the initial calculation values at only (m, n) were used.
- h) Completing the solution at ξ_{m+1} we then proceed to ξ_{m+2} and repeat all of the above.

The above procedure has been programmed for solution on a high speed digital computer (GE635) using Fortran IV. The flow chart is shown in Appendix G and the program listing in Appendix H.

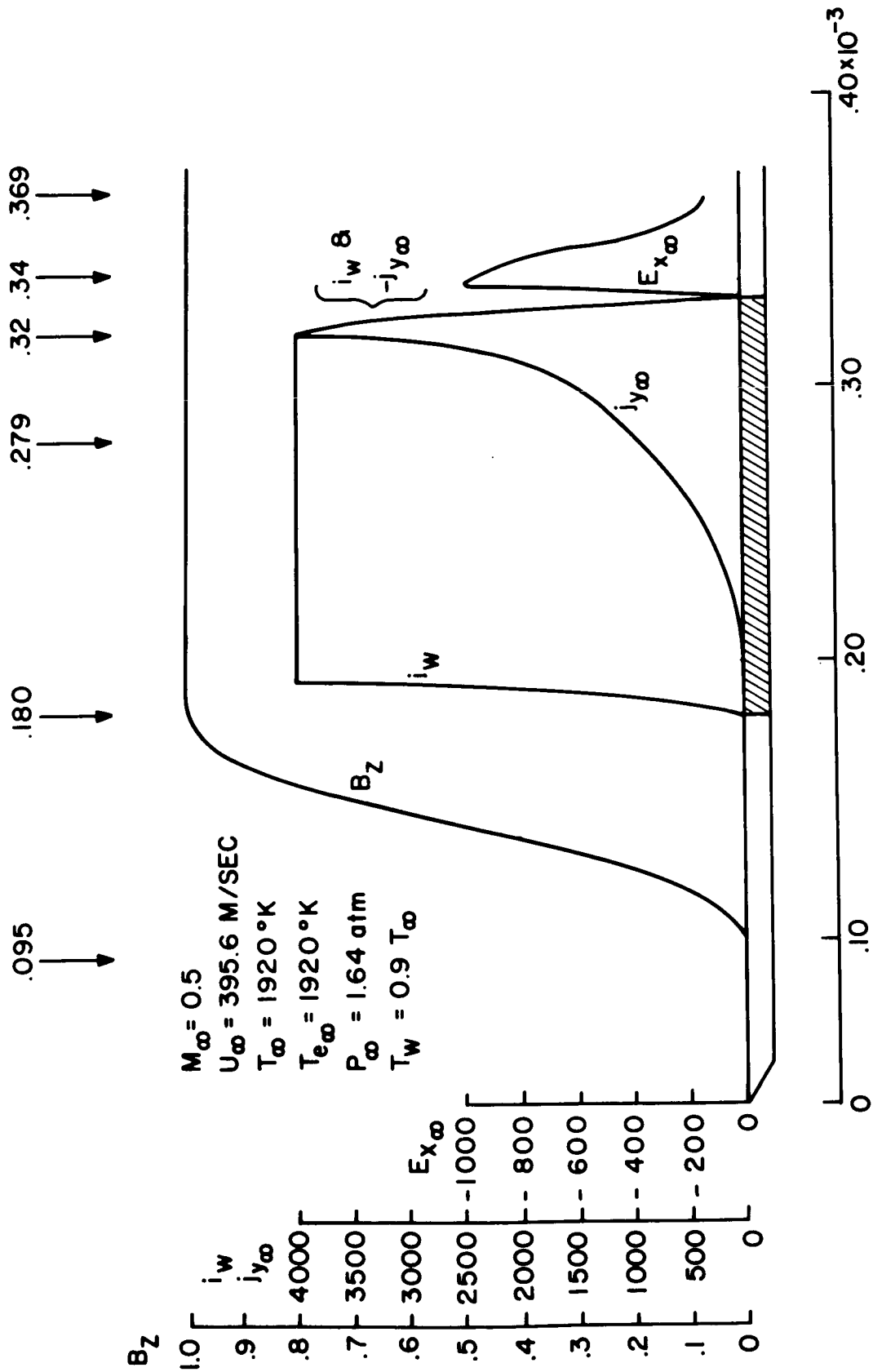
As noted earlier initial calculations using the finite difference technique have been carried out from a sharp leading edge. The distribution of imposed conditions is illustrated in Figure 5. The magnetic field was not taken to be uniform in ξ , but was instead allowed to rise from zero to its final value before the first electrode. Due to computational difficulties the emission could not be taken as a step function, but was instead represented by a smooth but rapid variation to its final value on the electrode. The current was brought up gradually to a peak at the downstream edge of the electrode. This is the expected form of the current distribution over a cathode. The current and the emission were brought back to zero smoothly but rapidly and together. Next, the electric field was introduced rapidly and then allowed to fall off gradually as the second electrode was approached.

Some of the results of our calculations using the above inputs are shown in Figures 6-10. For the hot wall case studied the voltage drop across the boundary layer was small. Some values at several ξ locations are presented in Table I.

ξ	$\Delta\phi_{\text{sheath}}$	$\Delta\phi_{\text{B.L.}}$	ΔV	(volts)
0.95×10^{-3}	.772	.011	.783	
.180	.676	.013	.689	
.189	.358	.015	.373	
.198	.381	.019	.400	
.252	.972	.162	1.13	
.280	.994	.300	1.29	
.320	1.05	.350	1.40	
.333	1.04	.547	1.59	
.337	1.06	.567	1.63	
.370	.940	.679	1.62	

Table I. Boundary Layer and Sheath Voltage Drop

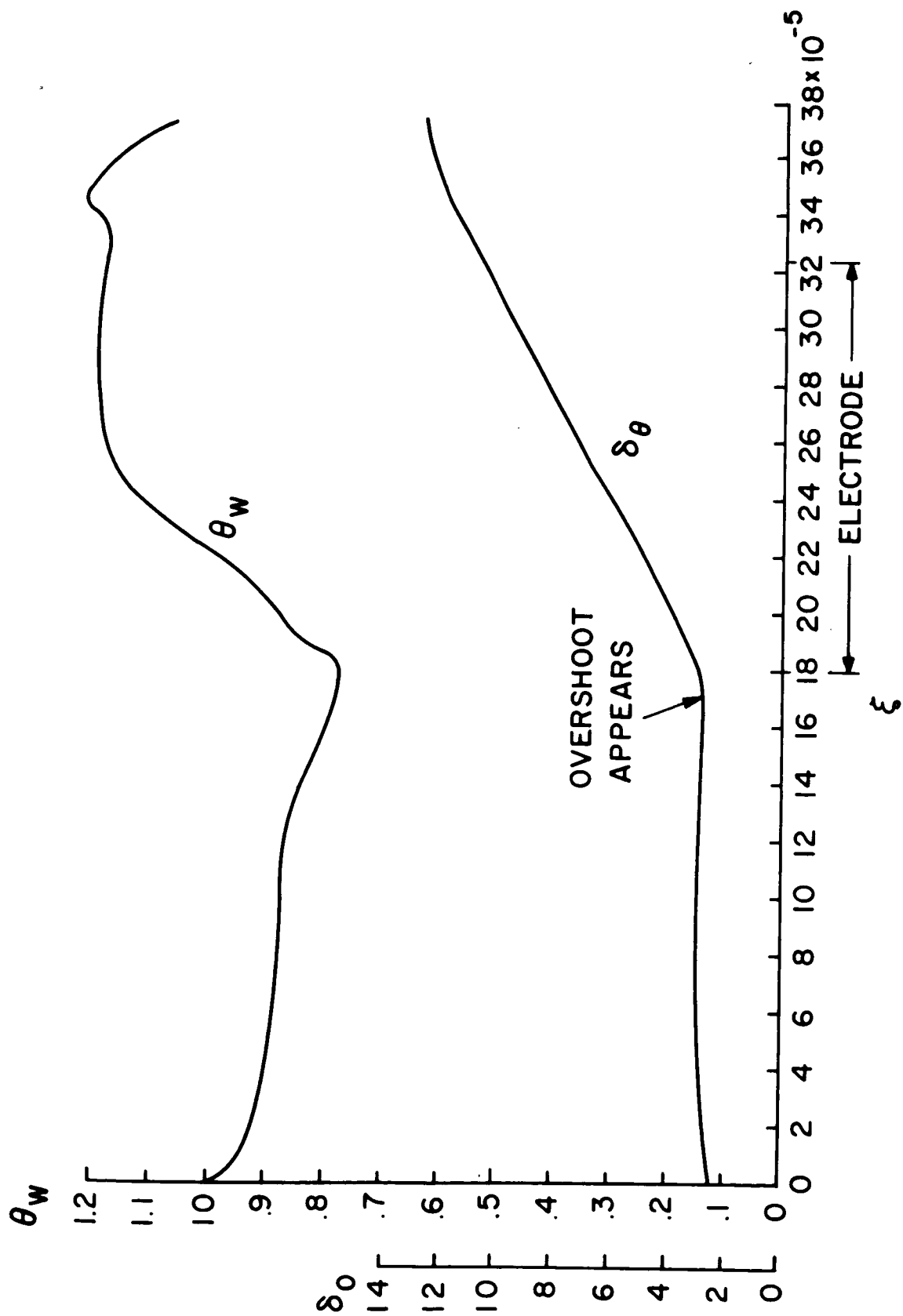
The velocity and heavy particle temperature profiles were relatively unaffected for the case studied. The heat flux was influenced somewhat more due to changes in $\partial T_e / \partial y$ and n_e . Values at several ξ values are given in Table II in watts/cm².



TRANSFORMED LONGITUDINAL COORDINATE, ξ

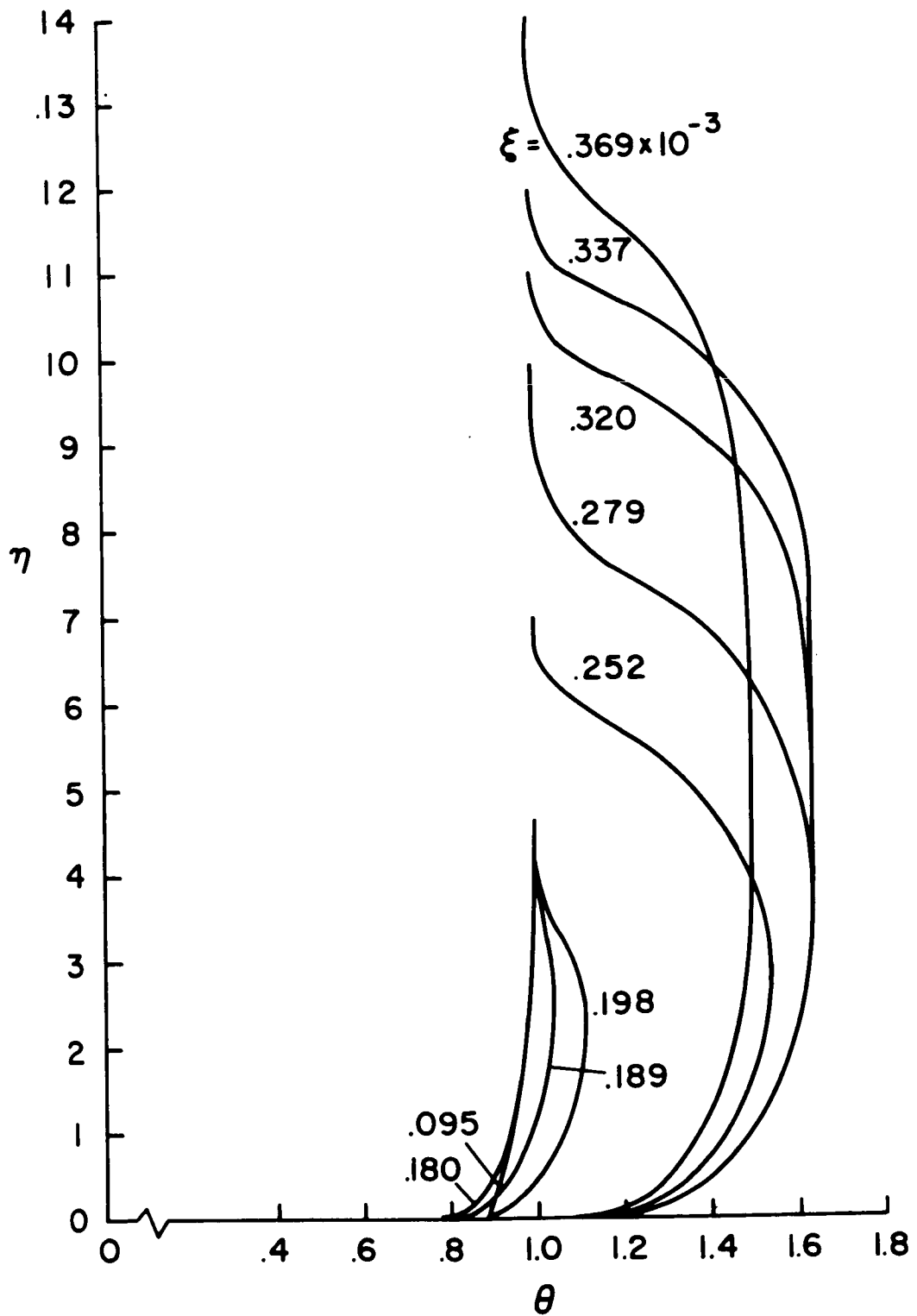
N208-650

Figure 5. Conditions imposed on boundary layer



N 208-644

Figure 6. Longitudinal variations of selected quantities



N208-642

Figure 7. Electron temperature profiles

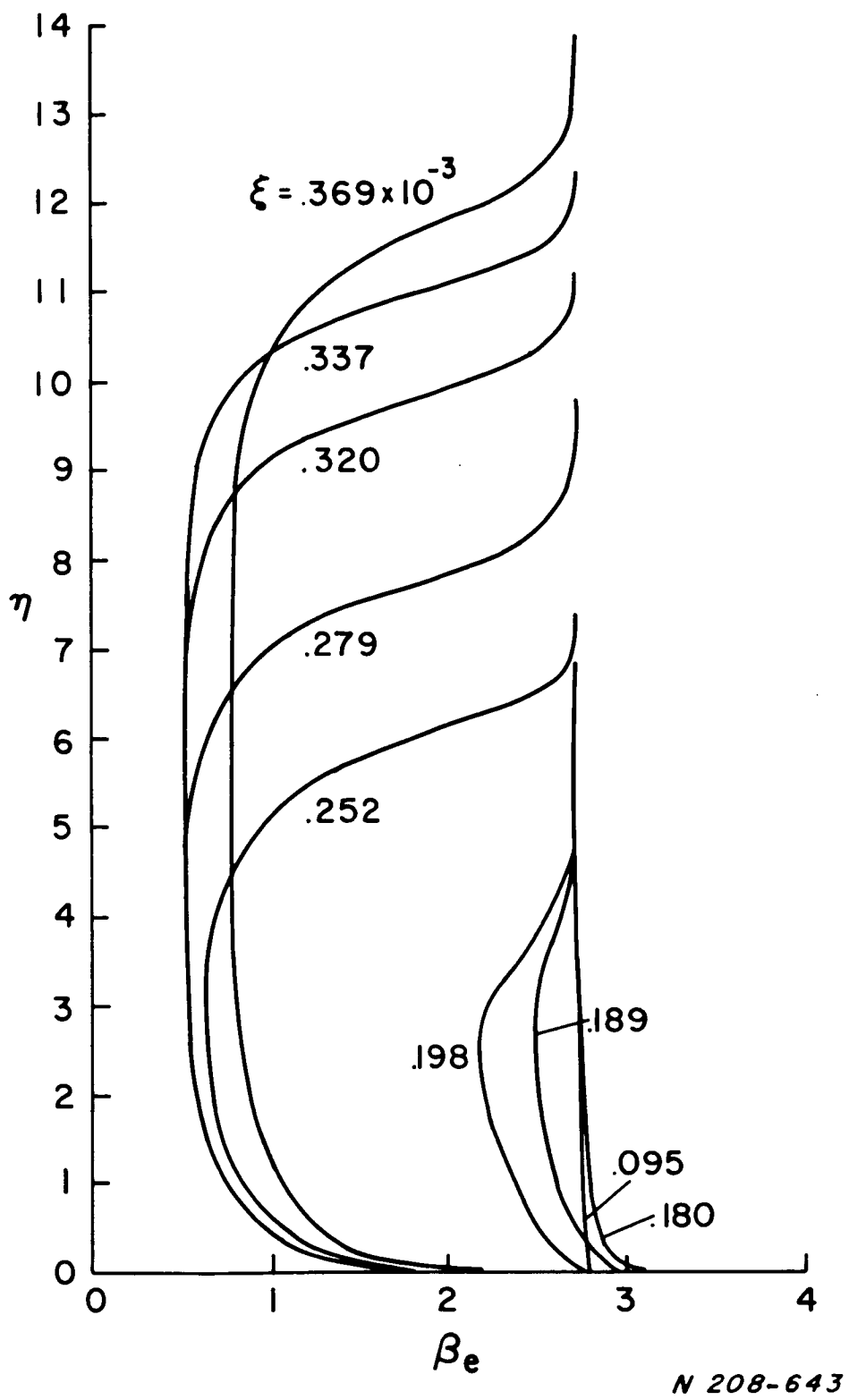
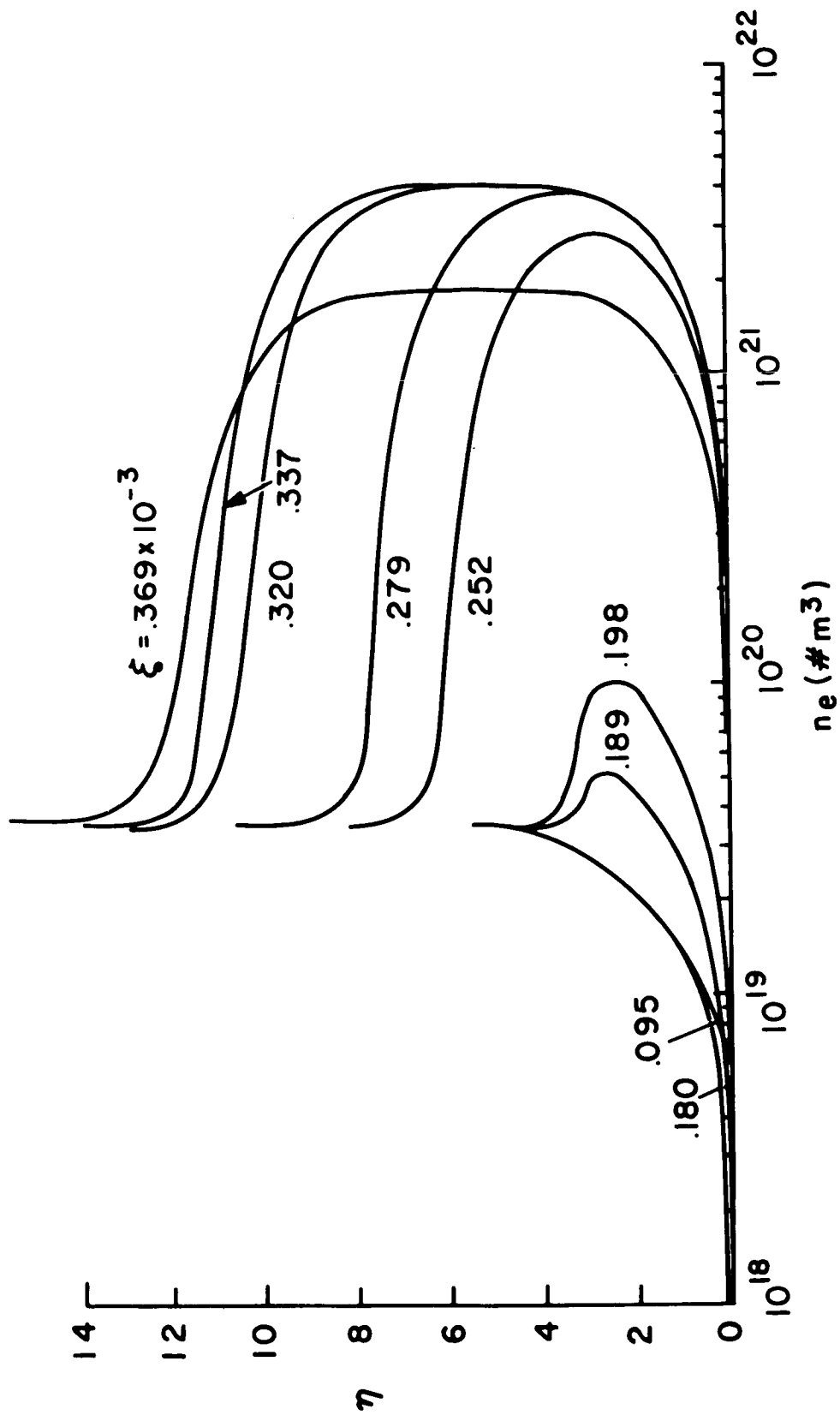


Figure 8. Electron Hall parameter



N208-641

Figure 9. Electron density profiles

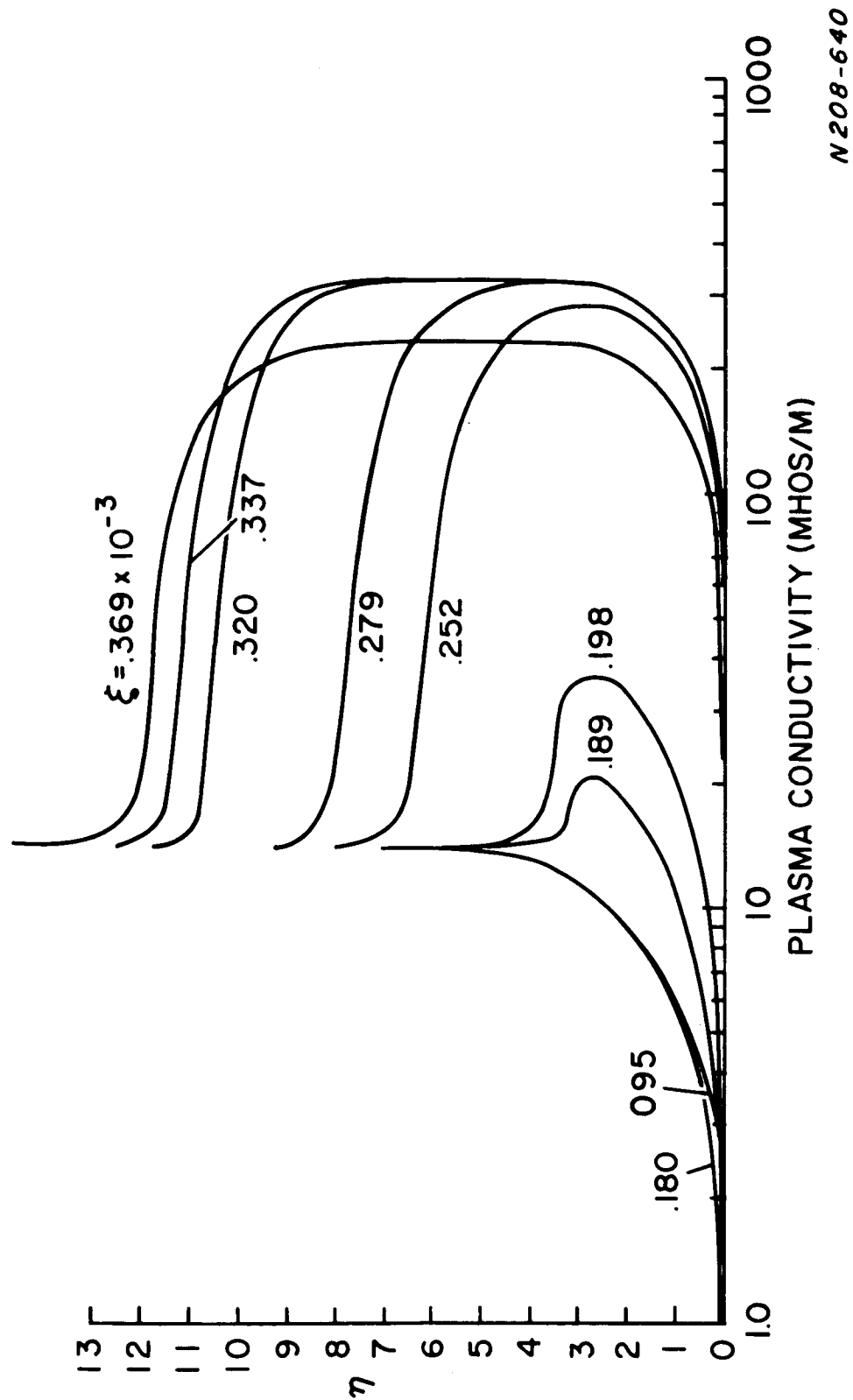


Figure 10. Electron conductivity profiles

ξ	$K \frac{\partial T}{\partial y}$	$K_e \frac{\partial T_e}{\partial y}$	$n_e \sqrt{\frac{kT_e}{m_s}} (eI)$	$q_{TOT.} \text{ (watts/cm}^2\text{)}$
0.95×10^{-3}	12.6	.041	.113	12.7
.180	9.16	.039	.015	9.21
.189	8.97	.070	.053	9.09
.198	8.75	.023	.115	8.88
.252	7.88	2.00	4.52	14.4
.280	7.91	2.28	5.29	15.5
.320	7.91	2.65	6.10	16.7
.333	7.85	2.32	5.37	15.5
.337	7.95	1.85	6.10	15.9
.370	7.75	.570	1.78	10.1

Table II. Component of Wall Heat Flux

Also, it may be of interest to note the boundary layer thickness in physical dimensions. Compared to an electrode width of ~ 1.4 cm we have a maximum boundary layer thickness of $\sim 10^{-1}$ cm.

From these results we can make a number of significant comments as to the quantitative effects of a magnetic field, thermionic emission, net current flow, and axial electric fields on the boundary layer. First, we see that introducing a magnetic field substantially lowers the electron temperature at the wall. This is caused by the lowering of K_e by the factor $(1 + \beta_e^2)$ which in turn has a profound effect on the electron temperature boundary condition such that θ'_w is much larger. In fact, the electron temperature is lowered enough so that the electron Debye length approaches the electron gyro radius at 10,000 gauss. For stronger magnetic fields it will be necessary to allow for magnetic effects in the sheath.

Next, we introduce thermionic emission before any net current is drawn. As shown in Figure 6 we see that the electron temperature at the wall rises rapidly over the initial portion of the electrode. Again this behaviour is caused by the modification of the electron temperature boundary condition. It is also interesting to note that an overshoot develops in the electron temperature in this region for the same reason.

As the level of net current passing through the boundary layer is increased (to a maximum equal to the emission assumed) we discover that the electron temperature at the wall no longer is increasing rapidly. This is again related to the boundary condition where $(i_w + j_{y\infty})$ appears and on a cathode they are of opposite sign.

As the electrode is traversed we see, from Figure 7, that the overshoot becomes substantial. Aside from the influence of the boundary condition this arises from the Joule heating due to the current. The related electron density, β_e , and plasma conductivity profiles are shown in Figures 8, 9, and 10.

At the end of the electrode the current and emission are reduced to zero rapidly and simultaneously with no significant effect on the profiles. Next, the axial electric field is introduced rapidly and sustained for some distance before falling slowly to a low value. Due to the energy input $(j_x E_x)$ associated with this field, the electron temperature profile becomes thicker although the peak electron temperature is somewhat reduced from its maximum value at the end of the electrode.

Finally, as E_x is reduced the boundary layer growth falls off. At the next electrode one would expect it to resume again. In any event, the electron temperature boundary layer thickness has grown to perhaps 4 times that of the velocity boundary layer.

As noted earlier, the electrons contribute to the heat flux somewhat in the electrode region. It should also be pointed out that, for the case studied here, the heavy particle temperature profile also develops a slight overshoot.

V. SUGGESTIONS FOR FURTHER WORK

The initial results we have obtained have been significant in that they demonstrate important effects in a quantitative way. They however apply only to a boundary layer starting from a sharp leading edge and extending past one cathode segment.

To extend the present calculations we should first examine more carefully the numerical difficulties found. The primary problem was a tendency for the electron temperature at the wall to oscillate with increasing ξ , thereby requiring a very small $\Delta\xi$ and some iteration. Such small $\Delta\xi$'s make extensive calculations very time consuming and expensive.

Additional calculations should be made over the anode wall as well as over the insulator wall normal to the applied magnetic field.

Any refinements of the sheath that can be fitted into the present framework should be made. Also, one should reexamine the assumptions relative to the $j_{y\infty}$ and $E_{x\infty}$ as obtained from the inviscid solution and how this solution would be revised by the boundary layer solution we have found.

A more extensive revision would involve reformulating the problem to allow for finite recombination and ionization rates.

References

1. Kerrebrock, J. L., "Electrode Boundary Layers in Direct Current Plasma Accelerators", J. Aerosp. Sci. 28, 631 (1961).
2. Hale, F. J. and Kerrebrock, J. L., "Insulator Boundary Layers in MHD Channels", AIAA J. 2, 461 (1964).
3. Oates, G. C., Richmond, J. K., Aoki, Y., and Grohs, G., "Loss Mechanisms of a Low Temperature Plasma Accelerator", Proceedings of the Fourth Biennial Gas Dynamics Symposium, Northwestern Univ. Press, Evanston, 1962.
4. Camac, M., and Kemp, N. H., "A Multi-temperature Boundary Layer", AVCO/Everett Research Laboratory Research Report 184, August 1964.
5. Dix, D. M., "Energy Transfer Processes in a Partially Ionized Two Temperature Gas", AIAA J., 2, 2081 (1964).
6. Hurwitz, H., Jr., Kilb, R. W., and Sutton, G. W., "Influence of Tensor Conductivity on Current Distribution in an MHD Generator", J. Appl. Phys., 32, 205 (1961).
7. Blottner, F. G., and Flügge-Lotz, I., "Finite Difference Computation of the Boundary Layer with Displacement Thickness Interaction". J. de Mecanique 2, 397 (1963).
8. Blottner, F. G., "Non-equilibrium Laminar Boundary Layer Flow of a Binary Gas", GE TIS R63SD17, June 1963.
9. Fay, J. A., "Hypersonic Heat Transfer in the Air Laminar Boundary Layer", AVCO/Everett Research Laboratory, AMP 71, March 1962.
10. Heighway, J. E., and Nichols, L. D., "Brayton Cycle MHD Power Generation with Non-Equilibrium Conductivity", NASA TN D-2651, Feb. 1965.
11. Sherman, A., "MHD Channel Flows with Non-equilibrium Ionization", Phys. Fl. 9, 1782 (1966).

APPENDIX A

Overall Energy Conservations for an Electrode Wall:

$$\rho u \frac{\partial h^*}{\partial x} + \rho v \frac{\partial h^*}{\partial y} = u \frac{\partial p}{\partial x} + \mu \left(\frac{\partial u}{\partial y} \right)^2 - \frac{\partial}{\partial y} (q_y) + j_x E_x + j_y (E_y - uB) \quad (A1)$$

The heat flux vector is assumed to be of the following form.

$$q = \sum_i q_i \text{ where } q_i = -K_i \nabla T_i + \rho_i h_i^* V_i$$

Now, let us express h^* more explicitly.

$$h^* = \frac{1}{\rho} \sum_i \rho_i h_i^* \quad h^* = \frac{5}{2} \frac{kT_i}{m_i} + \frac{I_i}{m_i}$$

so that

$$h^* = \frac{\rho_A}{\rho} \frac{5}{2} \frac{kT}{m_A} + \frac{\rho_s}{\rho} \frac{5}{2} \frac{kT}{m_s} + \frac{\rho_s^+}{\rho} \frac{5}{2} \frac{kT}{m_s} + \frac{\rho_e}{\rho} \frac{5}{2} \frac{kT_e}{m_e} + \frac{\rho_s^+}{\rho} \frac{I}{m_s}$$

or

$$h^* = h + \frac{n_e}{\rho} I$$

We can rewrite the heat flux vector for s as follows

$$q_i = -K_i \nabla T_i + m_i n_i h_i V_i + \frac{m_i n_i^2}{\rho} I_i V_i$$

so that

$$q = -\sum_i K_i \nabla T_i + m_e n_e \frac{5}{2} \frac{kT_e}{m_e} V_e = -\sum_i K_i \nabla T_i - \frac{5kT_e}{2e} j_e$$

Then, the overall energy equation becomes

$$\rho u \frac{\partial h}{\partial x} + \rho v \frac{\partial h}{\partial y} = u \frac{\partial p}{\partial x} + \mu \left(\frac{\partial u}{\partial y} \right)^2 + \frac{\partial}{\partial y} \left(\sum_i K_i \frac{\partial T}{\partial y} + \frac{5kT_e}{2e} j_{ey} \right)$$

$$+ j_x E_x + j_y (E_y - uB) - \rho u I \frac{\partial}{\partial x} \left(\frac{n_e}{\rho} \right) - \rho v I \frac{\partial}{\partial y} \left(\frac{n_e}{\rho} \right) \quad (A2)$$

Next, let us write

$$\rho u I \frac{\partial}{\partial x} \left(\frac{n_e}{\rho} \right) + \rho v I \frac{\partial}{\partial y} \left(\frac{n_e}{\rho} \right) = I \left[u \frac{\partial n_e}{\partial x} + v \frac{\partial n_e}{\partial y} - n_e \left(u \frac{\partial \rho}{\partial x} + v \frac{\partial \rho}{\partial y} \right) \right]$$

and the energy equation can be rewritten as

$$\rho u \frac{\partial h}{\partial x} + \rho v \frac{\partial h}{\partial y} = u \frac{\partial p}{\partial x} + \mu \left(\frac{\partial u}{\partial y} \right)^2 + \frac{\partial}{\partial y} \left(\sum_i K_i \frac{\partial T}{\partial y} + \frac{5kT_e}{2e} j_{ey} \right) + j_x E_x + j_y (E_y - uB) - I \left[u \frac{\partial n_e}{\partial x} + v \frac{\partial n_e}{\partial y} - n_e \left(u \frac{\partial \rho}{\partial x} + v \frac{\partial \rho}{\partial y} \right) \right] \quad (A3)$$

and the last two terms are equivalent to the \sum_{ions}

$\omega_i I_i$ term commonly included in the energy equation.

Next $\frac{\partial p}{\partial x}$ can be obtained from the momentum equation evaluated at the free stream. Then

$$\rho u \frac{\partial u}{\partial x} + \rho v \frac{\partial u}{\partial y} = -\frac{\partial p}{\partial x} + \frac{\partial}{\partial y} \left(\mu \frac{\partial u}{\partial y} \right) + j_y B_z$$

and at ∞

$$\rho_\infty u_\infty \frac{du_\infty}{dx} = -\frac{\partial p}{\partial x} + j_y B_z$$

$$\therefore \frac{\partial p}{\partial x} = j_y B_z - \rho_\infty u_\infty \frac{du_\infty}{dx}$$

and the energy equation becomes

$$\rho u \frac{\partial h}{\partial x} + \rho v \frac{\partial h}{\partial y} = -\rho_\infty u_\infty \frac{du_\infty}{dx} + \mu \left(\frac{\partial u}{\partial y} \right)^2 + \frac{\partial}{\partial y} \left(\sum_i K_i \frac{\partial T}{\partial y} + \frac{5kT_e}{2e} j_{ey} \right) + j_x E_x + j_y E_y - I \left[u \frac{\partial n_e}{\partial x} + v \frac{\partial n_e}{\partial y} - n_e \left(u \frac{\partial \rho}{\partial x} + v \frac{\partial \rho}{\partial y} \right) \right] \quad (A4)$$

Finally, we have to re-express the two last terms on the RHS in terms of T_e , T , u . Now, n_e can be obtained from the Saha relation.

$$\frac{n_e n_e}{n_s} = \left(\frac{2\pi m_e k T_e}{h^2} \right)^{3/2} \exp \left[-\frac{eI}{kT_e} \right] = S(T_e)$$

The ratio of the original number density of seed atoms as compared to the inert carrier will be specified. So

$$P \equiv \frac{n_e + n_s}{n_A}$$

Also, assuming each species is a P.G.

$$p = \sum p_i = k [n_A + n_s + n_e] T + k n_e T_e$$

$$\text{or } p \approx k n_A T$$

Now, we write from Saha

$$n_e^2 = S(T_e) n_s$$

But from the definition of P

$$n_s = P n_A - n_e$$

$$\therefore n_e^2 = S(T_e) \left[P \frac{p}{kT} - n_e \right]$$

$$\text{or } n_e^2 + S(T_e) n_e - \frac{P p S}{kT} = 0$$

$$\text{and } n_e = -\frac{S}{2} + \sqrt{\frac{S^2}{4} + \frac{P p S}{kT}}$$

$$\text{or } n_e = \frac{S}{2} \left\{ \sqrt{1 + \frac{4Pp}{kTS}} - 1 \right\} \quad \text{when } \frac{4Pp}{kTS} \geq 10^{-2}$$

when S is very large, corresponding to nearly full ionization, the above may prove very inaccurate for numerical calculation. For this case, we expand the $\sqrt{\quad}$ and use

$$n_e = \frac{pP}{kT} \left[1 - \frac{Pp}{kTS} \right] \quad \text{when } \frac{4Pp}{kTS} < 10^{-2}$$

If we wish, we can also write

$$S(T_e) = C_1 T_e^{3/2} e^{-C_2/T_e}$$

where

$$C_1 = \left(\frac{2\pi m_e k T_e}{h^2} \right)^{3/2}$$

$$C_2 = eI/k$$

Thus we can write out to begin with $\frac{\partial n_e}{\partial x}$ using

$$n_e = -\frac{S}{2} + \sqrt{\frac{S^2}{4} + \frac{PpS}{kT}}$$

and S(T_e) directly above.

Now

$$\frac{\partial n_e}{\partial x} = S_1 \frac{\partial T_e}{\partial x} - S_2 \frac{\partial h}{\partial x} + S_3 \frac{dp}{dx}$$

where

$$S_1 = S \left(\frac{3}{2T_e} + \frac{C_2}{T_e^2} \right) \left[-\frac{1}{2} + \frac{\frac{S}{2} + \frac{2Pp}{kT}}{S \sqrt{1 + \frac{4Pp}{kTS}}} \right]$$

$$S_2 = \frac{2Pp}{kC_p T^2 \sqrt{1 + \frac{4Pp}{kTS}}}$$

$$S_3 = \frac{2P}{kT \sqrt{1 + \frac{4Pp}{kTS}}}$$

Similarly

$$\frac{\partial n_e}{\partial y} = S_1 \frac{\partial T_e}{\partial y} - S_2 \frac{\partial h}{\partial y} \left(\frac{\partial p}{\partial y} = 0 \right)$$

Accordingly, neglecting argon ionization the overall energy equation becomes

$$\begin{aligned} \rho u \frac{\partial h}{\partial x} + \rho v \frac{\partial h}{\partial y} = & -\rho_\infty u_\infty \frac{du_\infty}{dx} \\ & + \mu \left(\frac{\partial u}{\partial y} \right)^2 + \left(\sum_i K_i \frac{\partial T}{\partial y} + \frac{5kT_e}{2e} j_{ey} \right) + j_x E_x \\ & + j_y E_y - I \left[u S_1 \frac{\partial T_e}{\partial x} - u S_2 \frac{\partial h}{\partial x} + u S_3 \frac{dp}{dx} \right. \\ & \left. + v S_1 \frac{\partial T_e}{\partial y} - v S_2 \frac{\partial h}{\partial y} - n_e \left(\frac{u}{\rho} \frac{\partial \rho}{\partial x} + \frac{v}{\rho} \frac{\partial \rho}{\partial y} \right) \right] \end{aligned} \quad (A5)$$

but the last two terms can be rewritten as follows: Assume the overall plasma density, pressure, et al, is that of a perfect gas (argon). Then

$$p = \rho RT = \rho \frac{R}{C_p} h \quad \therefore \quad \rho = \frac{C_p}{R} \frac{p}{h}$$

Then

$$\begin{aligned} \frac{1}{\rho} \frac{\partial \rho}{\partial x} = & -\frac{1}{\rho} \frac{C_p}{R} p \frac{1}{h} \frac{\partial h}{\partial x} + \frac{1}{\rho} \frac{C_p}{R} \frac{1}{h} \frac{dp}{dx} \\ = & -\frac{1}{h} \frac{\partial h}{\partial x} + \frac{1}{p} \frac{dp}{dx} \end{aligned}$$

$$\frac{u}{\rho} \frac{\partial \rho}{\partial x} + \frac{v}{\rho} \frac{\partial \rho}{\partial y} = -\frac{u}{h} \frac{\partial h}{\partial x} - \frac{v}{h} \frac{\partial h}{\partial y} + \frac{u}{p} \frac{dp}{dx}$$

The overall energy equation is then

$$\begin{aligned}
\rho u \frac{\partial h}{\partial x} + \rho v \frac{\partial h}{\partial y} = & - \rho_{\infty} u_{\infty} u \frac{du_{\infty}}{dx} + \mu \left(\frac{\partial u}{\partial y} \right)^2 \\
& + \frac{\partial}{\partial y} \left(\sum_i K_i \frac{\partial T}{\partial y} + \frac{5kT_e}{2e} j_{ey} \right) + j_x E_x + j_y E_y \\
& - I \left[u S_1 \frac{\partial T_e}{\partial x} - u S_2 \frac{\partial h}{\partial x} + u S_3 \frac{dp}{dx} \right. \\
& + v S_1 \frac{\partial T_e}{\partial y} - v S_2 \frac{\partial h}{\partial y} - n_e \left(\frac{u}{p} \frac{dp}{dx} \right. \\
& \left. \left. - \frac{u}{h} \frac{\partial h}{\partial x} - \frac{v}{h} \frac{\partial h}{\partial y} \right) \right] \quad (A6)
\end{aligned}$$

But we know $\frac{dp}{dx}$ to be $= j_y B_z - \rho_{\infty} u_{\infty} \frac{du_{\infty}}{dx}$. Then

we obtain Eq. (5).

APPENDIX B

Consider Eq. (4) specialized to an electrode wall. Then we have, as before

$$\frac{\partial n_e}{\partial x} = S_1 \frac{\partial T_e}{\partial x} - S_2 \frac{\partial h}{\partial x} + S_3 \frac{dp}{dx} \quad (B1)$$

$$\frac{\partial n_e}{\partial y} = S_1 \frac{\partial T_e}{\partial y} - S_2 \frac{\partial h}{\partial y} \quad (B2)$$

Also we have to reexpress $\frac{\partial u}{\partial x} + \frac{\partial v}{\partial y}$. Thus

$$\frac{\partial}{\partial x} (\rho u) + \frac{\partial}{\partial y} (\rho v) = 0 \quad (B3)$$

and

$$\rho \left(\frac{\partial u}{\partial x} + \frac{\partial v}{\partial y} \right) + u \frac{\partial \rho}{\partial x} + v \frac{\partial \rho}{\partial y} = 0 \quad (B4)$$

$$\frac{\partial u}{\partial x} + \frac{\partial v}{\partial y} = - \frac{u}{\rho} \frac{\partial \rho}{\partial x} - \frac{v}{\rho} \frac{\partial \rho}{\partial y} = \rho \left[u \frac{\partial \rho^{-1}}{\partial x} + v \frac{\partial \rho^{-1}}{\partial y} \right]$$

and we as well replace $\frac{dp}{dx}$ from before

$$\frac{dp}{dx} = j_y B_z - \rho_\infty u \frac{du}{dx} \quad (B5)$$

Making all of the above substitutions into Eq. (4) yields Eq. (6).

Appendix C

Eq. 's (9) and (10) can be written as

$$j_x = \frac{\sigma}{(1+\beta_{e_i}\beta_i)^2 + \beta_e^2} \left\{ (1+\beta_{e_i}\beta_i) E_{x_\infty} - \beta_e (E_y - uB_z) \right\}$$

$$j_{y_\infty} = \frac{\sigma}{(1+\beta_{e_i}\beta_i)^2 + \beta_e^2} \left\{ (1+\beta_{e_i}\beta_i) (E_y - uB_z) + \beta_e E_{x_\infty} \right\}$$

using the 2nd relation to replace $(E_y - uB_z)$ in 1st

we get

$$j_x = \frac{\sigma}{1+\beta_{e_i}\beta_i} \left\{ E_{x_\infty} - \frac{\beta_e}{\sigma} j_{y_\infty} \right\}$$

and

$$j_x E_{x_\infty} = \frac{\sigma}{1+\beta_{e_i}\beta_i} E_{x_\infty}^2 - \frac{\beta_e}{1+\beta_{e_i}\beta_i} j_{y_\infty} E_{x_\infty}$$

\downarrow
 $\rightarrow 0$

$$\begin{cases} j_{y_\infty} = 0 \text{ where } E_{x_\infty} \neq 0 \\ E_{x_\infty} = 0 \text{ where } j_{y_\infty} \neq 0 \end{cases}$$

So

$$j_x E_{x_\infty} = \frac{\sigma}{1+\beta_{e_i}\beta_i} E_{x_\infty}^2$$

Next, solve the 2nd of the above eq's. for E_y .

$$E_y = \frac{j_{y_\infty} \left[(1+\beta_{e_i}\beta_i)^2 + \beta_e^2 \right]}{\sigma (1+\beta_{e_i}\beta_i)} - \frac{\beta_e}{1+\beta_{e_i}\beta_i} E_{x_\infty} + uB_z$$

Then

$$j_y E_y = \frac{j_{y_\infty}^2}{\sigma} \left[\frac{(1+\beta_{e_i}\beta_i)^2 + \beta_e^2}{1+\beta_{e_i}\beta_i} \right] + uB_z j_{y_\infty}$$

Now, we need an expression for j_{e_x} and j_{e_y} . This we obtain from

$$\vec{j}_e = \vec{j} + \beta_i \frac{\vec{B} \times \vec{j}}{B_z}$$

Then

$$j_{e_x} = j_x - \frac{\beta_i}{B_z} B_z j_y = j_x - \beta_i j_y$$

$$j_{e_y} = j_y + \frac{\beta_i B_z}{B_z} j_x = j_y + \beta_i j_x$$

also as before

$$j_x = \frac{\sigma}{1+\beta_{e_i}\beta_i} \left[E_{x_\infty} - \frac{\beta_e}{\sigma} j_{y_\infty} \right]$$

So that

$$j_{e_y} = j_{y_\infty} \left[\frac{1}{1+\beta_{e_i}\beta_i} \right] + \left(\frac{\sigma \beta_i}{1+\beta_{e_i}\beta_i} \right) E_{x_\infty}$$

or

$$j_{e_y} = a_1 j_{y_\infty} + a_2 E_{x_\infty}$$

then

$$E_{x_\infty} j_{e_x} = E_{x_\infty} j_x - \beta_i j_{y_\infty} E_{x_\infty}$$

\downarrow
 $\rightarrow 0$

or

$$E_{x_\infty} j_{e_x} = \frac{\sigma}{1+\beta_{e_i}\beta_i} E_{x_\infty}^2$$

and

$$(E_y - uB) j_{e_y} = \frac{\left[(1+\beta_{e_i}\beta_i)^2 + \beta_e^2 \right]}{\sigma (1+\beta_{e_i}\beta_i)^2} j_{y_\infty}^2$$

$$- \frac{\beta_e}{(1+\beta_{e_i}\beta_i)^2} \cdot \sigma \beta_i E_{x_\infty}^2$$

then

$$j_{e_x} E_{x_\infty} + j_{e_y} (E_y - uB_z)$$

$$= \left[\frac{(1+\beta_{e_i}\beta_i)^2 + \beta_e^2}{(1+\beta_{e_i}\beta_i)^2} \right] \frac{j_{y_\infty}^2}{\sigma} + \frac{\sigma}{(1+\beta_{e_i}\beta_i)^2} E_{x_\infty}^2$$

APPENDIX D

Momentum eq.:

$$A_{11} f_{m+1, n+1} + B_{11} f'_{m+1, n} + B_{12} g_{m+1, n} + C_{11} f'_{m+1, n-1} = D_1$$

where

$$A_{11} = \frac{V \Delta \xi}{8 \xi f' \Delta \eta} - \frac{l \Delta \xi}{4 \xi f' (\Delta \eta)^2} - \frac{l' \Delta \xi}{8 \xi f'}$$

$$B_{11} = 1 + \frac{\Delta \xi}{2 u_{\infty}} \frac{du_{\infty}}{d\xi} + \frac{l \Delta \xi}{2 \xi f' (\Delta \eta)^2}$$

$$B_{12} = - \frac{\Delta \xi}{2 u_{\infty} f'} \frac{du_{\infty}}{d\xi}$$

$$C_{11} = - \frac{V \Delta \xi}{8 \xi f' \Delta \eta} - \frac{l \Delta \xi}{4 \xi f' (\Delta \eta)^2} + \frac{l' \Delta \xi}{8 \xi f' (\Delta \eta)}$$

$$D_1 = f'_{m, n} \left(1 - \frac{\Delta \xi}{2 u_{\infty}} \frac{du_{\infty}}{d\xi} \right) - \frac{V \Delta \xi}{4 \xi f'} f'_{\eta} + \frac{\Delta \xi}{2 u_{\infty} f} \frac{du_{\infty}}{d\xi} g_{m, n} \\ + \frac{l \Delta \xi}{4 \xi f'} f'_{\eta \eta} + \frac{l' (\Delta \xi)}{4 \xi f'} f'_{\eta}$$

Overall Energy Equation

$$A_{21} f'_{m+1,n+1} + A_{22} g_{m+1,n+1} + A_{23} \theta_{m+1,n+1} + B_{21} f'_{m+1,n} \\ + B_{22} g_{m+1,n} + B_{23} \theta_{m+1,n} + C_{21} f'_{m+1,n-1} + C_{22} g_{m+1,n-1} \\ + C_{23} \theta_{m+1,n-1} = D_2$$

where

$$A_{21} = \frac{-\Delta\xi}{2\xi f'} \frac{u_\infty^2}{C_p T_\infty} \frac{l f'_n}{2\Delta\eta}$$

$$A_{22} = \frac{\Delta\xi}{8\xi f' \Delta\eta} \left[V - \frac{2l}{P_R \Delta\eta} - \left(\frac{l}{P_R} \right)' + \frac{In_e V}{C_p T_\infty \rho_\infty} - \frac{IS_2 V}{\rho_\infty} g_{m,n} \right]$$

$$A_{23} = \frac{\Delta\xi}{8\xi f' \Delta\eta} \left[-\frac{2\lambda}{\Delta\eta} \frac{T_{e_\infty}}{T_\infty} - \lambda' \frac{T_{e_\infty}}{T_\infty} \right. \\ \left. + \frac{5 \sqrt{2\xi} k T_\infty}{2(\rho\mu)_r u_\infty C_p T_\infty e} \left(\alpha_1 j_{y_\infty} + \alpha_2 E_{x_\infty} \right) + \frac{IS_1 T_{e_\infty} V}{\rho_\infty C_p T_\infty} g_{m,n} \right]$$

$$B_{21} = 0$$

$$B_{22} = 1 - \frac{\Delta\xi}{2} \left\{ -\frac{u_\infty}{C_p T_\infty} \frac{du_\infty}{d\xi} (1-IS_3) - \frac{1}{T_\infty} \frac{dT_\infty}{d\xi} \right. \\ \left. + \frac{1}{f' C_p T_\infty (\rho\mu)_r \rho_\infty u_\infty^2} \left[\frac{\sigma E_{x_\infty}^2}{1+\beta_e \beta_i} + \frac{j_{y_\infty}^2}{\sigma} \frac{(1+\beta_e \beta_i)^2 + \beta_e^2}{1+\beta_e \beta_i} \right] \right. \\ \left. + \frac{B_z j_{y_\infty}}{(\rho\mu)_r C_p T_\infty \rho_\infty u_\infty} (1-IS_3) - \frac{In_e}{C_p T_\infty^2 \rho_\infty} \frac{dT_e}{d\xi} \right. \\ \left. + \frac{In_e j_{y_\infty} B_z}{p(\rho\mu)_2 \rho_\infty C_p T_\infty u_\infty} - \frac{I u_{\infty n e}}{p C_p T_\infty} \frac{du_\infty}{d\xi} \right\} + \frac{IS_1(\Delta\xi)}{\rho_\infty C_p T_\infty} \frac{dT_{e_\infty}}{d\xi} \theta_{m,n} \\ - \frac{IS_2}{\rho_\infty} g_{m,n} - \frac{(\Delta\xi) IS_2}{\rho_\infty T_\infty} \frac{dT_\infty}{d\xi} g_{m,n} + \frac{In_e}{C_p \rho_\infty T_\infty} + \frac{\Delta\xi}{2\xi f' (\Delta\eta)^2} \frac{l}{P_R}$$

$$\begin{aligned}
B_{23} &= \frac{\Delta \xi}{2 \xi f' (\Delta \eta)^2} \frac{T_{e\infty}}{T_{\infty}} \lambda - \frac{\Delta \xi}{4 \xi f'} \frac{5}{2} \frac{\sqrt{2 \xi} k T_{e\infty}}{(\rho \mu)_2^u C_p T_{\infty} e} (\alpha_1' j_{y_{\infty}} + \alpha_2' E_{x_{\infty}}) \\
&+ \frac{IS_1 T_{e\infty}}{C_p T_{\infty} \rho_{\infty}} g_{m,n} + \frac{IS_1 (\Delta \xi)}{\rho_{\infty} C_p T_{\infty}} \frac{dT_{e\infty}}{d\xi} g_{m,n} \\
C_{21} &= \frac{\Delta \xi}{4 \xi f' \Delta \eta} \frac{u_{\infty}^2}{C_p T_{\infty}} \ell f' \eta = -A_{21} \\
C_{22} &= \frac{\Delta \xi}{8 \xi f' \Delta \eta} \left[-V - \frac{2}{\Delta \eta} \left(\frac{\ell}{P_R} \right) + \left(\frac{\ell}{P_R} \right)' + \frac{IS_2 V}{\rho_{\infty}} g_{m,n} - \frac{In_e V}{C_p T_{\infty} \rho_{\infty}} \right] \\
C_{23} &= \frac{\Delta \xi}{8 \xi f' \Delta \eta} \left[-2 \frac{T_{e\infty}}{T_{\infty}} \frac{\lambda}{\Delta \eta} + \frac{T_{e\infty}}{T_{\infty}} \lambda' + \frac{5}{2} \frac{\sqrt{2 \xi} k T_{\infty}}{(\rho \mu)_r^u C_p T_{\infty} e} (\alpha_1 j_{y_{\infty}} + \alpha_2 E_{x_{\infty}}) \right. \\
&\quad \left. - \frac{IS_1 T_{e\infty} V}{\rho_{\infty} C_p T_{\infty}} g_{m,n} \right] \\
D_2 &= -\frac{\Delta \xi}{4 \xi f'} V g_{\eta} + \frac{1}{2} g_{m,n} \left[2 - \frac{(\Delta \xi) u_{\infty}}{C_p T_{\infty}} \frac{du_{\infty}}{d\xi} (1 - IS_3) - \frac{(\Delta \xi)}{T_{\infty}} \frac{dT_{\infty}}{d\xi} \right. \\
&\quad \left. + \frac{\Delta \xi}{f' C_p T_{\infty} (\rho \mu)_r \rho_{\infty} u_{\infty}^2} \left(\frac{\sigma E_{x_{\infty}}^2}{1 + \beta_e \beta_i} + \frac{j_{y_{\infty}}^2}{\sigma} \frac{(1 + \beta_e \beta_i)^2 + \beta_e^2}{1 + \beta_e \beta_i} \right) \right. \\
&\quad \left. + \frac{(\Delta \xi) B_z j_{y_{\infty}}}{(\rho \mu)_r C_p T_{\infty} \rho_{\infty} u_{\infty}} (1 - IS_3) - \frac{In_e (\Delta \xi)}{C_p T_{\infty}^2 \rho_{\infty}} \frac{dT_{\infty}}{d\xi} + \frac{In_e (\Delta \xi) j_{y_{\infty}} B_z}{p (\rho \mu)_r \rho_{\infty} C_p T_{\infty} u_{\infty}} \right. \\
&\quad \left. - \frac{I u_{\infty} n_e (\Delta \xi)}{p C_p T_{\infty}} \frac{du_{\infty}}{d\xi} \right] + \frac{\Delta \xi}{4 \xi f'} \left[\frac{\ell}{P_R} g_{\eta \eta} + \left(\frac{\ell}{P_R} \right)' g_{\eta} \right. \\
&\quad \left. + \frac{T_{e\infty}}{T_{\infty}} \lambda \theta_{\eta \eta} + \frac{T_{e\infty}}{T_{\infty}} \lambda' \theta_{\eta} + \frac{5}{2} \frac{\sqrt{2 \xi} k T_{\infty}}{(\rho \mu)_r^u C_p T_{\infty} e} (\alpha_1 j_{y_{\infty}} + \alpha_2 E_{x_{\infty}}) \theta_{\eta} \right]
\end{aligned}$$

$$\begin{aligned}
& + \frac{5}{2} \frac{\sqrt{2\xi} k T_{e\infty}}{(\rho\mu)_r u_\infty C_p T_\infty e} \left(\alpha'_1 j_{y_\infty} + \alpha'_2 E_{x_\infty} \right) \theta_{m,n} - \frac{IS_1 T_{e\infty} V}{\rho_\infty C_p T_\infty} g_{m,n} \theta_\eta \\
& + \left[\frac{IS_2 V}{\rho_\infty} g_{m,n} g_\eta - \frac{I n_e V}{C_p T_\infty \rho_\infty} g_\eta \right] \\
& + \frac{IS_1 T_{e\infty}}{C_p T_\infty \rho_\infty} g_{m,n} \theta_{m,n} - \frac{IS_2}{\rho_\infty} g_{m,n}^2 + \frac{I n_e}{C_p T_\infty \rho_\infty} g_{m,n}
\end{aligned}$$

Electron Energy Equation

$$\begin{aligned}
& A_{31} f'_{m+1,n+1} + A_{32} g_{m+1,n+1} + A_{33} \theta_{m+1,n+1} + B_{31} f'_{m+1,n} \\
& + B_{32} g_{m+1,n} + B_{33} \theta_{m+1,n} + C_{31} f'_{m+1,n-1} + C_{32} g_{m+1,n-1} \\
& + C_{33} \theta_{m+1,n-1} = D_3
\end{aligned}$$

where

$$A_{31} = 0$$

$$A_{32} = \left[-\frac{n_e \left(\frac{5}{2} k T_{e\infty} \theta + I \right)}{g} - \left(\frac{3}{2} k T_{e\infty} \theta + I \right) S_2 C_p T_\infty \right] \frac{(\rho\mu)_r u_\infty^2 V}{8\xi (\Delta\eta)}$$

$$A_{33} = \left[\frac{3}{2} k n_e + \left(\frac{3}{2} k T_{e\infty} \theta + I \right) S_1 \right] \frac{(\rho\mu)_r T_{e\infty} u_\infty^2 V}{8\xi \Delta\eta}$$

$$- \frac{(\rho\mu)_r C_p \rho_\infty u_\infty^2 T_{e\infty} \lambda}{4\xi g (\Delta\eta)^2} - \frac{(\rho\mu)_r C_p \rho_\infty u_\infty^2 T_{e\infty} \lambda'}{8\xi g \Delta\eta}$$

$$- \frac{5k\rho_\infty u_\infty T_{e\infty}}{8eg \sqrt{2\xi} \Delta\eta} \left(\alpha_1 j_{y_\infty} + \alpha_2 E_{x_\infty} \right)$$

$$B_{31} = \left[\frac{3}{2} k n_e + \left(\frac{3}{2} k T_{e\infty} \theta + I \right) S_1 \right] \frac{(\rho\mu)_r u_\infty^2}{2} \frac{dT_{e\infty}}{d\xi} \theta_{m,n}$$

$$- n_e \left(\frac{5}{2} k T_{e\infty} \theta + I \right) \frac{(\rho\mu)_r u_\infty^2}{2} \frac{1}{\rho_\infty} \frac{d\rho_\infty}{d\xi}$$

$$\begin{aligned}
& - S_2 \left(\frac{3}{2} k T_{e_\infty} \theta + I \right) \frac{(\rho\mu)_r u_\infty^2}{2} C_p \frac{dT_\infty}{d\xi} g_{m,n} \\
& - \frac{3}{4} k T_{e_\infty} S_3 (\rho\mu)_r \rho_\infty u_\infty^3 \frac{du_\infty}{d\xi} \theta_{m,n} - \frac{IS_3}{2} (\rho\mu)_r \rho_\infty u_\infty^3 \frac{du_\infty}{d\xi} \\
& + \frac{3}{4} k T_{e_\infty} S_3 u_\infty j_{y_\infty} B_z \theta_{m,n} + \frac{IS_3 u_\infty}{2} j_{y_\infty} B_z \\
B_{32} = & \left[\frac{n_e \left(\frac{5}{2} k T_{e_\infty} \theta + I \right)}{g} - \left(\frac{3}{2} k T_{e_\infty} \theta + I \right) S_2 C_p T_\infty \right] (\rho\mu)_r u_\infty^2 \frac{f'_{m,n}}{\Delta \xi} \\
& - S_2 \left(\frac{3}{2} k T_{e_\infty} \theta + I \right) \frac{(\rho\mu)_r u_\infty^2}{2} C_p \frac{dT_\infty}{d\xi} f'_{m,n} \\
& - \frac{3}{2} m_e n_e k T_\infty \sum_s \frac{\nu_{es}}{m_s} \\
B_{33} = & \left[\frac{3}{2} k n_e + \left(\frac{3}{2} k T_{e_\infty} \theta + I \right) S_1 \right] \frac{(\rho\mu)_r T_{e_\infty} u_\infty^2 f'}{\Delta \xi} \\
& + \left[\frac{3}{2} k n_e + \left(\frac{3}{2} k T_{e_\infty} \theta + I \right) S_1 \right] \frac{(\rho\mu)_r u_\infty^2}{2} \frac{dT_{e_\infty}}{d\xi} f'_{m,n} \\
& - \frac{3}{4} k T_{e_\infty} S_3 (\rho\mu)_r \rho_\infty u_\infty^3 \frac{du_\infty}{d\xi} f'_{m,n} \\
& + \frac{(\rho\mu)_r C_p \rho_\infty u_\infty^2 T_{e_\infty} \lambda}{2\xi g (\Delta\eta)^2} - \frac{\rho_\infty u_\infty T_{e_\infty}}{\sqrt{2\xi} g} \frac{5k}{4e} \left(\alpha_1' j_{y_\infty} + \alpha_2' E_{x_\infty} \right) \\
& + \frac{3}{2} m_e n_e k T_{e_\infty} \sum_s \frac{\nu_{es}}{m_s} + \frac{3}{4} k T_{e_\infty} S_3 u_\infty B_z f'_{m,n}
\end{aligned}$$

$$C_{31} = 0$$

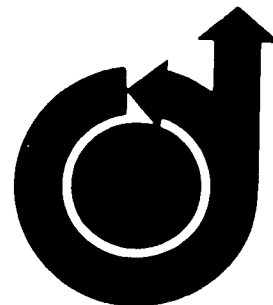
$$C_{32} = - \left[\frac{n_e \left(\frac{5}{2} k T_{e_\infty} \theta + I \right)}{g} - \left(\frac{3}{2} k T_{e_\infty} \theta + I \right) S_2 C_p T_\infty \right] \frac{(\rho\mu)_r u_\infty^2 v}{8\xi \Delta\eta}$$

$$\begin{aligned}
C_{33} = & - \left[\frac{3}{2} k n_e + \left(\frac{3}{2} k T_{e\infty} \theta + I \right) S_1 \right] \frac{(\rho\mu)_r T_{e\infty} u_\infty^2 v}{8\xi(\Delta\eta)} \\
& - \frac{(\rho\mu)_r C_p \rho_\infty u_\infty^2 T_{e\infty} \lambda}{4\xi g (\Delta\eta)^2} + \frac{(\rho\mu)_r C_p \rho_\infty u_\infty^2 T_{e\infty} \lambda'}{8\xi g (\Delta\eta)} \\
& + \frac{\rho_\infty u_\infty T_{e\infty}}{2\sqrt{2\xi} g(\Delta\eta)} \frac{5k}{4e} \left(\alpha_1 j_{y_\infty} + \alpha_2 E_{x_\infty} \right) \\
D_3 = & \left[\frac{3}{2} k n_e + \left(\frac{3}{2} k T_{e\infty} \theta + I \right) S_1 \right] \frac{(\rho\mu)_r T_{e\infty} u_\infty^2 f'}{\Delta\xi} \theta_{m,n} \\
& - \left[\frac{3}{2} k n_e + \left(\frac{3}{2} k T_{e\infty} \theta + I \right) S_1 \right] \frac{(\rho\mu)_r T_{e\infty} u_\infty^2 v}{4\xi} \theta_\eta \\
& + \left[n_e \frac{\left(\frac{5}{2} k T_{e\infty} \theta + I \right)}{g} - \left(\frac{3}{2} k T_{e\infty} \theta + I \right) S_2 C_p T_\infty \right] (\rho\mu)_r u_\infty^2 \frac{f'_{m,n}}{\Delta\xi} g_{m,n} \\
& - \left[n_e \frac{\left(\frac{5}{2} k T_{e\infty} \theta + I \right)}{g} - \left(\frac{3}{2} k T_{e\infty} \theta + I \right) S_2 C_p T_\infty \right] \frac{(\rho\mu)_r u_\infty^2 v}{4\xi} g_\eta \\
& + n_e \left(\frac{5}{2} k T_{e\infty} \theta + I \right) (\rho\mu)_r u_\infty^2 \frac{1}{\rho_\infty} \frac{d\rho_\infty}{d\xi} \frac{f'_{m,n}}{2} \\
& + \frac{IS_3}{2} (\rho\mu)_r \rho_\infty u_\infty^3 \frac{du_\infty}{d\xi} f'_{m,n} + \frac{(\rho\mu)_r C_p \rho_\infty u_\infty^2 T_{e\infty} \lambda}{4\xi g} \theta_{\eta\eta} \\
& + \frac{(\rho\mu)_r C_p \rho_\infty u_\infty^2 T_{e\infty} \lambda'}{4\xi g} \theta_\eta + \frac{\rho_\infty u_\infty T_{e\infty}}{\sqrt{2\xi} g} \frac{5k}{4e} \left(\alpha_1 j_{y_\infty} + \alpha_2 E_{x_\infty} \right) \theta_\eta
\end{aligned}$$

$$\begin{aligned}
& + \frac{\rho_{\infty} u_{\infty} T_{e_{\infty}}}{\sqrt{2\xi} g} \frac{5k}{4e} \left(\alpha_1' j_{y_{\infty}} + \alpha_2' E_{x_{\infty}} \right) \theta_{m,n} + \frac{\sigma}{(1+\beta_e \beta_i)^2} E_{x_{\infty}}^2 \\
& + \frac{j_{y_{\infty}}^2}{\sigma} \frac{[(1+\beta_e \beta_i)^2 + \beta_e^2]}{(1+\beta_e \beta_i)^2} + \frac{3}{2} m_e n_e k T_{\infty} \frac{\Sigma}{s} \frac{\nu_{es}}{m_s} g_{m,n} \\
& - \frac{3}{2} m_e n_e k T_{e_{\infty}} \frac{\hat{\Sigma}}{s} \frac{\nu_{es}}{m_s} \theta_{m,n} - IS_3 \frac{u_{\infty} j_{y_{\infty}}}{2} B_z f'_{m,n}
\end{aligned}$$

No. 68-134

APPENDIX E



THE NONEQUILIBRIUM BOUNDARY LAYER ALONG A CHANNEL WALL

by

ARTHUR SHERMAN

General Electric Space Sciences Laboratory
Valley Forge, Pennsylvania

and

ELI RESHOTKO

Case Western Reserve University
Cleveland, Ohio

AIAA Paper

No. 68-134

**AIAA 6th Aerospace Sciences
Meeting**

NEW YORK, NEW YORK / JANUARY 22-24, 1968

First publication rights reserved by American Institute of Aeronautics and Astronautics, 1290 Avenue of the Americas, New York, N. Y. 10019.
Abstracts may be published without permission if credit is given to author and to AIAA. Price—AIAA Member \$1.00, Nonmember \$1.50.

THE NONEQUILIBRIUM BOUNDARY LAYER ALONG A CHANNEL WALL

Arthur Sherman
Consultant - Space Power and Propulsion
General Electric Space Sciences Laboratory
Valley Forge, Pennsylvania

and

Eli Reshotko*
Professor of Engineering
Case Western Reserve University
Cleveland, Ohio

Abstract

The present paper studies the boundary layer in a plasma in which the electron and heavy particle temperatures can be different. The formulation is from the point of view of multifluid magnetohydrodynamics but differs from earlier treatments in that the complete electron energy equation is retained. This requires a boundary condition on electron temperature at the wall, which is obtained by considering the sheath. A steady, laminar, two-dimensional boundary layer is assumed in which the electron density can be predicted by the Saha equation evaluated at the local electron temperature. The equations for flow velocity, gas, and electron temperature are reduced to ordinary differential equations by assuming local similarity and are integrated simultaneously. Solutions obtained along an insulator wall show electron temperature distributions that differ significantly from the overall gas temperature even when the free stream is in equilibrium.

I. Introduction

Several attempts have been made to analyze the magnetohydrodynamic boundary layer occurring in the internal flow of a compressible plasma, in order to determine skin friction, heat transfer, and potential differences between wall and external stream for both electrode and insulator surfaces. The first such attempt was by Kerrebrock^{1,2}. He considered the equilibrium electrode boundary layer in a magnetohydrodynamic accelerator having constant external static temperature and cooled electrodes. He argued that in the immediate vicinity of the electrode the conductivity would be low because of the cooling. This would lead to considerable Joule heating of the gas near the wall resulting in large temperature gradients and high heat transfer rates. Kerrebrock's calculations bore out these expectations. It was felt that these

results were not realistic because the electrons would not be in equilibrium with the heavy species. Accordingly, Oates³ made a rough estimate of boundary layer behavior considering the electrons to be at an elevated temperature. He found that the increased conductivity near the wall over that found on the basis of equilibrium theory greatly reduced the Joule heating. He found that transport of enthalpy to the walls by electrons was enhanced because of the increased electron temperature. He further pointed out that when the electron transport of enthalpy is significant, there is a considerably larger heat flux to the anode than to the cathode. In Oates' analysis, the electron temperature was determined on the basis of a simple energy balance rather than the complete electron energy equation, and as a result no "sheath" analysis was carried out.

In the above described analyses the Hall effect, ion slip, and electron pressure gradient effects, were neglected in the Ohm's Law. Finally, the solutions were obtained by the approximate method of local similarity, and did not allow for such things as finite segmentation of the electrodes.

For the insulator boundary layer an analysis has been carried out by Hale² who also used the assumption of local similarity, but did include the Hall effect. Hale, however, considered the nonequilibrium effect by assuming a conductivity relationship $\sigma = \sigma(j)$ rather than by accounting for the behavior of electron temperature. This again obviated the need for an examination of the "sheath". Nonetheless, this study did demonstrate the possibility of enhanced heat flux due to nonequilibrium ionization, as well as temperature and velocity overshoots.

The present study has as its objective a more refined treatment of the nonequilibrium boundary layer development through the use of multifluid magnetohydrodynamics. A set of conservation equations is written for each constituent of the working fluid. These equations are in turn reduced and combined to achieve a usable set of equations for a two temperature plasma - one where the

*Consultant to General Electric Company Space Sciences Laboratory

electrons may be at a temperature that is significantly different from that of the heavy particles. The formulation is somewhat like those of the two temperature treatments of Camac and Kemp⁴ and Dix⁵ except that their problems were generally nonflowing and noncurrent carrying, whereas Joule heating and Lorentz forces are essential features of generators and accelerators.

In its more general form the present formulation is applicable to both electrode and insulator walls of both accelerators and generators. The present paper is more specifically concerned with nonequilibrium boundary layer development on the channel walls that contain the electrode segments. These walls are made up of an electric insulator upstream of the first electrode segment and have insulator segments between subsequent electrode segments. The calculations presented and discussed in the present paper are for the insulator upstream of the first electrode segment and ahead of the region of the applied magnetic field. These provide initial boundary layer profiles for a later study of boundary layer development over the finite electrode and insulator segments. However it is readily evident that these results apply to the non-equilibrium boundary layer development over any electrically insulated surface in the absence of magnetic field.

II. Analysis

The formulation of our problem will be for a two temperature plasma under the following simplifying assumptions:

1. Steady flow $\frac{\partial}{\partial t} = 0$
2. Laminar flow
3. No induced magnetic fields $R_m \approx 0$
4. Plasma consists only of electrons, atoms (carrier and seed), and singly ionized seed ions
5. Plasma composition determined by Saha equation evaluated at the electron temperature
6. No continuum radiation losses
7. Collision free plasma sheath
8. Only thermionic emission
9. Neglect pressure differences normal to wall.

The geometry of the wall along which the boundary layer will develop is shown in Figure 1.

The basic equations are developed below in boundary layer form.

Mass Conservation:

$$\frac{\partial}{\partial x} (\rho u) + \frac{\partial}{\partial y} (\rho v) = 0 \quad (1)$$

Momentum Conservation:

$$\rho u \frac{\partial u}{\partial x} + \rho v \frac{\partial u}{\partial y}$$

$$= -\frac{\partial p}{\partial x} + \frac{\partial}{\partial y} \left(\mu \frac{\partial u}{\partial y} \right) + j_y B_z \quad (2)$$

Overall Energy Conservation:

$$\begin{aligned} \rho u \frac{\partial h}{\partial x} + \rho v \frac{\partial h}{\partial y} = & -\rho_\infty u_\infty \frac{du_\infty}{dx} u + \mu \left(\frac{\partial u}{\partial y} \right)^2 \\ & + \frac{\partial}{\partial y} \left(\sum_i K_i \frac{\partial T}{\partial y} + \frac{5kT_e}{2e} j_{ey} \right) \\ & + j_x E_x + j_y E_y - I \left[u S_1 \frac{\partial T_e}{\partial x} - u S_2 \frac{\partial h}{\partial x} \right. \\ & + u S_3 j_y B_z - u S_3 \rho_\infty u_\infty \frac{du_\infty}{dx} + v S_1 \frac{\partial T_e}{\partial y} \\ & - v S_2 \frac{\partial h}{\partial y} - n_e \left(\frac{u}{p} j_y B_z - \frac{u}{p} \rho_\infty u_\infty \frac{du_\infty}{dx} \right. \\ & \left. \left. - \frac{u}{h} \frac{\partial h}{\partial x} - \frac{v}{h} \frac{\partial h}{\partial y} \right) \right] \end{aligned} \quad (3)$$

The details of the development of the above equation are presented in Appendix A, where the Saha relation has been used at the electron temperature to calculate the electron density.

Electron Energy Conservation:

$$\begin{aligned} \frac{3}{2} k n_e \frac{\partial T_e}{\partial x} + \frac{3}{2} k v n_e \frac{\partial T_e}{\partial y} \\ + \left(\frac{3}{2} k T_e + I \right) u \left\{ S_1 \frac{\partial T_e}{\partial x} - S_2 \frac{\partial h}{\partial x} \right. \\ \left. + S_3 \left(j_{y_\infty} B_z - \rho_\infty u_\infty \frac{du_\infty}{dx} \right) \right\} \\ + \left(\frac{3}{2} k T_e + I \right) v \left\{ S_1 \frac{\partial T_e}{\partial y} - S_2 \frac{\partial h}{\partial y} \right\} \\ + n_e \left[\frac{5}{2} k T_e + I \right] \left\{ \rho u \frac{\partial \rho^{-1}}{\partial x} + \rho v \frac{\partial \rho^{-1}}{\partial y} \right\} \\ - \frac{\partial}{\partial y} \left(K_e \frac{\partial T_e}{\partial y} + \frac{5}{2} \frac{k}{e} T_e j_{ey} \right) \\ = E_x j_{ex} + \left(E_y - u B_z \right) j_{ey} \\ + 3 \rho_e k \left(T - T_e \right) \sum_s \frac{\nu_{es}}{m_s} \end{aligned} \quad (4)$$

The details of the development of Eq. (4) are given in Appendix B.

To complete the formulation of our problem, we must conserve current and satisfy Maxwell's equations. Thus,

Current Conservation:

$$\nabla \cdot \mathbf{j} = 0 \quad (5)$$

Electric Field Relation:

$$\nabla \times \mathbf{E} = 0 \quad (6)$$

Finally, the individual species momentum is conserved by satisfying a generalized Ohm's law.

Generalized Ohm's Law:

$$\mathbf{J}_x = \frac{\sigma}{(1+\beta_e \beta_i)^2 + \beta_e^2} \times \quad (7)$$

$$[(1+\beta_e \beta_i) E_x - \beta_e (E_y - u B_z)]$$

$$\mathbf{J}_y = \frac{\sigma}{(1+\beta_e \beta_i)^2 + \beta_e^2} \times \quad (8)$$

$$[(1+\beta_e \beta_i) (E_y - u B_z) + \beta_e E_x]$$

where the electron inertia and electron pressure gradients have been neglected.

Next, we observe that if we try to satisfy (Eq's. (5) and (6) explicitly we have for the two-dimensional problem the following relations:

$$\frac{\partial j_x}{\partial x} + \frac{\partial j_y}{\partial y} = 0 \quad (5a)$$

and

$$\frac{\partial E_x}{\partial y} = \frac{\partial E_y}{\partial x} \quad (6a)$$

along with Eq's. (7) and (8). Now, even if we assumed the flow field, gas conditions, and electron temperature known, the above four equations lead to a nonlinear "elliptic" partial differential equation for the current stream function. If this equation must then be solved as part of the system, one cannot solve a boundary layer problem which is "parabolic" in character. Furthermore, the effects of finite electrical resistivity of the plasma are such that the significant variations in current density and electric field are not restricted to a narrow layer in the neighborhood of the wall.

Accordingly, since we still wish to treat a boundary layer type of problem we must abandon hope of satisfying (5) and (6) exactly and look for a procedure whereby they can be satisfied approximately. Such a procedure is available if we assume that the boundary layer thickness is small compared to the electrode or insulator segment lengths on the electrode wall.

In the analysis of the inviscid problem⁶, one obtains $j_y(x)$ along the electrode and $E_x(x)$ along the insulator. The boundary layer problem can then be handled by making the following assumptions:

1. Over an electrode segment $j_y = j_{y_e}(x)$, $E_x = 0$ for all y 's.

2. Over an insulator segment $j_y = 0$, $E_x = E_{x_o}(x)$ for all y 's.

With these assumptions Eq's. (5a) and (6a) are satisfied approximately and one must then only satisfy the Ohm's law at every point within the boundary layer.

Working with Eq's. (7) and (8) we can obtain expressions for $j_x E_x$, $j_y E_y$, $j_e x$, and $j_e y$ as is shown in Appendix C. Substituting these into Eq's. (3) and (4) yield the following results.

Overall Energy Conservation:

$$\begin{aligned} \rho u \frac{\partial h}{\partial x} + \rho v \frac{\partial h}{\partial y} = & - \left(\rho_x u_x \frac{du_x}{dx} \right) u + \mu \left(\frac{\partial u}{\partial y} \right)^2 \\ & + \frac{\partial}{\partial y} \left[\sum_i K_i \frac{\partial T}{\partial y} + \frac{5kT_e}{2e} \left(\alpha_1 j_{y_e} + \alpha_2 E_{x_e} \right) \right] \\ & + \frac{\sigma}{1+\beta_e \beta_i} E_{x_e}^2 + \frac{j_{y_e}^2}{\sigma} \left[\frac{(1+\beta_e \beta_i)^2 + \beta_e^2}{1+\beta_e \beta_i} \right] \\ & + u B_z j_{y_e} - I \left[u S_1 \frac{\partial T_e}{\partial x} - u S_2 \frac{\partial h}{\partial x} \right. \\ & + u S_3 j_{y_e} B_z - u S_3 \rho_x u_x \frac{du_x}{dx} + v S_1 \frac{\partial T_e}{\partial y} \\ & - v S_2 \frac{\partial h}{\partial y} - n_e \left(\frac{u}{p} j_{y_e} B_z - \frac{u}{p} \rho_x u_x \frac{du_x}{dx} \right. \\ & \left. \left. - \frac{u}{h} \frac{\partial h}{\partial x} - \frac{v}{h} \frac{\partial h}{\partial y} \right) \right] \quad (9) \end{aligned}$$

Electron Energy Conservation:

$$\begin{aligned} \frac{3}{2} k n_e \frac{\partial T_e}{\partial x} + \frac{3}{2} k v n_e \frac{\partial T_e}{\partial y} + \left(\frac{3}{2} k T_e + I \right) x \\ u \left\{ S_1 \frac{\partial T_e}{\partial x} - S_2 \frac{\partial h}{\partial x} + S_3 j_{y_e} B_z - S_3 \rho_x u_x \frac{du_x}{dx} \right\} \\ + \left(\frac{3}{2} k T_e + I \right) v \left\{ S_1 \frac{\partial T_e}{\partial y} - S_2 \frac{\partial h}{\partial y} \right\} \\ + n_e \left[\frac{5}{2} k T_e + I \right] \left\{ \rho u \frac{\partial \rho^{-1}}{\partial x} + \rho v \frac{\partial \rho^{-1}}{\partial y} \right\} \\ - \frac{\partial}{\partial y} \left[K_e \frac{\partial T_e}{\partial y} + \frac{5}{2} \frac{k}{e} T_e \left(\alpha_1 j_{y_e} + \alpha_2 E_{x_e} \right) \right] \\ = \left[\frac{(1+\beta_e \beta_i)^2 + \beta_e^2}{(1+\beta_e \beta_i)^2} \right] \frac{j_{y_e}^2}{\sigma} \end{aligned}$$

$$+ \frac{\sigma}{(1+\beta_e \beta_i)^2} E_{x_\infty}^2$$

$$+ 3m_e n_e k (T - T_e) \sum_s \frac{\nu_e^s}{m_s}$$

Boundary Conditions:

To complete the formulation, we must specify boundary conditions. At the outer edge of the boundary layer we have from the results of channel flow calculations

$$\begin{aligned} u(\infty) &= u_\infty(x) \\ p(\infty) &= p_\infty(x) \\ T(\infty) &= T_\infty(x) \\ T_e(\infty) &= T_{e_\infty}(x) \end{aligned}$$

Along the wall we have

$$\begin{aligned} u(0) &= v(0) = 0 \\ T(0) &= T_w(x) \quad \text{or} \quad q(0) = q_w(x) \end{aligned}$$

To establish the inner boundary condition on the electron temperature T_e , we must consider the nature of the plasma sheath. The sheath will be considered collision-free and free of magnetic effects. The validity of such a treatment depends on the Debye length being much smaller than both the electron cyclotron radius and the electron mean free path. Such conditions obtain in the external channel flow but it is not clear that the desired length ordering is appropriate at the wall. In fact, it can be shown that if in the external stream the electron gyro radius is say ten times the Debye length, then just a 25% reduction in electron temperature will equalize the two lengths. Such a reduction may well occur in the boundary layer. Nevertheless, let us now consider the ideal sheath.

Consider the surface at $y = 0$ (Fig. 2). The net current density in the positive y direction is that due to electron arrival at the wall minus the sum of the current densities due to ion arrival at the wall and electron emission from the wall⁴. For the present problem where the only ions present are seed ions, the net current density normal to the wall can be expressed as

$$(j_y)_w = \frac{n_e e \langle V_e \rangle}{4} e^{-\frac{e \Delta \phi}{k T_{ew}}} - n_i e V_i - i_w \quad (11)$$

where n_e , n_i refer to the number densities at the edge of the sheath ($n_e = n_i$ for singly ionized ions), where

$$\langle V_e \rangle = \sqrt{\frac{8 k T_{ew}}{\pi m_e}}$$

$$V_i = \sqrt{\frac{k T_{ew}}{m_i}}$$

T_{ew} being the electron temperature at the sheath edge, and where the emission current density i_w is dependent on the surface temperature and work function of the surface. This gives one relation between the electron temperature at the sheath edge T_{ew} and the sheath drop, $\Delta \phi$.*

A second relation is obtained from continuity of electron energy flux at the sheath interface between continuum and molecular descriptions⁴. Thus,

$$\begin{aligned} K_e \left(\frac{\partial T_e}{\partial y} \right)_w + \frac{5}{2} \frac{j_e}{e} k T_{ew} &= (2 K T_{ew})_{ew} \\ &+ e |\Delta \phi| \frac{n_e \langle V_e \rangle}{4} e^{-\frac{e \Delta \phi}{k T_{ew}}} - i_w \frac{\bar{\epsilon}}{e} \quad (12) \end{aligned}$$

where $\bar{\epsilon}$ is the average energy of a thermionically emitted electron as it crosses the sheath interface. Between the two relations (11) and (12) we have the sheath drop $\Delta \phi$ and the mixed inner boundary condition on T_e .

Coordinate Transformation:

The boundary layer equations so far presented are a set of nonlinear partial differential equations dependent on two space variables. It has been common at this point to seek a similarity transformation that would reduce the dependence to just one independent variable. Such a transformation has in fact been carried out. While complete similarity is not attainable, by suitable approximations a form of local similarity (the longitudinal distance appears as a parameter but not in differentiations) can be obtained. While clearly inadequate for the regions of finite segmentation, the local similarity procedure allows solution of the boundary layer equations from a stagnation point or from a leading edge up to the region of segmentation. The solution may then be continued by a finite difference procedure in the plane of the transformed variables with the longitudinal step size determined by electrode length and spacing.

The new independent variables are those of the Levy-Lees transformation.

$$F(x) = \int_0^x (\rho \mu)_r u_\infty dx$$

$$\eta(x, y) = \frac{u_\infty}{\sqrt{2 \xi}} \int_0^y \rho dy$$

*The anode sheath drop is slightly less than the difference between plasma and floating potentials while the cathode sheath drop exceeds the aforementioned potential difference.

so that

$$\frac{\partial}{\partial x} = (\rho\mu)_r u_\infty \frac{\partial}{\partial \xi} + \eta_x \frac{\partial}{\partial \eta}$$

$$\frac{\partial}{\partial y} = \frac{\rho u_\infty}{\sqrt{2\xi}} \frac{\partial}{\partial \eta}$$

and where

$$V = \frac{2\xi}{(\rho\mu)_r u_\infty} \left(f' \eta_x + \frac{\rho v}{\sqrt{2\xi}} \right)$$

Equations (1), (2), (9), and (10) become

Continuity:

$$2\xi \frac{\partial f'}{\partial \xi} + \frac{\partial V}{\partial \eta} + f' = 0 \quad (13)$$

Momentum:

$$2\xi f' \frac{\partial f'}{\partial \xi} + V \frac{\partial f'}{\partial \eta} = \frac{2\xi}{u_\infty} \frac{du_\infty}{d\xi} [g - f'^2] + \frac{\partial}{\partial \eta} \left(\lambda \frac{\partial f'}{\partial \eta} \right) \quad (14)$$

Energy:

$$2\xi f' \frac{\partial g}{\partial \xi} + V \frac{\partial g}{\partial \eta} + \frac{2\xi f' g}{h_\infty} \frac{dh_\infty}{d\xi}$$

$$= - \frac{2\xi u_\infty}{h_\infty} \frac{du_\infty}{d\xi} (1 - IS_3) f' g + \frac{u_\infty^2}{h_\infty} \ell \left(\frac{\partial f'}{\partial \eta} \right)^2$$

$$+ \frac{\partial}{\partial \eta} \left[\frac{\ell}{P_R} \frac{\partial g}{\partial \eta} \right] + \frac{T_{e_\infty}}{T_\infty} \frac{\partial}{\partial \eta} \left[\lambda \frac{\partial \theta}{\partial \eta} \right]$$

$$+ \frac{5}{2} \frac{\sqrt{2\xi} k T_{e_\infty} \alpha_1 j_{y_\infty}}{(\rho\mu)_r u_\infty C_p T_\infty e} \frac{\partial \theta}{\partial \eta}$$

$$+ \frac{5}{2} \frac{\sqrt{2\xi} k T_{e_\infty} \alpha_2 E_{x_\infty}}{(\rho\mu)_r u_\infty C_p T_\infty e} \frac{\partial \theta}{\partial \eta}$$

$$+ \frac{5}{2} \frac{\sqrt{2\xi} k T_{e_\infty} \alpha'_1 j_{y_\infty}}{(\rho\mu)_r u_\infty C_p T_\infty e} \theta$$

$$+ \frac{5}{2} \frac{\sqrt{2\xi} k T_{e_\infty} \alpha'_2 E_{x_\infty}}{(\rho\mu)_r u_\infty C_p T_\infty e} \theta$$

$$+ \frac{2\xi}{C_p T_\infty} \frac{1}{(\rho\mu)_r \rho_\infty u_\infty^2} \left[\frac{\sigma E_{x_\infty}^2}{1 + \beta_e \beta_i} \right.$$

$$+ \left. \frac{j_{y_\infty}^2}{\sigma} \frac{(1 + \beta_e \beta_i)^2 + \beta_e^2}{1 + \beta_e \beta_i} \right] g$$

$$+ \frac{2\xi B_z j_{y_\infty} f' g}{(\rho\mu)_r C_p T_\infty \rho_\infty u_\infty} (1 - IS_3)$$

$$- \frac{IS_1 T_{e_\infty} (2\xi)}{C_p T_\infty \rho_\infty} g f' \frac{\partial \theta}{\partial \xi} - \frac{IS_1 T_{e_\infty} V}{\rho_\infty C_p T_\infty} g \frac{\partial \theta}{\partial \eta}$$

$$- \frac{IS_1 (2\xi) \frac{dT_{e_\infty}}{d\xi}}{\rho_\infty C T_\infty} g f' \theta$$

$$+ \frac{IS_2 (2\xi)}{\rho_\infty} g f' \frac{\partial g}{\partial \xi} + \frac{IS_2 V}{\rho_\infty} g \frac{\partial g}{\partial \eta}$$

$$+ \frac{IS_2 (2\xi)}{\rho_\infty T_\infty} \left(\frac{dT_\infty}{d\xi} \right) g^2 f' - \frac{2\xi I n_e}{C_p T_\infty \rho_\infty} f' \frac{\partial g}{\partial \xi}$$

$$- \frac{I n_e}{C_p T_\infty \rho_\infty} V \frac{\partial g}{\partial \eta} - \frac{I n_e (2\xi)}{C_p T_\infty \rho_\infty} \frac{dT_\infty}{d\xi} f' g$$

$$+ \frac{I n_e j_{y_\infty} (2\xi) B_z}{p (\rho\mu)_r \rho_\infty C_p T_\infty u_\infty} g f'$$

$$- \frac{I u_\infty n_e (2\xi)}{p C_p T_\infty} \frac{du_\infty}{d\xi} g f' \quad (15)$$

Electron Energy:

$$\left(\frac{3}{2} k n_e + \left[\frac{3}{2} k T_{e_\infty} \theta + I \right] S_1 \right) \left(\frac{(\rho\mu)_r T_{e_\infty} u_\infty}{2\xi} \right) \left[2\xi f' \frac{\partial \theta}{\partial \xi} \right.$$

$$+ \left. V \frac{\partial \theta}{\partial \eta} + 2\xi \frac{f' \theta}{T_{e_\infty}} \frac{dT_{e_\infty}}{d\xi} \right]$$

$$- S_2 \left[\frac{3}{2} k T_{e_\infty} \theta + I \right] \left(\frac{(\rho\mu)_r h_\infty u_\infty^2}{2\xi} \right) \left[2\xi f' \frac{\partial g}{\partial \xi} \right.$$

$$+ \left. V \frac{\partial g}{\partial \eta} + 2\xi \frac{f' g}{T_\infty} \frac{dT_\infty}{d\xi} \right]$$

$$- \left(\frac{3}{2} k T_{e_\infty} \theta + I \right) S_3 \rho_\infty u_\infty^3 \frac{du_\infty}{d\xi} (\rho\mu)_r f'$$

$$+ \left(\frac{3}{2} k T_{e_\infty} \theta + I \right) S_3 j_{y_\infty} B_z u_\infty f'$$

$$- \frac{\rho_\infty u_\infty^2 C_p (\rho\mu)_r T_{e_\infty}}{2\xi g} \frac{\partial}{\partial \eta} \left(\lambda \frac{\partial \theta}{\partial \eta} \right)$$

$$\begin{aligned}
& - \frac{\rho_{\infty} u_{\infty}}{g\sqrt{2\xi}} \frac{5}{2} \frac{k}{e} T_{e\infty} j_{y\infty} \frac{\partial}{\partial \eta} (\theta \alpha_1) \\
& - \frac{\rho_{\infty} u_{\infty}}{g\sqrt{2\xi}} \frac{5}{2} \frac{k}{e} T_{e\infty} E_{x\infty} \frac{\partial}{\partial \eta} (\theta \alpha_2) \\
& + n_e \left[\frac{5}{2} k T_{e\infty} \theta + I \right] \left[\frac{(\rho \mu)_r u_{\infty}^2}{2\xi g} \right] \left[2\xi f' \frac{\partial g}{\partial \xi} \right. \\
& \left. + v \frac{\partial g}{\partial \eta} - \frac{2\xi f' g}{\rho_{\infty}} \frac{d\rho_{\infty}}{d\xi} \right] = E_{x\infty}^2 \frac{\sigma}{(1+\beta_e \beta_i)^2} \\
& + \frac{j_{y\infty}^2}{\sigma} \frac{[(1+\beta_e \beta_i)^2 + \beta_e^2]}{(1+\beta_e \beta_i)^2} \\
& + 3m_e n_e k T_{e\infty} \left(g \frac{T_{\infty}}{T_{e\infty}} - \theta \right) \frac{\nu_s}{m_s} \quad (16)
\end{aligned}$$

Nonequilibrium Boundary Layer Development Over Initial Insulator:

Upstream of any electrode segment, Eq's. (13) to (16) are simplified by assuming local similarity. That is, we take $\frac{\partial}{\partial \eta} = 0$ and treat ξ as a parameter. In the absence of currents, magnetic, and electric fields, Eq's. (13) to (16) become

Momentum:

$$(\ell f')' + ff'' = 0 \quad (17)$$

Overall Energy:

$$\begin{aligned}
& \left(\frac{\ell}{P_R} g' \right)' + fg' + \frac{u_{\infty}^2}{h_{\infty}} [\ell (f'')^2] + \frac{T_{e\infty}}{T_{\infty}} (\lambda \theta')' \\
& + I \left(\frac{S_1 T_{e\infty}}{\rho_{\infty} C_p T_{\infty}} fg\theta' - \frac{S_2 fg g'}{\rho_{\infty}} \right. \\
& \left. + \frac{n_e}{\rho_{\infty} C_p T_{\infty}} fg' \right) = 0 \quad (18)
\end{aligned}$$

Electron Energy:

$$\begin{aligned}
& (\lambda \theta')' + \left[\frac{\frac{3}{2} k n_e + \left(\frac{3}{2} k T_{e\infty} \theta + I \right) S_1}{\rho_{\infty} C_p} \right] fg\theta' \\
& - \left[\frac{\left(\frac{3}{2} k T_{e\infty} \theta + I \right) T_{\infty} S_2}{\rho_{\infty} T_{e\infty}} \right] fgg'
\end{aligned}$$

$$\begin{aligned}
& + \left[\frac{n_e \left(\frac{5}{2} k T_{e\infty} \theta + I \right)}{\rho_{\infty} C_p T_{e\infty}} \right] fg' - \left[\frac{2\xi}{(\rho \mu)_r u_{\infty}^2} \times \right. \\
& \left. \left(\frac{3n_e k}{\rho_{\infty} C_p} \right) \left(m_e \Sigma \frac{\nu_s}{m_s} \right) g \left(\theta - \frac{T_{\infty}}{T_{e\infty}} g \right) \right] = 0 \quad (19)
\end{aligned}$$

where $(\cdot)' = \frac{d}{d\eta}$.

Boundary Conditions:

$$\eta = \infty \quad f' = g = \theta = 1$$

$$\eta = 0 \quad f = f' = 0, \quad g = g_w,$$

$$\begin{aligned}
\theta'_w &= \frac{2}{5} \frac{\sqrt{2\xi} m_c n_{ew}}{\lambda (\rho \mu)_r u_{\infty}} \sqrt{\frac{k T_{e\infty}}{m_s}} \\
&\times \left(2 + \ell n \sqrt{\frac{m_s}{2\pi m_e}} \right) \theta_w^{3/2}
\end{aligned}$$

The viscosity-temperature relation is assumed to be such that $\ell = g^{-1/4}$ and Fay's⁷ approximate mixing rule is used to evaluate the electron thermal conductivity parameter.

$$\lambda = \frac{\rho K_e}{C_p (\rho \mu)_r} = \left[\frac{\ell}{P_R} \left(\frac{K_e}{K_{A*}} \right) \right] \quad (20)$$

where

$$\frac{K_e}{K_{A*}} = \frac{K_s/K_{A*}}{1 + \sqrt{2} \left(\frac{1-\alpha}{\alpha} \right) \frac{K_s}{K_{A*}} \frac{Q_{en}}{Q_{nn}} \sqrt{\frac{m_e}{m_c} \frac{T}{T_e}}}$$

$$\begin{aligned}
\frac{K_s}{K_{A*}} &= \frac{7.5 \times 10^{-7} \frac{T_e^{5/2}}{T^{3/4}}}{\frac{1}{4} \ell n [55 + \Lambda_1^4 + \Lambda_2^4]}
\end{aligned}$$

$$\alpha = \frac{n_e}{n}$$

$$\Lambda_1 = \frac{1.24 \times 10^7 T_e^{3/2}}{n_e^{1/2}}$$

$$\Lambda_2 = \frac{1.8 \times 10^5 T_e}{n_e^{1/3}}$$

Eq's. (17) to (19) are three coupled nonlinear ordinary differential equations that have to be solved simultaneously while satisfying two-point boundary conditions. Such calculations have been carried out on a high speed digital computer.

III. Example and Discussions

The nonequilibrium boundary layer development over an initial insulator has been carried out for argon gas (inert) seeded with 1% by volume of cesium. The free stream conditions selected are

$$\begin{aligned}u_{\infty} &= 395.6 \text{ m/sec} \\T_{\infty} &= T_{e\infty} = 1920^{\circ}\text{K} \\p_{\infty} &= 1.64 \text{ atmospheres} \\M_{\infty} &= 0.5\end{aligned}$$

The Prandtl number of the mixture is assumed to be $2/3$.

Calculations are presented for values of ξ between 0 and 0.01. This would correspond to a maximum distance of one meter from the leading edge of a flat plate having the above uniform free stream conditions and $(\rho\mu)_{\infty} = 4.5 \times 10^{-5} \frac{\text{kg}^2}{\text{m}^4 \cdot \text{sec}}$. The results are tabulated in Table I.

Table I

ξ	g_w	f_w''	g_w'	θ_w^*
0	0.9	.4598	.0655	1.0000
.005	0.9	.4596	.0656	.7791
.010	0.6	.4257	.1709	.7194
.010	0.8	.4498	.1030	.7553
.010	0.9	.4596	.0657	.7745
.010	1.0	.4689	.0261	.7940
.010	1.2	.4847	-.0574	.8384

Typical profiles obtained at $\xi = .01$ and $g_w = 0.9$ are shown in Figs. (3), (4), and (5).[†] Here we observe that the velocity and overall gas temperature profiles are relatively unaffected by the electron temperature variation. Significantly, however, we find that the electron temperature differs considerably from the heavy particle temperature. This occurs in spite of the fact that the electrons are in equilibrium in the free stream.

There are several causes for the difference between T_e and T . Most important is the fact that the sheath boundary condition for an insulated wall requires a large $\frac{\partial T_e}{\partial y}$. Then T_e must be low at the wall to allow $T_e \rightarrow T$ at infinity. Such a large value for $\frac{\partial T_e}{\partial y}$ is necessary in order for the continuum heat flux to equal the microscopic electron heat flux at the sheath interface. The other cause for differing T_e and T arises due to the flow and overall gas temperature gradients and their contribution to the electron energy equation.

One consequence of the lowered T_e is that the electron density and electrical conductivity are lowered near the wall. These are shown in Fig. (6).

* Changes in θ_w in the sixth and seventh places were found to be necessary in order to obtain accurate profiles.

† The profiles all approached one at infinity to within an accuracy of better than one part in a thousand.

To illustrate the longitudinal development of the boundary layer, calculations have been made at several values of ξ . Curves showing f'' , g' , and θ at the wall are shown in Fig. (7). Most noticeably, we see that aside from a rapid drop of θ near $\xi = 0$ that all three unknowns vary rather slowly in the coordinate system chosen.

The influence of g_w on the profiles is shown in Figs. (8) and (9). Interestingly, we find that increasing g_w increases θ_w . In fact at $g_w = 1.2$ we find θ reaches a maximum of 1.016 at $\eta \approx 2$ before returning to unity at ∞ . This establishes the fact that the variations in g and f throughout the boundary layer can even cause T_e to rise above its free stream value.

The total heat transfer to the wall may be evaluated using the continuum description developed in formulating Eq. (3). In general, it will consist of the sum of the conduction terms for each species, and the flux of the particles to the wall carrying their enthalpy (both due to random thermal motion and recombination energy). The latter will con-

sist primarily of $\frac{5}{2} \frac{kT_e}{e} j_{ey}$ which represents the

flux of electrons carrying their thermal energy,

and $n_i \sqrt{\frac{kT_e}{m_s}} I$ which represents the flux of ions

carrying their recombination energy. For the calculations presented over an insulator wall, we have no current, $j_e = j = 0$. As well, we have

neglected $n_i \sqrt{\frac{kT_e}{m_s}} I$ in Eq. (3) since for the con-

ditions being considered it amounts to less than 1% of the heavy particle conduction. The electronic heat conduction has been included, however, in the analysis; but a check shows that it is no more than 2% of the heavy particle conduction. Since the g distribution seems little affected by the electron temperature we must conclude that the heat flux seems unaffected by the variations in the electron temperature found here.

IV. Summary

In the present paper we have developed a general procedure for estimating boundary layer development for a nonequilibrium plasma. An important feature of the method is the separate treatment of the electron energy equation subject to electric and thermal boundary conditions obtained through a description of the sheath.

Calculations made assuming local similarity have been presented for an insulator wall that shows that the electron temperature is much different from the gas temperature even though the plasma is in equilibrium in the free stream. Also, the velocity and overall gas temperature profiles are little influenced by the electron temperature, although small changes in the former cause large

changes in the latter. Specifically, small changes in the wall temperature are shown to change the electron temperature considerably.

Acknowledgment

The research reported on in the present paper was carried out as a part of NASA program NASw-1586.

Appendix A

Overall Energy Conservation:

$$\rho u \frac{\partial h^*}{\partial x} + \rho v \frac{\partial h^*}{\partial y} = u \frac{\partial p}{\partial x} + \mu \left(\frac{\partial u}{\partial y} \right)^2 - \frac{\partial}{\partial y} (q_y) + j_x E_x + j_y (E_y - uB) \quad (A1)$$

The heat flux vector is assumed to be of the following form.

$$q = \sum_i q_i \text{ where } q_i = -K_i \nabla T_i + \rho_i h_i^* V_i$$

Now, let us express h^* more explicitly.

$$h^* = \frac{1}{\rho} \sum_i \rho_i h_i^* \quad h^* = \frac{5}{2} \frac{kT_i}{m_i} + \frac{I_i}{m_i}$$

so that

$$h^* = \frac{\rho_A}{\rho} \frac{5}{2} \frac{kT}{m_A} + \frac{\rho_s}{\rho} \frac{5}{2} \frac{kT}{m_s} + \frac{\rho_s^+}{\rho} \frac{5}{2} \frac{kT}{m_s} + \frac{\rho_e}{\rho} \frac{5}{2} \frac{kT_e}{m_e} + \frac{\rho_s^+}{\rho} \frac{I}{m_s}$$

or

$$h^* = h + \frac{n_e}{\rho} I$$

We can rewrite the heat flux vector for s as follows

$$q_i = -K_i \nabla T_i + m_i n_i h_i V_i + \frac{m_i n_i^2}{\rho} I_i V_i$$

so that

$$q = -\sum_i K_i \nabla T + m_e n_e \frac{5}{2} \frac{kT_e}{m_e} V_e = -\sum_i K_i \nabla T - \frac{5kT_e}{2e} j_e$$

Then, the overall energy equation becomes

$$\rho u \frac{\partial h}{\partial x} + \rho v \frac{\partial h}{\partial y} = u \frac{\partial p}{\partial x} + \mu \left(\frac{\partial u}{\partial y} \right)^2 + \frac{\partial}{\partial y} \left(\sum_i K_i \frac{\partial T}{\partial y} + \frac{5kT_e}{2e} j_{ey} \right)$$

$$+ j_x E_x + j_y (E_y - uB) - \rho u I \frac{\partial}{\partial x} \left(\frac{n_e}{\rho} \right) - \rho v I \frac{\partial}{\partial y} \left(\frac{n_e}{\rho} \right) \quad (A2)$$

Next, let us write

$$\rho u I \frac{\partial}{\partial x} \left(\frac{n_e}{\rho} \right) + \rho v I \frac{\partial}{\partial y} \left(\frac{n_e}{\rho} \right) = I \left[u \frac{\partial n_e}{\partial x} + v \frac{\partial n_e}{\partial y} - n_e \left(\frac{u}{\rho} \frac{\partial \rho}{\partial x} + \frac{v}{\rho} \frac{\partial \rho}{\partial y} \right) \right]$$

and the energy equation can be rewritten as

$$\rho u \frac{\partial h}{\partial x} + \rho v \frac{\partial h}{\partial y} = u \frac{\partial p}{\partial x} + \mu \left(\frac{\partial u}{\partial y} \right)^2 + \frac{\partial}{\partial y} \left(\sum_i K_i \frac{\partial T}{\partial y} + \frac{5kT_e}{2e} j_{ey} \right) + j_x E_x + j_y (E_y - uB) - I \left[u \frac{\partial n_e}{\partial x} + v \frac{\partial n_e}{\partial y} - n_e \left(\frac{u}{\rho} \frac{\partial \rho}{\partial x} + \frac{v}{\rho} \frac{\partial \rho}{\partial y} \right) \right] \quad (A3)$$

and the last two terms are equivalent to the \sum_{ions}

$\omega_i I_i$ term commonly included in the energy equation.

Next $\frac{\partial p}{\partial x}$ can be obtained from the momentum equation evaluated at the free stream. Then

$$\rho u \frac{\partial u}{\partial x} + \rho v \frac{\partial u}{\partial y} = -\frac{\partial p}{\partial x} + \frac{\partial}{\partial y} \left(\mu \frac{\partial u}{\partial y} \right) + j_y B_z$$

and at ∞

$$\rho_\infty u_\infty \frac{du_\infty}{dx} = -\frac{\partial p}{\partial x} + j_y B_z$$

$$\therefore \frac{\partial p}{\partial x} = j_y B_z - \rho_\infty u_\infty \frac{du_\infty}{dx}$$

and the energy equation becomes

$$\rho u \frac{\partial h}{\partial x} + \rho v \frac{\partial h}{\partial y} = -\rho_\infty u_\infty \frac{du_\infty}{dx} + \mu \left(\frac{\partial u}{\partial y} \right)^2 + \frac{\partial}{\partial y} \left(\sum_i K_i \frac{\partial T}{\partial y} + \frac{5kT_e}{2e} j_{ey} \right) + j_x E_x + j_y E_y - I \left[u \frac{\partial n_e}{\partial x} + v \frac{\partial n_e}{\partial y} - n_e \left(\frac{u}{\rho} \frac{\partial \rho}{\partial x} + \frac{v}{\rho} \frac{\partial \rho}{\partial y} \right) \right] \quad (A4)$$

Finally, we have to re-express the two last terms on the RHS in terms of T_e , T , u . Now, n_e can be obtained from the Saha relation.

$$\frac{n_e n_e}{n_s} = \left(\frac{2\pi m_e k T_e}{h^2} \right)^{3/2} \exp \left[-\frac{eI}{k T_e} \right] = S(T_e)$$

The ratio of the original number density of seed atoms as compared to the inert carrier will be specified. So

$$P = \frac{n_e + n_s}{n_A}$$

Also, assuming each species is a P.G.

$$p = \sum p_i = k [n_A + n_s + n_e] T + k n_e T_e$$

$$\text{or } p \approx k n_A T$$

Now, we write from Saha

$$n_e^2 = S(T_e) n_s$$

But from the definition of P

$$n_s = P n_A - n_e$$

$$\therefore n_e^2 = S(T_e) \left[P \frac{p}{kT} - n_e \right]$$

$$\text{or } n_e^2 + S(T_e) n_e - \frac{P p S}{kT} = 0$$

$$\text{and } n_e = -\frac{S}{2} + \sqrt{\frac{S^2}{4} + \frac{P p S}{kT}}$$

$$\text{or } n_e = \frac{S}{2} \left\{ \sqrt{1 + \frac{4Pp}{kTS}} - 1 \right\} \quad \text{when } \frac{4Pp}{kTS} \gg 10^{-2}$$

when S is very large, corresponding to nearly full ionization, the above may prove very inaccurate for numerical calculation. For this case, we expand the $\sqrt{\quad}$ and use

$$n_e = \frac{pP}{kT} \left[1 - \frac{Pp}{kTS} \right] \quad \text{when } \frac{4Pp}{kTS} < 10^{-2}$$

If we wish, we can also write

$$S(T_e) = C_1 T_e^{3/2} e^{-C_2/T_e}$$

where

$$C_1 = \left(\frac{2\pi m_e k T_e}{h^2} \right)^{3/2}$$

$$C_2 = eI/k$$

Thus we can write out to begin with $\frac{\partial n_e}{\partial x}$ using

$$n_e = -\frac{S}{2} + \sqrt{\frac{S^2}{4} + \frac{PpS}{kT}}$$

and $S(T_e)$ directly above.

Now

$$\frac{\partial n_e}{\partial x} = S_1 \frac{\partial T_e}{\partial x} - S_2 \frac{\partial h}{\partial x} + S_3 \frac{dp}{dx}$$

where

$$S_1 = S \left(\frac{3}{2T_e} + \frac{C_2}{T_e^2} \right) \left[-\frac{1}{2} + \frac{\frac{S}{2} + \frac{2Pp}{kT}}{S \sqrt{1 + \frac{4Pp}{kTS}}} \right]$$

$$S_2 = \frac{2Pp}{k C_p T^2 \sqrt{1 + \frac{4Pp}{kTS}}}$$

$$S_3 = \frac{2P}{kT \sqrt{1 + \frac{4Pp}{kTS}}}$$

Similarly

$$\frac{\partial n_e}{\partial y} = S_1 \frac{\partial T_e}{\partial y} - S_2 \frac{\partial h}{\partial y} \left(\frac{\partial p}{\partial y} = 0 \right)$$

Accordingly, neglecting argon ionization the overall energy equation becomes

$$\begin{aligned} \rho u \frac{\partial h}{\partial x} + \rho v \frac{\partial h}{\partial y} = & -\rho_\infty u_\infty \frac{du_\infty}{dx} \\ & + \mu \left(\frac{\partial u}{\partial y} \right)^2 + \left(\sum K_i \frac{\partial T}{\partial y} + \frac{5kT_e}{2e} j_{ey} \right) + j_{ex} E_x \\ & + j_{ey} E_y - I \left[u S_1 \frac{\partial T_e}{\partial x} - u S_2 \frac{\partial h}{\partial x} + u S_3 \frac{dp}{dx} \right. \\ & \left. + v S_1 \frac{\partial T_e}{\partial y} - v S_2 \frac{\partial h}{\partial y} - n_e \left(\frac{u}{\rho} \frac{\partial \rho}{\partial x} + \frac{v}{\rho} \frac{\partial \rho}{\partial y} \right) \right] \end{aligned} \quad (A5)$$

but the last two terms can be rewritten as follows: Assume the overall plasma density, pressure, et al, is that of a perfect gas (argon). Then

$$p = \rho RT = \rho \frac{R}{C_p} h \quad \therefore \quad \rho = \frac{C_p}{R} \frac{p}{h}$$

Then

$$\begin{aligned} \frac{1}{\rho} \frac{\partial \rho}{\partial x} = & -\frac{1}{\rho} \frac{C_p}{R} p \frac{1}{h^2} \frac{\partial h}{\partial x} + \frac{1}{\rho} \frac{C_p}{R} \frac{1}{h} \frac{dp}{dx} \\ = & -\frac{1}{h} \frac{\partial h}{\partial x} + \frac{1}{p} \frac{dp}{dx} \end{aligned}$$

$$\frac{u}{\rho} \frac{\partial \rho}{\partial x} + \frac{v}{\rho} \frac{\partial \rho}{\partial y} = -\frac{u}{h} \frac{\partial h}{\partial x} - \frac{v}{h} \frac{\partial h}{\partial y} + \frac{u}{p} \frac{dp}{dx}$$

The overall energy equation is then

$$\begin{aligned}
\rho u \frac{\partial h}{\partial x} + \rho v \frac{\partial h}{\partial y} = & -\rho_{\infty} u_{\infty} \frac{du_{\infty}}{dx} + \mu \left(\frac{\partial u}{\partial y} \right)^2 \\
& + \frac{\partial}{\partial y} \left(\sum_i K_i \frac{\partial T}{\partial y} + \frac{5kT_e}{2e} j_{ey} \right) + j_x E_x + j_y E_y \\
& - I \left[u S_1 \frac{\partial T_e}{\partial x} - u S_2 \frac{\partial h}{\partial x} + u S_3 \frac{dp}{dx} \right. \\
& + v S_1 \frac{\partial T_e}{\partial y} - v S_2 \frac{\partial h}{\partial y} - n_e \left(\frac{u}{p} \frac{dp}{dx} \right. \\
& \left. \left. - \frac{u}{h} \frac{\partial h}{\partial x} - \frac{v}{h} \frac{\partial h}{\partial y} \right) \right] \quad (A6)
\end{aligned}$$

But we know $\frac{dp}{dx}$ to be $= j_y B_z - \rho_{\infty} u_{\infty} \frac{du_{\infty}}{dx}$. Then we obtain Eq. (3).

Appendix B

General Form of Electron Energy Equation:

$$\begin{aligned}
\nabla \cdot \left(n_e v \left[\frac{3}{2} k T_e + I \right] \right) + \nabla \cdot \left[-K_e \nabla T_e \right. \\
\left. - \frac{5}{2} \frac{k}{e} T_e j_e - \frac{I}{e} j_e \right] + p_e \nabla \cdot v = E^* \cdot j_e \\
+ 3 \rho_e k (T - T_e) \sum_s \nu_{es}^* / m_s \quad (B1)
\end{aligned}$$

which we can rewrite as

$$\begin{aligned}
\nabla \cdot \left(n_e v \left[\frac{3}{2} k T_e \right] \right) - \nabla \cdot \left[K_e \nabla T_e + \frac{5}{2} \frac{k}{e} T_e j_e \right] \\
+ p_e \nabla \cdot v = E^* \cdot j_e + 3 \rho_e k (T - T_e) \sum_s \nu_{es}^* / m_s \\
+ \frac{I}{e} \nabla \cdot j_e - I \nabla \cdot (n_e v) \quad (B2)
\end{aligned}$$

In boundary layer form this can be simplified to

$$\begin{aligned}
\frac{3}{2} k n_e \frac{\partial T_e}{\partial x} + \frac{3}{2} k u T_e \frac{\partial n_e}{\partial x} + \frac{3}{2} k v n_e \frac{\partial T_e}{\partial y} \\
+ \frac{3}{2} k v T_e \frac{\partial n_e}{\partial y} + n_e \left[\frac{5}{2} k T_e + I \right] \left(\frac{\partial u}{\partial x} + \frac{\partial v}{\partial y} \right) \\
- \frac{\partial}{\partial y} \left[K_e \frac{\partial T_e}{\partial y} + \frac{5}{2} \frac{k}{e} T_e j_{ey} \right] = E_x j_{ex} \\
+ (E_y - u B_z) j_{ey} + 3 \rho_e k (T - T_e) \sum_s \frac{\nu_{es}^*}{m_s} \\
- I u \frac{\partial n_e}{\partial x} - I v \frac{\partial n_e}{\partial y} \quad (B3)
\end{aligned}$$

Now we have as before

$$\frac{\partial n_e}{\partial x} = S_1 \frac{\partial T_e}{\partial x} - S_2 \frac{\partial h}{\partial x} + S_3 \frac{dp}{dx}$$

$$\frac{\partial n_e}{\partial y} = S_1 \frac{\partial T_e}{\partial y} - S_2 \frac{\partial h}{\partial y}$$

Also we have to reexpress $\frac{\partial u}{\partial x} + \frac{\partial v}{\partial y}$. Thus

$$\frac{\partial}{\partial x} (\rho u) + \frac{\partial}{\partial y} (\rho v) = 0$$

and

$$\rho \left(\frac{\partial u}{\partial x} + \frac{\partial v}{\partial y} \right) + u \frac{\partial \rho}{\partial x} + v \frac{\partial \rho}{\partial y} = 0$$

$$\frac{\partial u}{\partial x} + \frac{\partial v}{\partial y} = -\frac{u}{\rho} \frac{\partial \rho}{\partial x} - \frac{v}{\rho} \frac{\partial \rho}{\partial y} = \rho \left[u \frac{\partial \rho^{-1}}{\partial x} + v \frac{\partial \rho^{-1}}{\partial y} \right]$$

and we as well replace $\frac{dp}{dx}$ from before

$$\frac{dp}{dx} = j_y B_z - \rho_{\infty} u_{\infty} \frac{du_{\infty}}{dx}$$

Making all of the above substitutions into Eq. (B3) yields Eq. (4).

Appendix C

Eq's. (7) and (8) can be written as

$$\begin{aligned}
j_x &= \frac{\sigma}{(1+\beta_e \beta_i)^2 + \beta_e^2} \left\{ (1+\beta_e \beta_i) E_{x_{\infty}} - \beta_e (E_y - u B_z) \right\} \\
j_{y_{\infty}} &= \frac{\sigma}{(1+\beta_e \beta_i)^2 + \beta_e^2} \left\{ (1+\beta_e \beta_i) (E_y - u B_z) + \beta_e E_{x_{\infty}} \right\}
\end{aligned}$$

using the 2nd relation to replace $(E_y - u B_z)$ in 1st we get

$$\begin{aligned}
j_x &= \frac{\sigma}{1+\beta_e \beta_i} \left\{ E_{x_{\infty}} - \frac{\beta_e}{\sigma} j_{y_{\infty}} \right\} \\
j_x E_x &= \frac{\sigma}{1+\beta_e \beta_i} E_{x_{\infty}}^2 - \frac{\beta_e}{1+\beta_e \beta_i} j_{y_{\infty}} E_{x_{\infty}} \\
&\quad \downarrow 0 \\
\begin{cases} j_{y_{\infty}} = 0 \text{ where } E_{x_{\infty}} \neq 0 \\ E_{x_{\infty}} = 0 \text{ where } j_{y_{\infty}} \neq 0 \end{cases}
\end{aligned}$$

So

$$j_x E_x = \frac{\sigma}{1+\beta_e \beta_i} E_{x_\infty}^2$$

Next, solve the 2nd of the above eq's. for E_y .

$$E_y = \frac{j_y \left[(1+\beta_e \beta_i)^2 + \beta_e^2 \right]}{\sigma (1+\beta_e \beta_i)} - \frac{\beta_e}{1+\beta_e \beta_i} E_{x_\infty} + u B_z$$

Then

$$j_y E_y = \frac{j_y^2}{\sigma} \left[\frac{(1+\beta_e \beta_i)^2 + \beta_e^2}{1+\beta_e \beta_i} \right] + u B_z j_y$$

Now, we need an expression for j_{e_x} and j_{e_y} . This we obtain from

$$j_e = j + \beta_i \frac{B \times j}{B_z}$$

Then

$$j_{e_x} = j_x - \frac{\beta_i}{B_z} B_z j_y = j_x - \beta_i j_y$$

$$j_{e_y} = j_y + \frac{\beta_i B_z}{B_z} j_x = j_y + \beta_i j_x$$

also as before

$$j_x = \frac{\sigma}{1+\beta_e \beta_i} \left[E_{x_\infty} - \frac{\beta_e}{\sigma} j_{y_\infty} \right]$$

So that

$$j_{e_y} = j_{y_\infty} \left[\frac{1}{1+\beta_e \beta_i} \right] + \left(\frac{\sigma \beta_i}{1+\beta_e \beta_i} \right) E_{x_\infty}$$

or

$$j_{e_y} = \alpha_1 j_{y_\infty} + \alpha_2 E_{x_\infty}$$

then

$$E_{x_\infty} j_{e_x} = E_{x_\infty} j_x - \beta_i j_{y_\infty} \begin{matrix} E_{x_\infty} \\ \downarrow \\ 0 \end{matrix}$$

or

$$E_{x_\infty} j_{e_x} = \frac{\sigma}{1+\beta_e \beta_i} E_{x_\infty}^2$$

and

$$(E_y - uB) j_{e_y} = \frac{\left[(1+\beta_e \beta_i)^2 + \beta_e^2 \right]}{\sigma (1+\beta_e \beta_i)^2} j_{y_\infty}^2$$

$$- \frac{\beta_e}{(1+\beta_e \beta_i)^2} \sigma \beta_i E_{x_\infty}^2$$

then

$$\begin{aligned} j_{e_x} E_{x_\infty} + j_{e_y} (E_y - uB_z) \\ = \left[\frac{(1+\beta_e \beta_i)^2 + \beta_e^2}{(1+\beta_e \beta_i)^2} \right] \frac{j_{y_\infty}^2}{\sigma} + \frac{\sigma}{(1+\beta_e \beta_i)^2} E_{x_\infty}^2 \end{aligned}$$

References

1. Kerrebrock, J. L., "Electrode Boundary Layers in Direct Current Plasma Accelerators", J. Aerosp. Sci. 28, 631 (1961).
2. Hale, F. J. and Kerrebrock, J. L., "Insulator Boundary Layers in MHD Channels", AIAA J. 2, 461 (1964).
3. Oates, G. C., Richmond, J. K., Aoki, Y., and Grohs, G., "Loss Mechanisms of a Low Temperature Plasma Accelerator", Proceedings of the Fourth Biennial Gas Dynamics Symposium, Northwestern Univ. Press, Evanston, 1962.
4. Camac, M., and Kemp, N.H., "A Multi-temperature Boundary Layer", AVCO/Everett Research Laboratory Research Report 184, August 1964.
5. Dix, D. M., "Energy Transfer Processes in a Partially Ionized Two Temperature Gas", AIAA J., 2, 2081 (1964).
6. Hurwitz, H., Jr., Kilb, R. W., and Sutton, G. W., "Influence of Tensor Conductivity on Current Distribution in an MHD Generator", J. Appl. Phys., 32, 205 (1961).
7. Fay, J. A., "Hypersonic Heat Transfer in the Air Laminar Boundary Layer", AVCO/Everett Research Laboratory, AMP 71, March 1962.

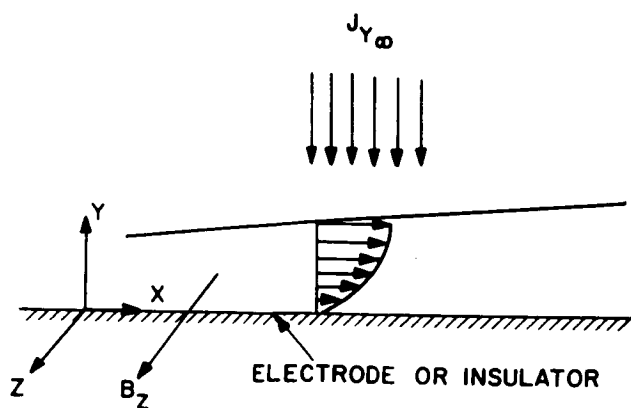
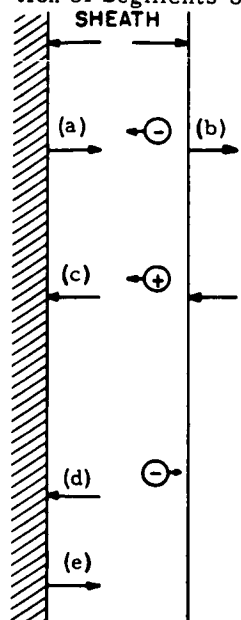


Figure 1. Channel Wall-Electrode or Insulator or Combination of Segments of Each



(a) current density due to electron arrival at wall

$$\frac{n_e e \langle V \rangle_e}{4} - \frac{e \Delta \phi}{KT_e}$$

(b) current density due to electron arrival at outer edge of sheath

$$\frac{n_e e \langle V \rangle_e}{4}$$

(c) current density due to ions entering sheath (all these ions reach the wall since they are accelerated by the sheath drop)

$$n_i e V_i$$

(d) electron emission current density i_w

(e) net current density j_y

Figure 2. Contributions to Current Density at Wall

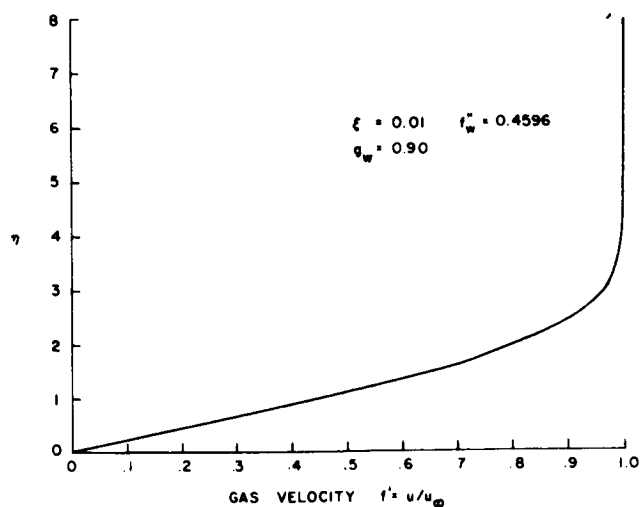


Figure 3. Velocity Profile at $\xi = .01$ for $g_w = 0.9$

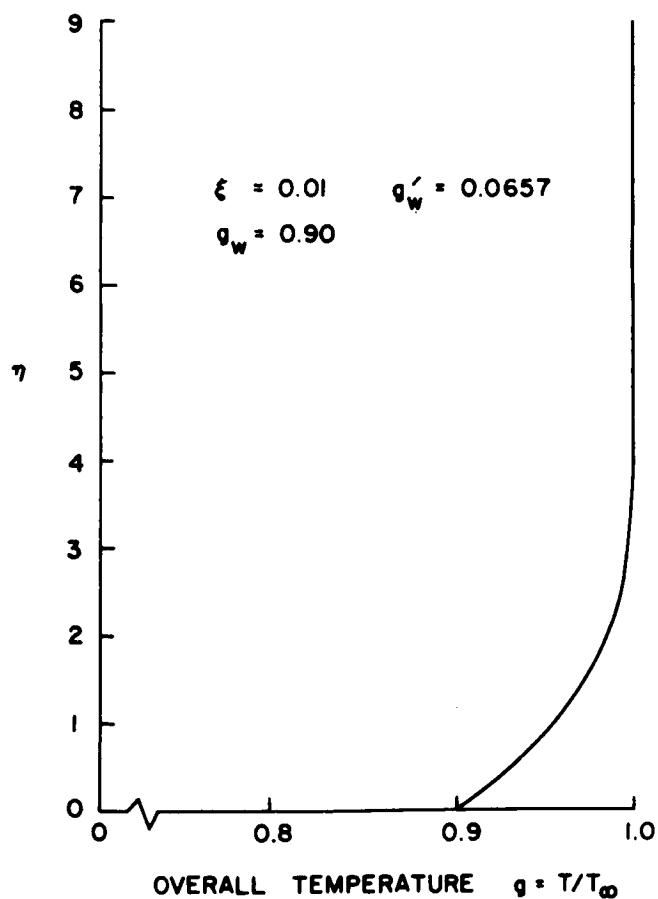


Figure 4. Overall Temperature Profile at $\xi = .01$ for $g_w = 0.9$

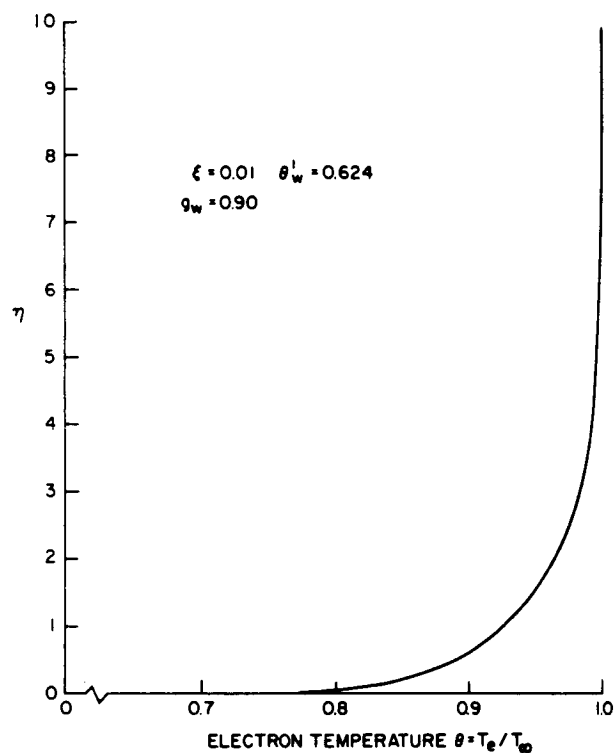


Figure 5. Electron Temperature Profile at $\xi = .01$ for $g_w = 0.9$

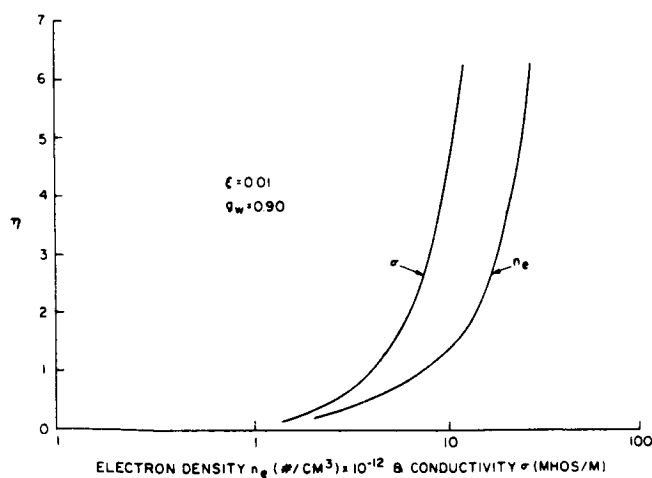


Figure 6. Electrical Conductivity and Electron Density vs. η at $\xi = .01$ for $g_w = 0.9$

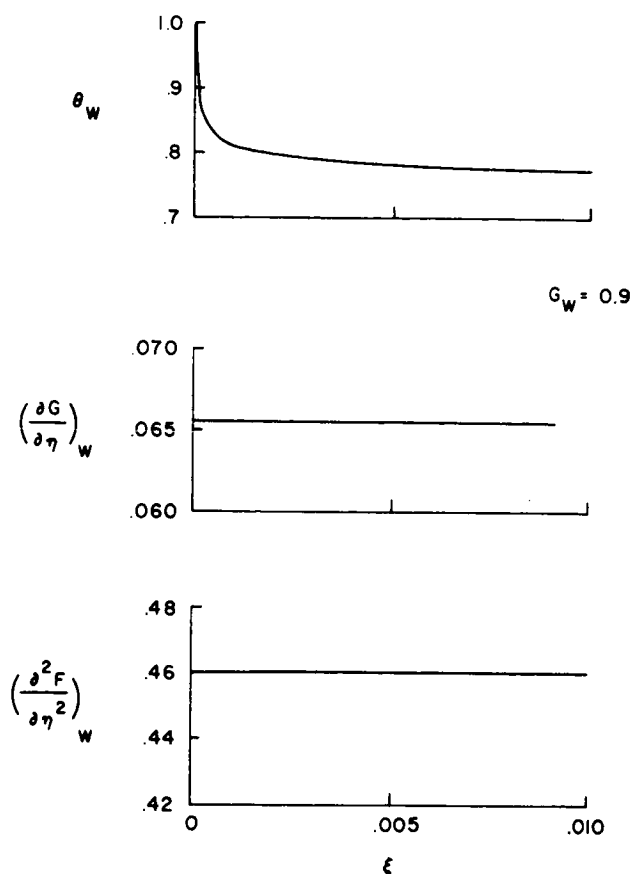


Figure 7. Wall Parameters vs. Distance ξ for $g_w = 0.9$

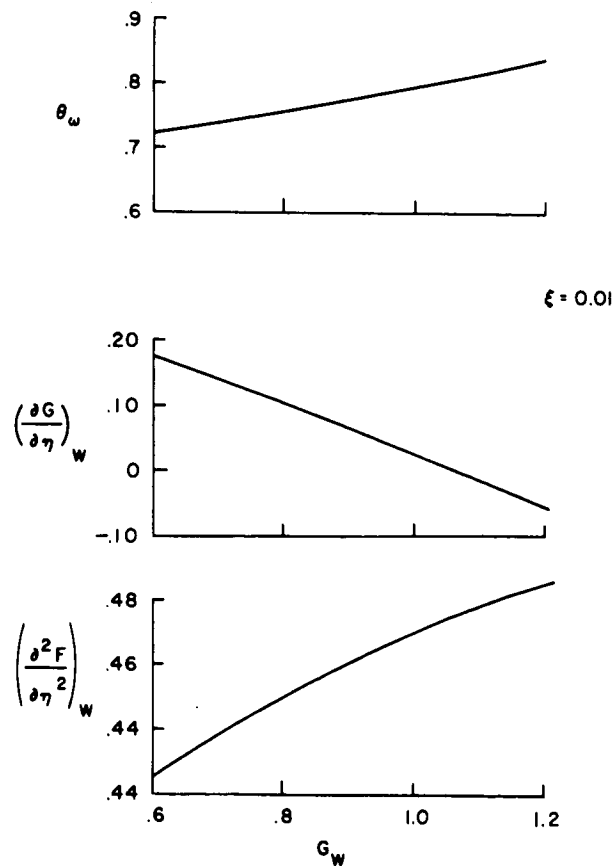


Figure 8. Wall Parameters vs. g_w at $\xi = .01$

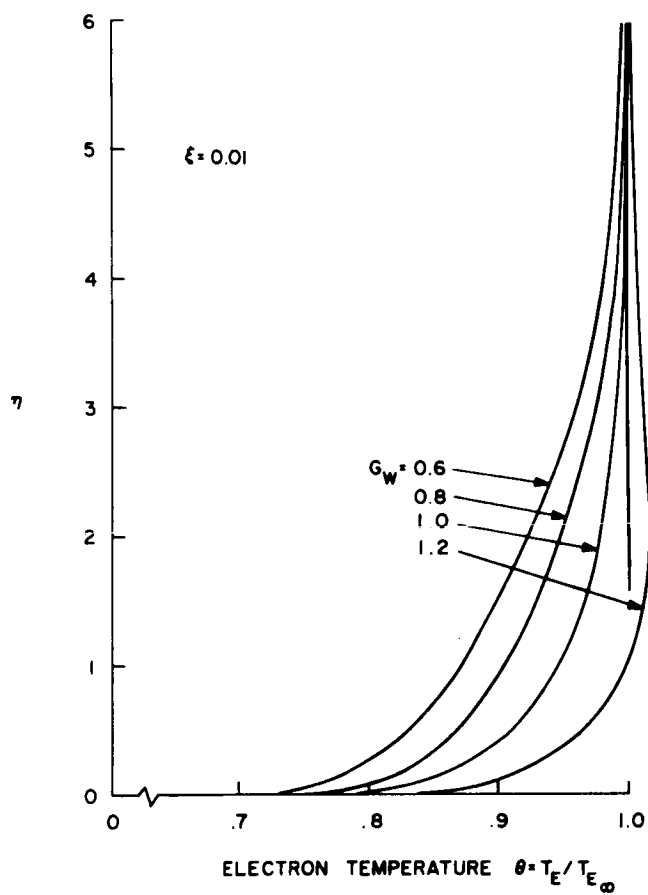


Figure 9. Electron Temperature Profiles with g_w as Parameter at $\xi = .01$

APPENDIX F

The flow diagram and listing included here are for the computer program written to carry out the calculation of the initial profile. A fourth order Runge-Kutta method subroutine is employed to solve the equations described in Sections II and III.

The following equivalence between major variable names employed in the equations and in the program should be noted:

$$U (1) = f = - V$$

$$U (2) = f'$$

$$U (3) = f''$$

$$U (4) = g$$

$$U (5) = g'$$

$$U (6) = \theta$$

$$U (7) = \theta'$$

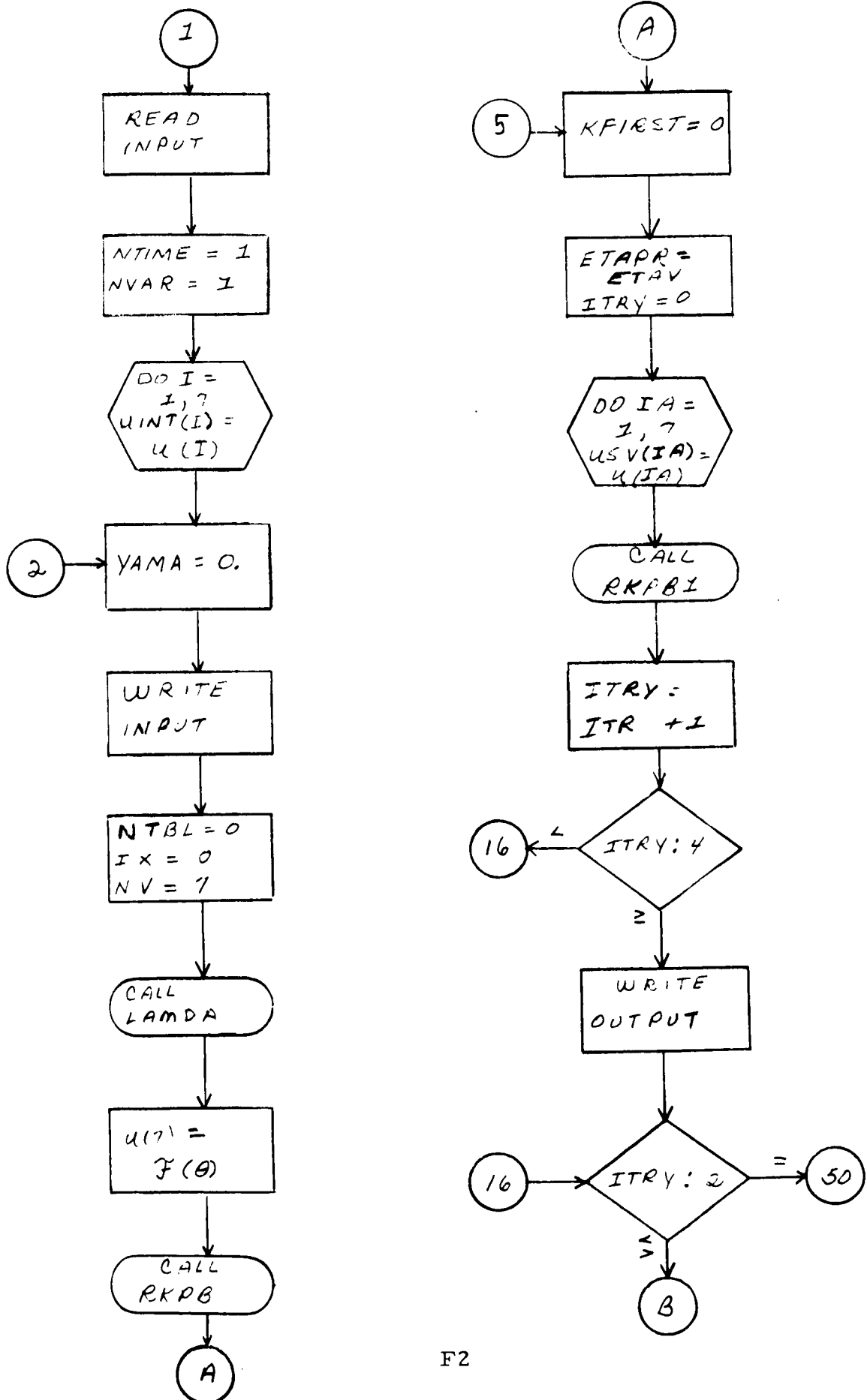
$$\mathcal{F} (\dots) = \text{function of } (\dots)$$

$$F (3) = f''' = \mathcal{F}(f, f'', g, g')$$

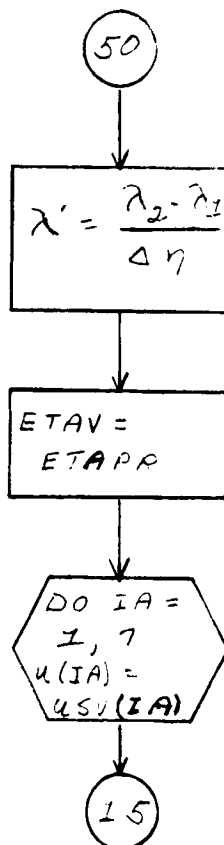
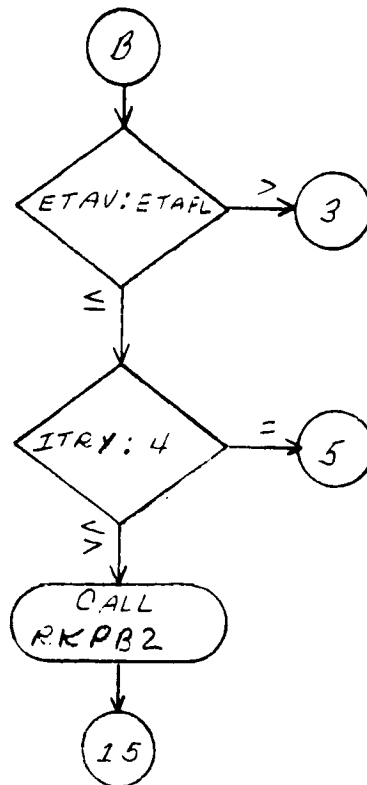
$$F (5) = g'' = \mathcal{F}(f, f'', g, g', \theta, \theta')$$

$$F (7) = \theta'' = \mathcal{F}(f, g, g', \theta, \theta')$$

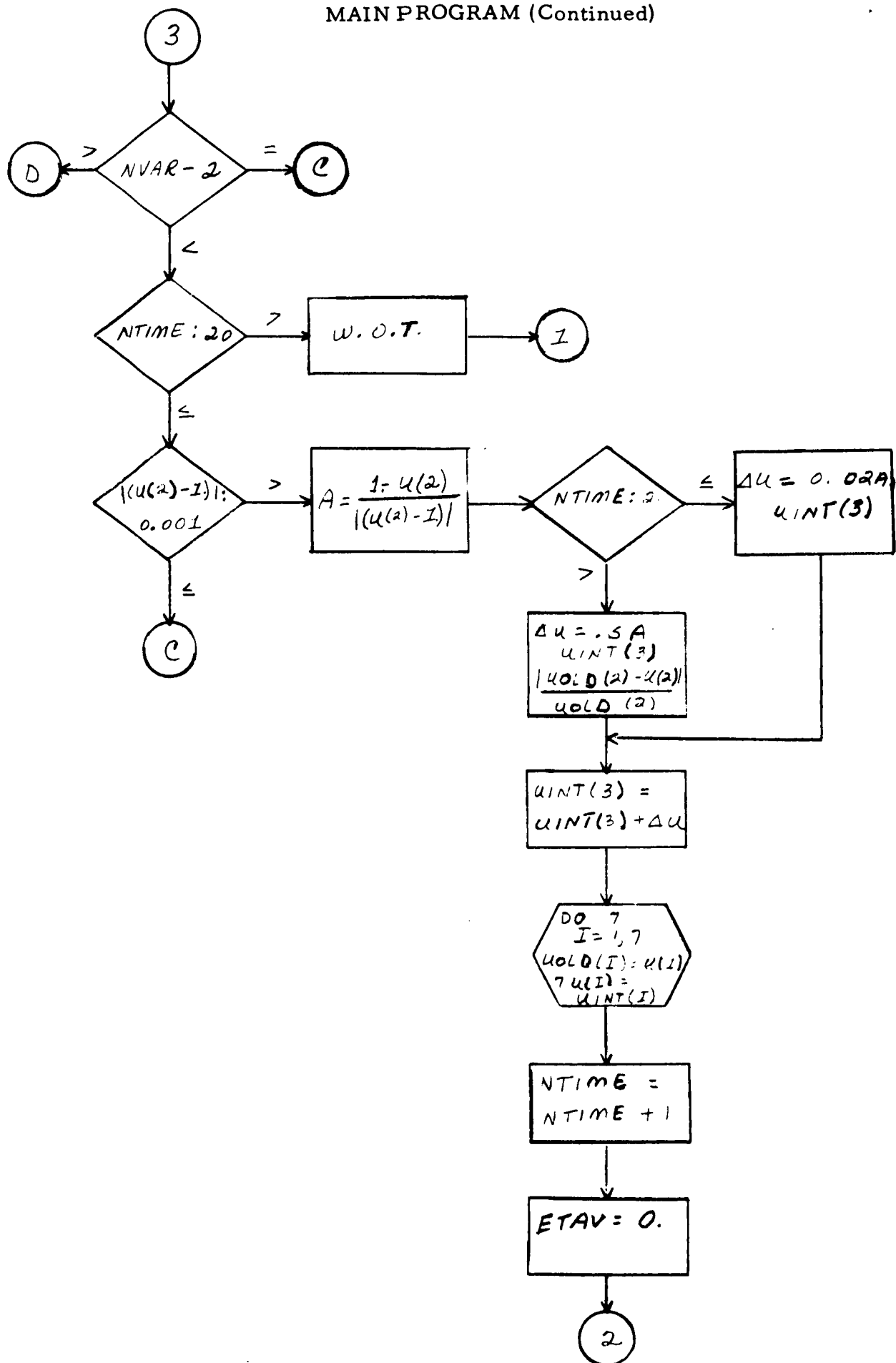
MAIN PROGRAM



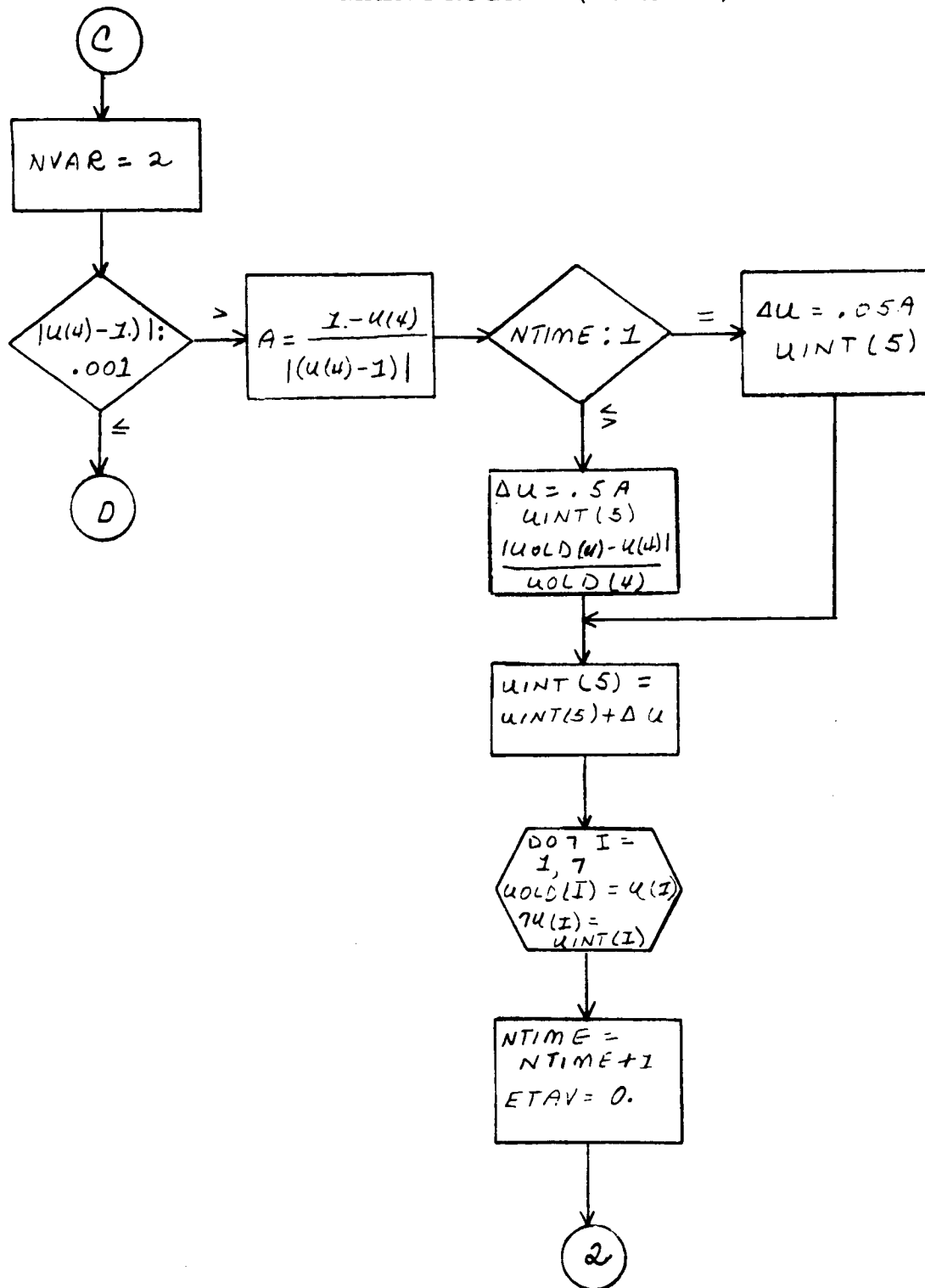
MAIN PROGRAM (Continued)



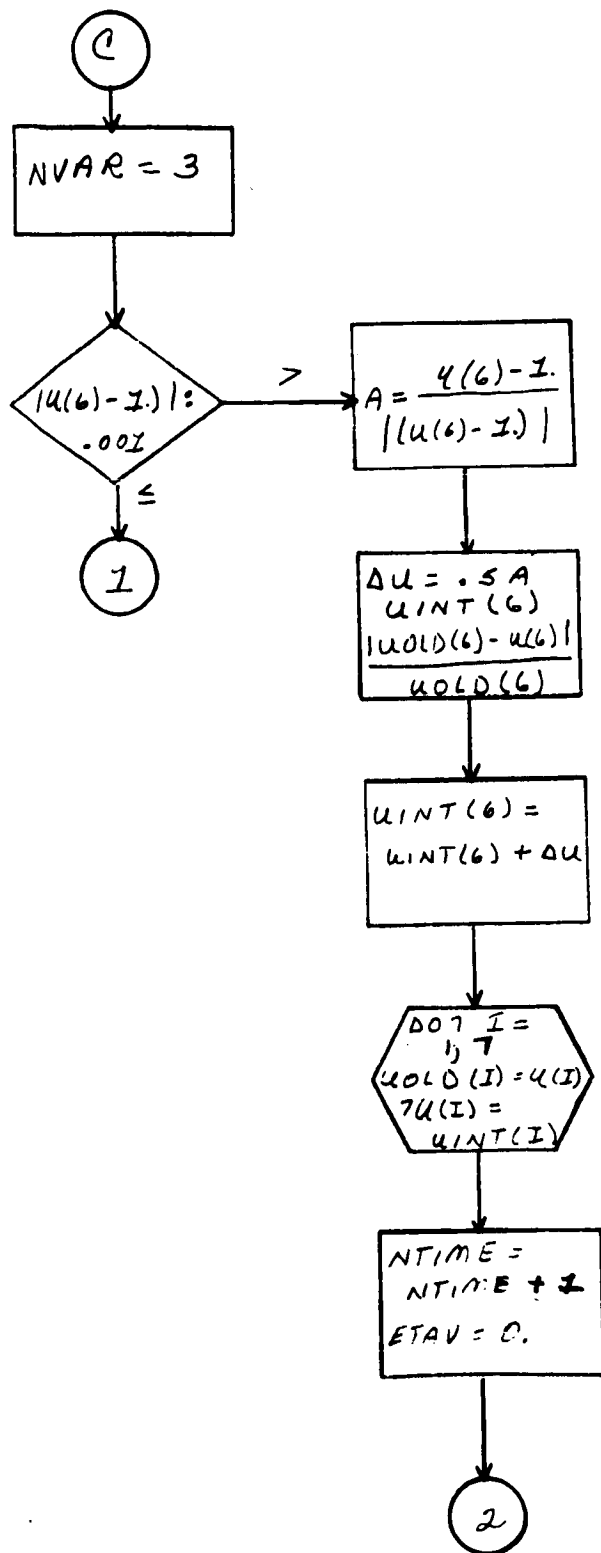
MAIN PROGRAM (Continued)



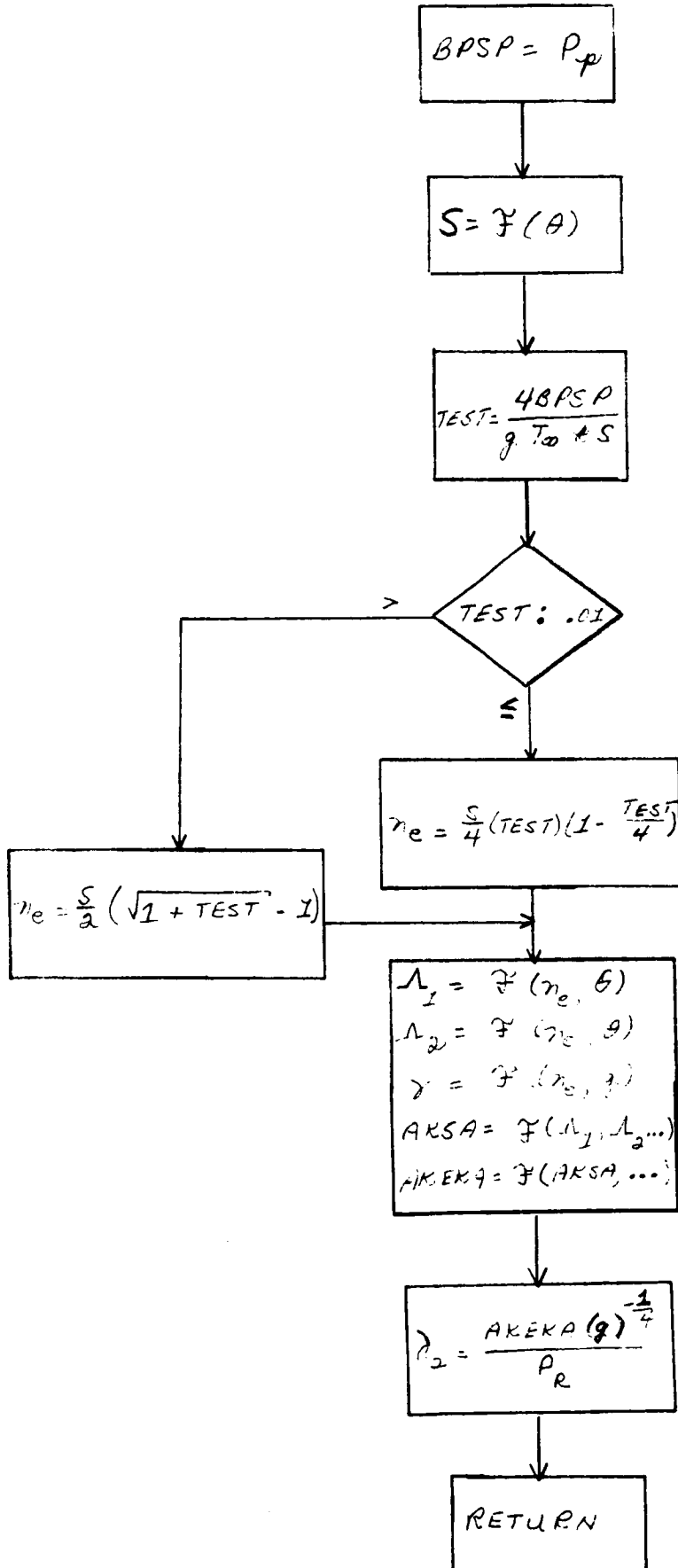
MAIN PROGRAM (Continued)



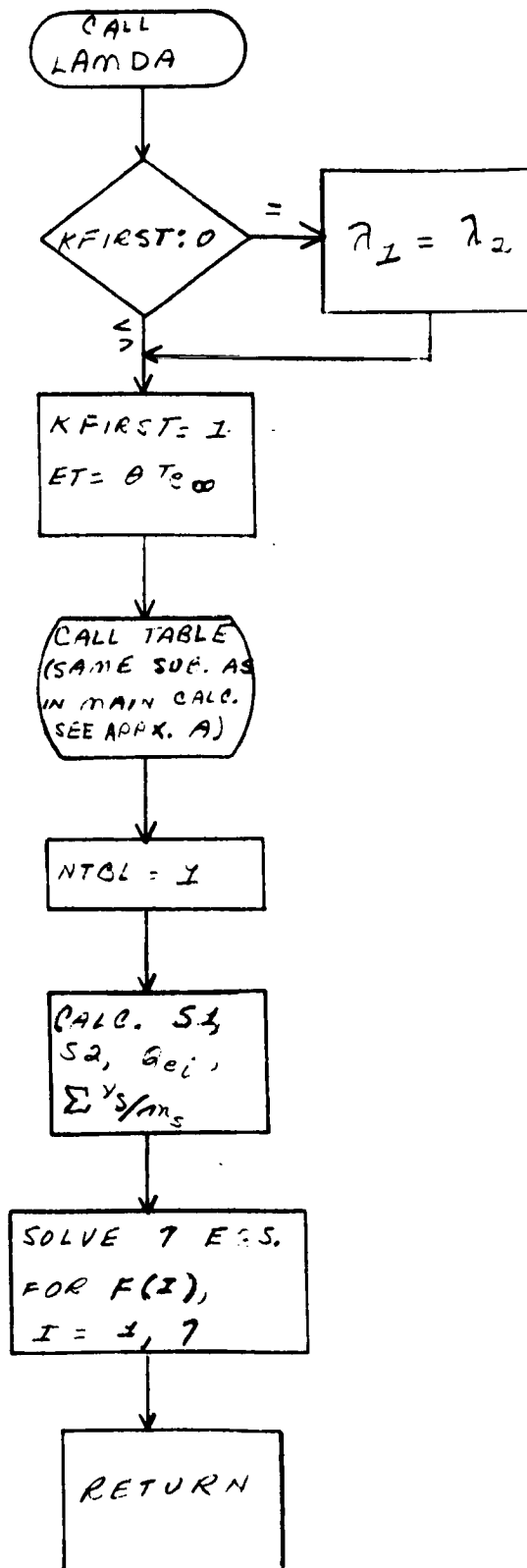
MAIN PROGRAM (Continued)



LAMDA



DERIV*



*The Runge-Kutta integration subroutine CALLS DERIV, which contains the seven first-order non-linear differential equations for simultaneous solution.

A20 1 07-25-67 MAIN PROGRAM

1	C MAIN	MAIN PROGRAM	
2		COMMON /CCOM1/ PIZ,CP,ETE,UE,CM,EM,IE,C1,C2,PER,PRN,EKS1,AK0,EC,	
3		1UEAQA,ROMR,HK,PRES,PI,SM,RHOE	
4		COMMON/CCOM2/ U(7),F(7),YAM1,YAM2,YAMA,KFIRST	
5		COMMON /CCOM3/ BPSP,ET,TEST,S,ENE,NIBL	
6		COMMON /CCOM4/ TEMPRA,QEAT,QECST,NTBA	
7		DIMENSION TEMPRA(50),QEAT(50),QECST(50)	
8		DIMENSION USV(7),ATEMP(32)	
9		DIMENSION UINT(7),UOLD(7)	
10		EXTERNAL DERIV	
11		NAMelist /INPUT/ U,DETA,ETAV,ETAFL,TEMPRA,QEAT,QECST,NTBA	
12		NAMelist/OUTPUT/ YAMA,U,F,ETAV,DETA,YAM1,YAM2,I TRY	
13		1 READ(5,INPUT)	
14		NIME = 1	2
15		NVAR = 1	3
16		DO 11 I=1,7	4
17	11	UINI(I)=U(I)	5
18	2	YAMA=U.	7
19		WRITE(6,INPUT)	8
20		NIBL=U	9
21		IX=U	10
22		NV=7	11
23	C		
24	C	FIND LAMDA FOR THETA PRIME CALCULATION	
25	C		
26		CALL LAMDA	12
27		U(7)=4.*SQRT(2.*EKS1)*(CM/ROMR/UE*SQRT(BK*ETE/SM))*(2,+.5*A LOG(SM/	13
28		1(2.*PI*EM)))*U(6)**1.5	
29		CALL MKPB(DERIV,ATEMP,ETAV,DETA,U,F,NV)	14
30	C		
31	C	ETAV IS THE INDEPENDENT VARIABLE	
32	C	DETA IS THE DELTA ETA	
33	C	U IS THE DEPENDENT VARIABLE ARRAY	
34	C	F IS THE DERIVATIVE ARRAY	
35	C	ETAFL IS THE FINAL ETA	
36	C		
37	5	KFIRST=U	15
38	C		
39	C	KFIRST IS A CONTROL TO SAVE YAM1 INITIALLY IN DERIV	
40	C		
41		ETAPR=ETAV	16
42		I TRY=U	17
43		DO 10 IA=1,7	18
44	10	USV(IA)=U(IA)	19
45	15	CALL MKPB1	21
46		I TRY=I TRY+1	22
47		IF (I TRY.LT.4) GO TO 16	23
48		WRITE(6,OUTPUT)	26
49	16	IF (I TRY.EQ.2) GO TO 50	27
50	C		
51	C	TEST FOR FINAL ETA	
52	C		

53	IF (ETAV.GE.ETAFL) GO TO 3	30
54	IF (ITRY.EQ.4) GO TO 5	33
55	CALL RKPR2	36
56	GO TO 15	37
57	C	
58	C RE-CALCULATE LAMDA PRIME	
59	C	
60	50 YAMA=(YAM2-YAM1)/DETA	38
61	C	
62	C RESET VALUES TO PREVIOUS POINT	
63	C	
64	ETAV=ETAPR	39
65	DO 60 I=1,7	40
66	60 U(I)=USV(I)	41
67	GO TO 15	43
68	3 IF (NVAR-2) 100,101,102	44
69	100 IF (NIME-20) 103,103,104	45
70	104 WRITE (6,105)	46
71	105 FORMAT (34H1 FAILED TO CONVERGE GO TO NEXT CASE)	48
72	GO TO 1	48
73	103 IF (ABS(U(2)-1.)-.001) 101,101,107	49
74	107 A = (1.-U(2))/ABS(U(2)-1.)	50
75	IF (NIME.GT.1) GO TO 108	51
76	DELU = .02*A*UINT(3)	54
77	GO TO 109	55
78	108 DELU = .5*A*UINT(3)*ABS(UOLD(2)-U(2))/UOLD(2)	56
79	109 UINI(3) = UINI(3)+DELU	57
80	DO 7 I=1,7	58
81	UOLD(I)=U(I)	59
82	7 U(I) = UINI(I)	60
83	NIME = NIME+1	62
84	ETAV = 0.	63
85	GO TO 2	64
86	101 NVAR = 2	65
87	IF (NIME-20) 111,111,104	66
88	111 IF (ABS(U(4)-1.)-.001) 102,102,110	67
89	110 A = (1.-U(4))/ABS(U(4)-1.)	68
90	IF (NIME.GT.1) GO TO 115	69
91	DELU = .05*A*UINT(5)	72
92	GO TO 116	73
93	115 DELU = .5*A*UINT(5)*ABS(UOLD(4)-U(4))/UOLD(4)	74
94	116 UINI(5) = UINI(5)+DELU	75
95	DO 8 I=1,7	76
96	UOLD(I) = U(I)	77
97	8 U(I) = UINI(I)	78
98	NIME = NIME+1	80
99	ETAV = 0.	81
100	GO TO 2	82
101	102 NVAR = 3	83
102	IF (NIME-20) 112,112,104	84
103	112 IF (ABS(U(6)-1.)-.001) 1,1,113	85
104	113 A = (U(6)-1.)/ABS(U(6)-1.)	86

02A20 1 07-25-67

MAIN PROGRAM

105	IF (N1IME.GT,1) GO TO 117	87
106	DELU = .01*A*U1NT(6)	90
107	GO TO 113	91
108	117 DELU = .5*A*U1NT(6)*ABS(UOLD(6)-U(6))/UOLD(6)	92
109	118 U1NT(6) = U1NT(6)+DELU	93
110	DO 9 I=1,7	94
111	UOLD(I) = U(I)	95
112	9 U(I) = U1NT(I)	96
113	N1IME = N1IME+1	98
114	ETAV = J.	99
115	GO TO 2	100
116	END	101

B1R09 2

07-17-67

BLOCK PROGRAM

```
1      C BLOCK      BLOCK PROGRAM
2      BLOCK DATA
3      COMMON /CCOM1/ PIZ,CP,ETE,UE,CM,FM,TF,C1,C2,PER,PRN,EKS1,AK0,EC,
4      1GEAQAA,ROMR,BK,PRES,PI,SM,RHOE
5      DATA PIZ/6.22E-19/,CP/515./,ETF/1920./,UE/395.4/,CM/6.67E-26/,
6      1FM/9.107E-31/,TE/1920./,C1/2.420E21/,C2/4.49E4/,PER/.01/,
7      2PRN/.666667/,EKS1/.01/,AK0/8.854E-12/,EC/1.602E-19/,GEAQAA/.1/,
8      3ROMR/449.5775E-7/,BK/1.38E-23/,PRES/164000./,PI/3.1416/,
9      4SM/2.2E-25/,RHOE/.5/
10     END
```

R1809 3 07-17-67

LAMDA CALCULATION

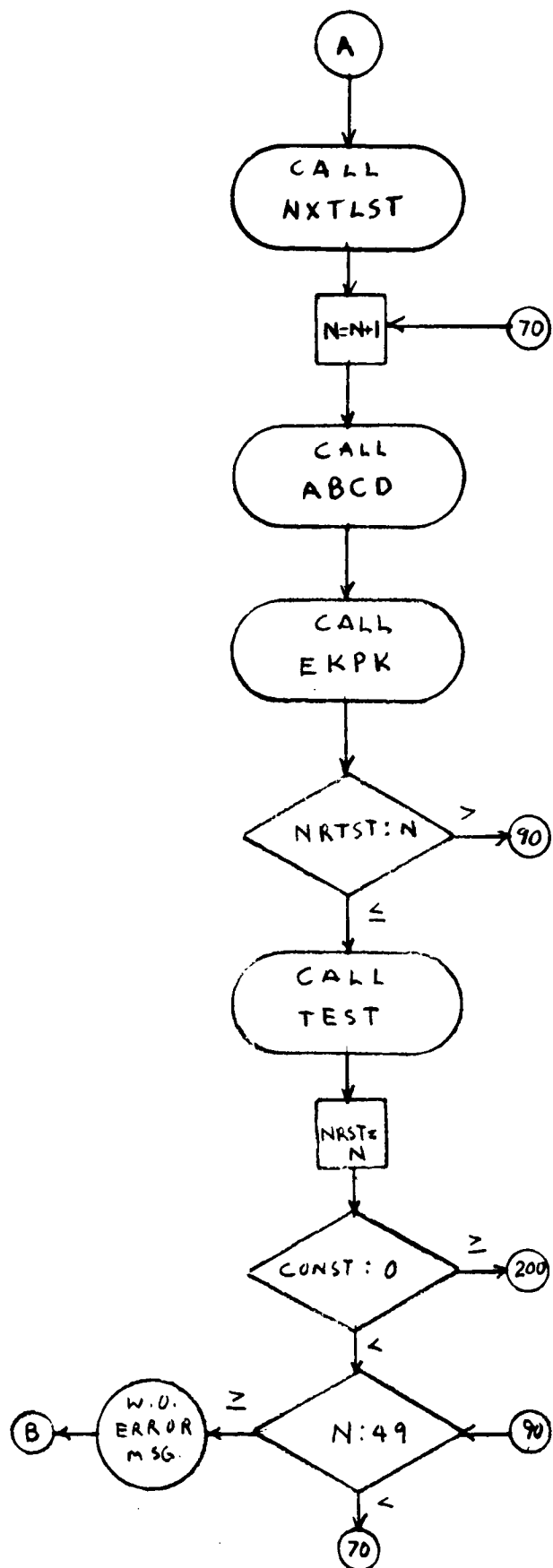
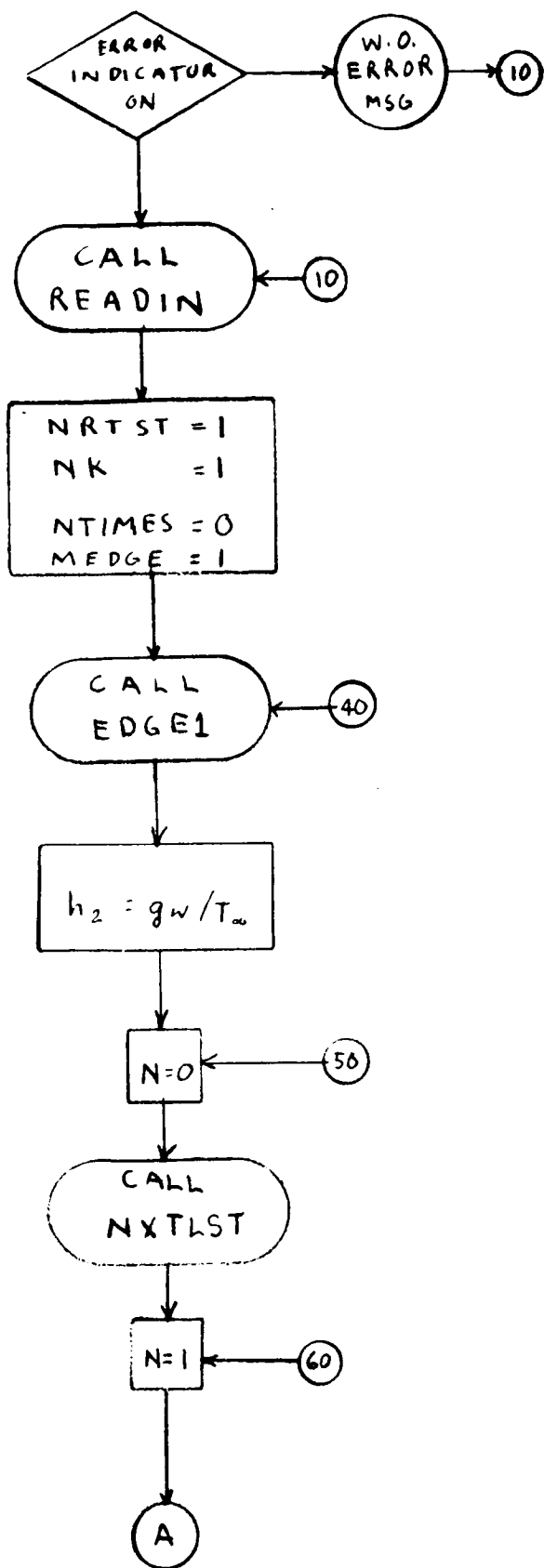
1	C LAMDA	LAMDA CALCULATION	
2		SUBROUTINE LAMDA	
3		COMMON /CCOM1/ PIZ,CP,ETE,UE,CM,FM,TE,C1,C2,PER,PRN,EKS1,AK0,EC,	
4		1QEAQAA,ROMR,BK,PRES,PI,SH,RHOE	
5		COMMON/CCOM2/ U(7),F(7),YAM1,YAM2,YAMA,KFIRST	
6		COMMON /CCOM3/ BPSP,ET,TEST,S,ENE,NTBL	
7		BPSP=PER*PRES	
8		S=C1*ETE**(1.5)*U(6)**(1.5)*EXP(-C2/(ETE*U(6)))	2
9		TEST=4.*BPSP/(U(4)*TE*S*BK)	3
10		IF(TEST,GT.,.01) GO TO 15	4
11		FNF=TEST*S/4.*(1.-TEST/4.)	7
12		GO TO 20	8
13	15	FNF=S/2.*(SQRT(1.+TEST)-1.)	9
14	20	ALAM1=1.24E7*(ETF*U(6))**1.5/ENE**5	10
15		ALAM2=1.8E5*ETE*U(6)/ENE**(1./3.)	11
16		GAMMA=BK*TE*ENE*U(4)/PRES	12
17		AKSKA=(7.5F-7*(U(6)*ETE)**2.5/(TE*U(4))**.75)/(1.25*ALOG(55.+ALAM1	13
18		1**4+ALAM2**4))	
19		AKFKA=AKSKA/(1.+1.414214*1./GAMMA*AKSKA*QEAQAA*SQRT((EM/CM)*(U(4)*	14
20		1TE)/(U(6)*ETE)))	
21		YAM2=AKEKA*U(4)**(-.25)/PRN	15
22	500	RETURN	16
23		END	17

```

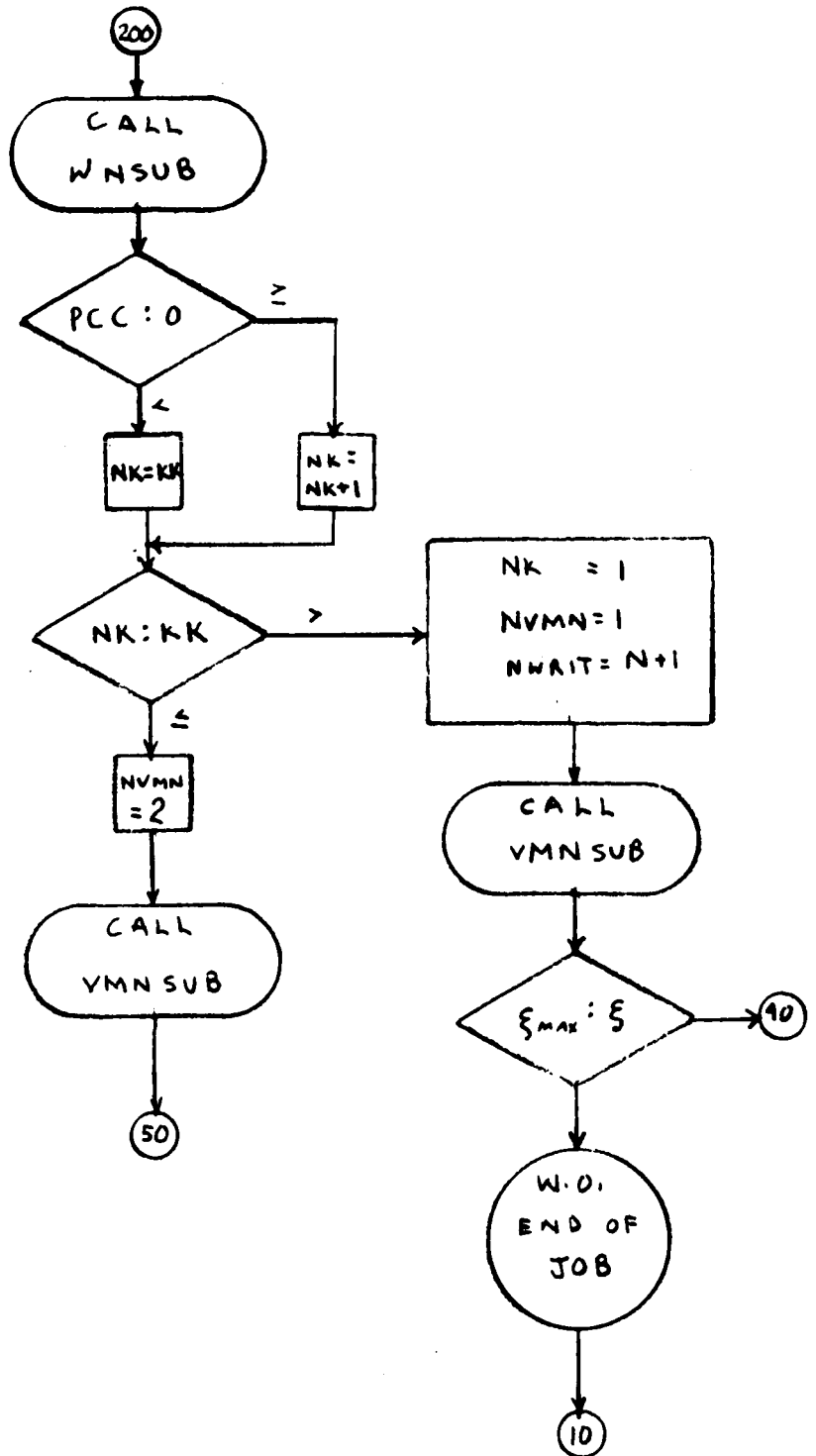
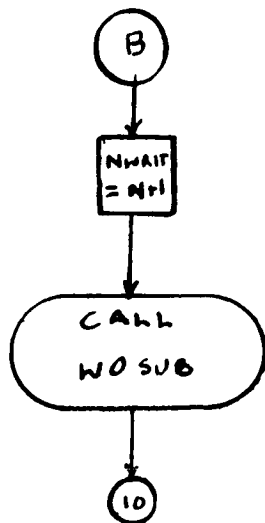
1      C DERIV      DERIVATIVE ROUTINE
2      SUBROUTINE DERIV
3      COMMON /CCOM1/ PIZ,CP,ETE,UE,CM,FM,TE,C1,C2,PER,PRN,EKS1,AK0,EC,
4      10EAQAA,ROMR,BK,PRES,PI,SM,RHOE
5      COMMON /CCOM2/ U(7),F(7),YAM1,YAM2,YAMA,KFIRST
6      COMMON /CCOM3/ BPSP,ET,TEST,S,ENE,NTBL
7      COMMON /CCOM4/ TEMPRA,QEAT,QECST,NTBA
8      DIMENSION TEMPRA(50),QEAT(50),QECST(50)
9      CALL LAMDA
10     IF(KFIRST.EQ.0) YAM1=YAM2
11     KFIRST=1
12     ET=U(6)*ETF
13     10 CALL TABLE(TEMPRA,QEAT,QECST,ET,NTBA,NTBL,QEA,QECS)
14     15 NTBL=1
15
16     C
17     C      CALCULATE VARIABLES
18     C
19     20 S1=S*(3./(2.*ETF*U(6))+C2/(ETE*U(6))**2)*(-.5+(S/2.+TEST*S/4.)/(S*
20     1SQRT(1.+TEST)))
21     TERM1=1./U(4)*BK
22     S2=((4.*CM*BPSP/(5.*TE**2))*TERM1)*(TERM1/(SQRT(1.+TEST)))
23     TERM1=PI*U(6)**(1.5)*((EC/(16.*BK))*(EC/(AK0*ETE))*(1./U(6))**2
24     1))*(SQRT(AK0*ETE))
25     30 QEI=TERM1*TERM2
26     TERM1=(QEA/CM)*(PRES/(BK*TE))*(1./U(4))+(QEC/SM)*((BPSP/(BK*TE))*
27     1(1./U(4))-ENE)+(QFI/SM)*ENE
28     40 SNUS=TERM1*SQRT(((8.*BK*ETE)/(PI*EM))*U(6))
29
30     C
31     C      CALCULATE DERIVATIVES
32     C
33     F(1)=U(2)
34     F(2)=U(3)
35     F(3)=U(4)**.25*U(3)*(.25*U(4)**(-1.25)*U(5)-U(1))
36     F(4)=U(5)
37     CSNT1=BK*ETE*U(6)
38     TERM1=YAMA*U(7)+(U(1)*U(4)*U(7)/(RHOE*CP))*(1.5*BK*ENE+(1.5*CSNT1+
39     1PIZ)*S1)
40     TERM2=U(5)*U(1)/(RHOE*CP*ETE)*((1.5*CSNT1+PIZ)*S2+ENE*(2.5*CSNT1+
41     1PIZ))
42     TERM3=(ENE*U(4)*2.*EKS1/(ROMR*UE**2))*(3.*BK*ETE/(RHOE*CP*TE))*(EM
43     1*SNUS)*(U(6)-TE*U(4)/ETE)
44     50 F(7)=-1./YAM2*(TERM1-TERM2+TERM3)
45     TERM1=U(1)*U(5)-(U(4)**(-1.25)*U(5)**2/(4.*PRN))*(UE*U(3))**2*U(4)
46     1*(-.25)/(CP*TE)
47     TERM2=ETE/TE*(U(7)*YAMA+YAM2*F(7))*PIZ*((ETE/(RHOE*CP*TE))*S1*U(1)
48     1*U(4)*U(7)-S2*U(1)*U(4)*U(5)/RHOE*ENE*U(1)*U(5)/(RHOE*CP*TE))
49     F(5)=-PRN*U(4)**(.25)*(TERM1+TERM2)
50     F(6)=U(7)
51     500 RETURN
      END

```

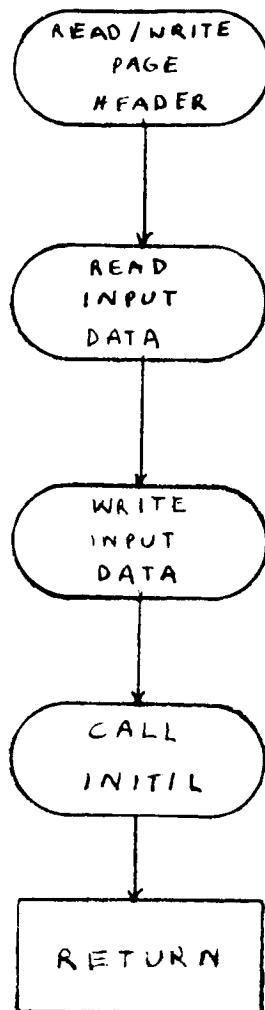
MHD BOUNDARY LAYER MAIN PROGRAM



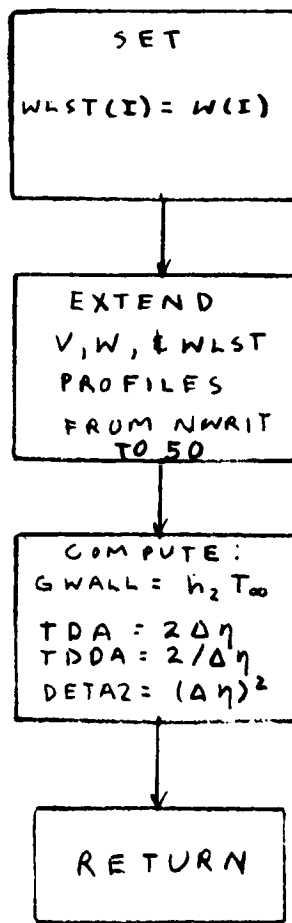
MAIN PROGRAM (Cont.)



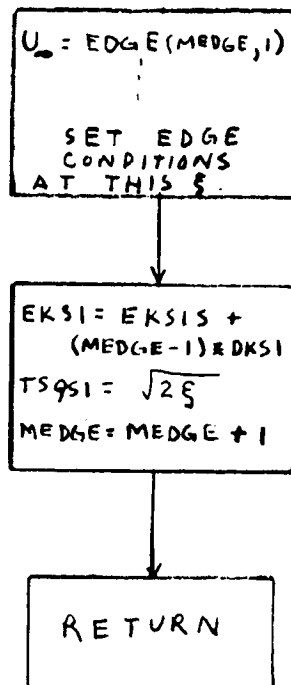
SUBROUTINE READIN



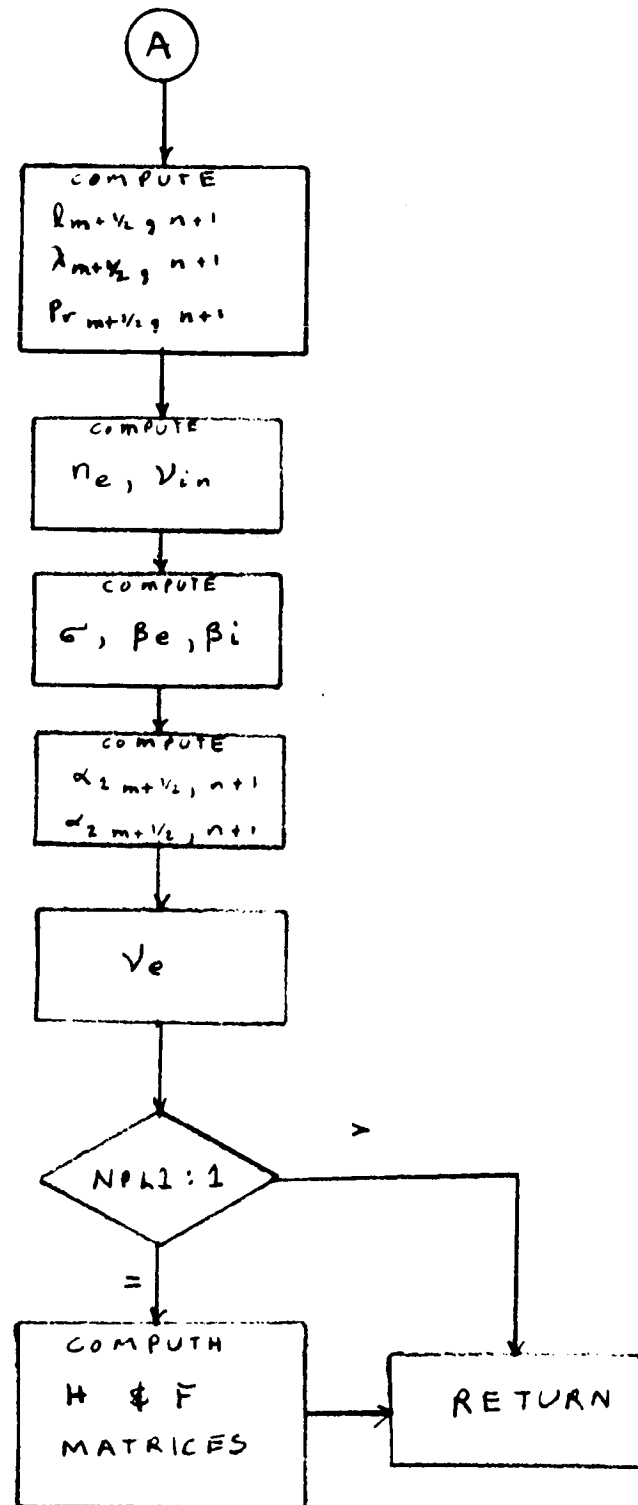
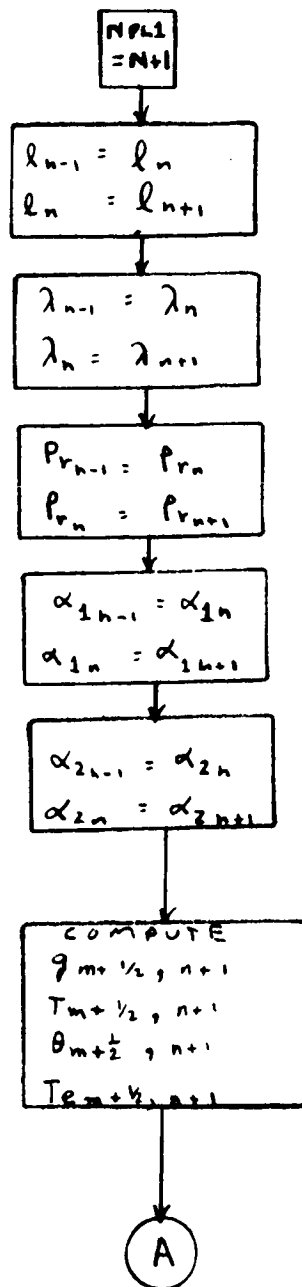
SUBROUTINE INITIAL



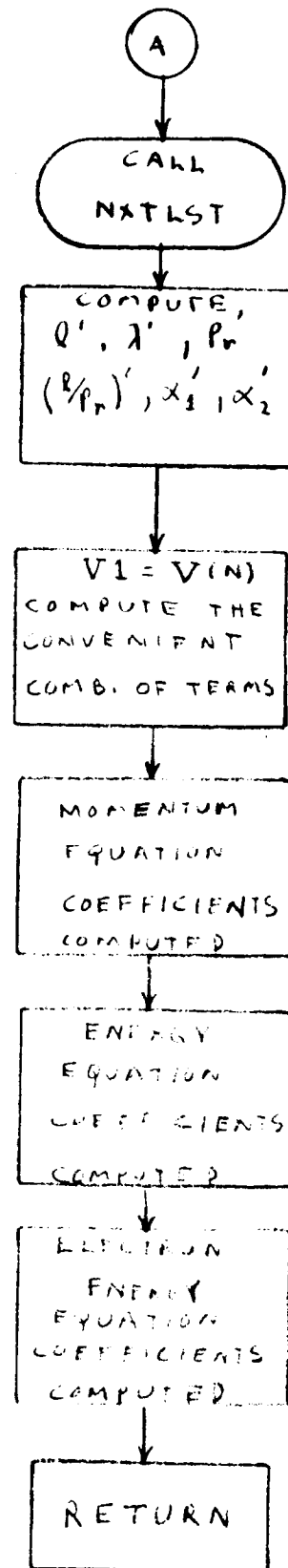
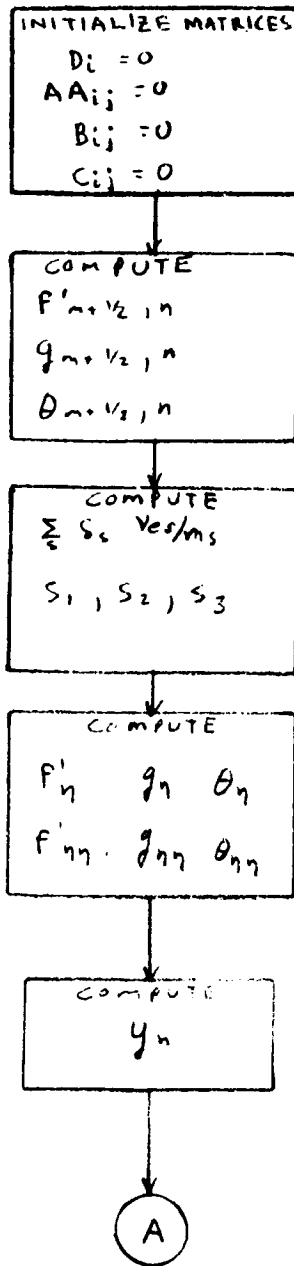
SUBROUTINE EDGE 1



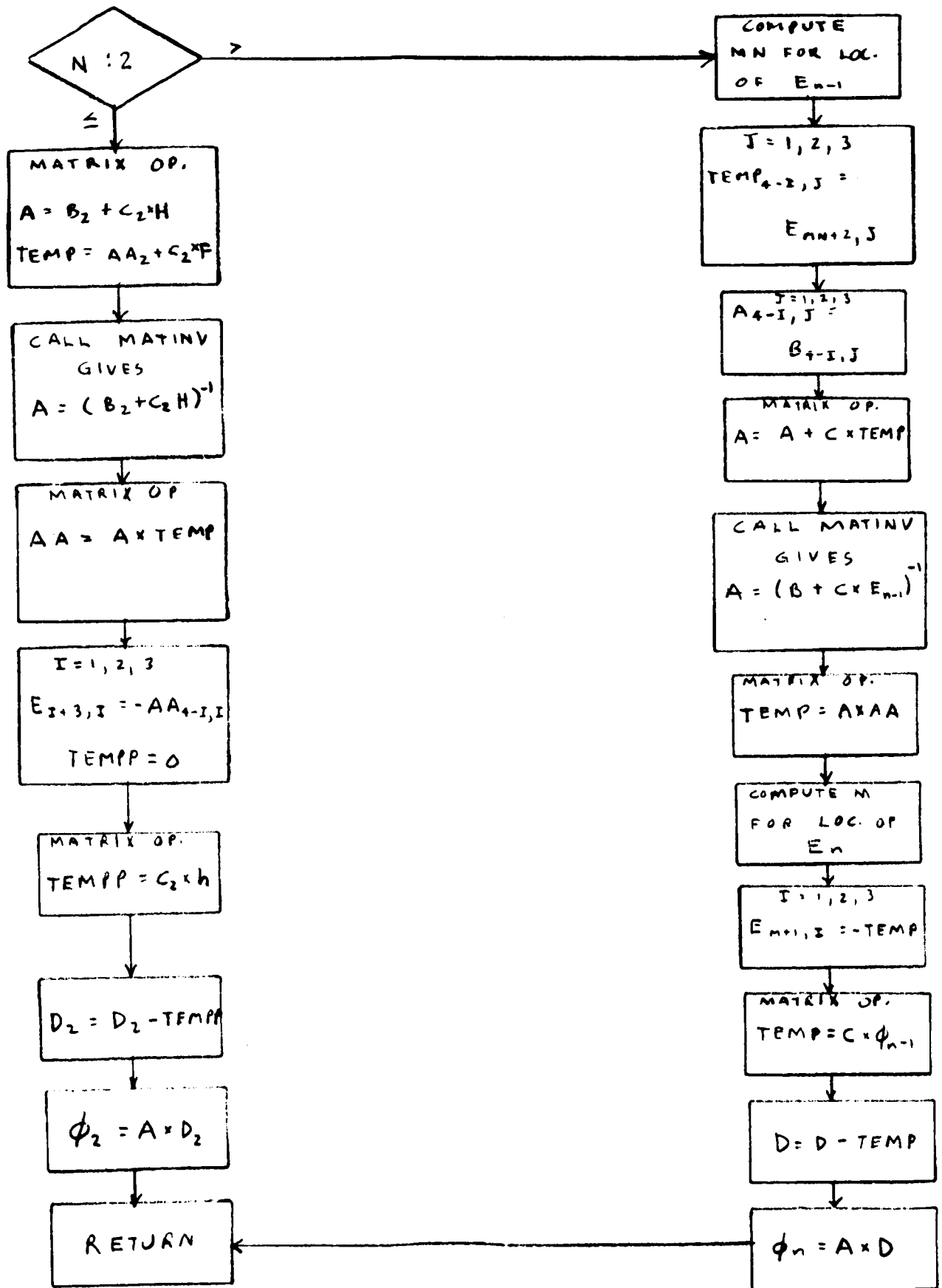
SUBROUTINE NXTLST



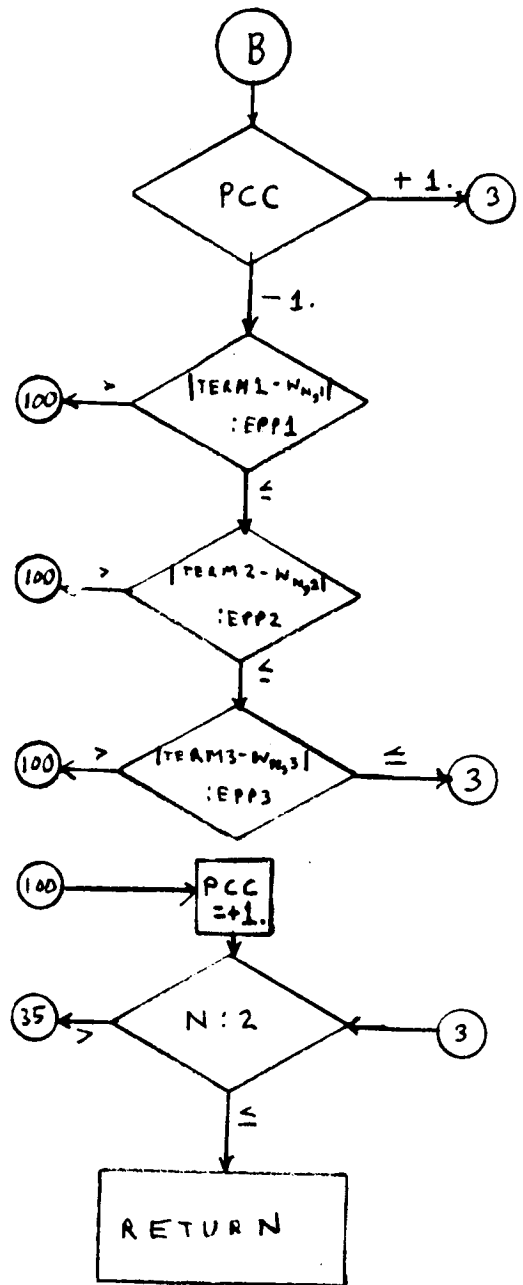
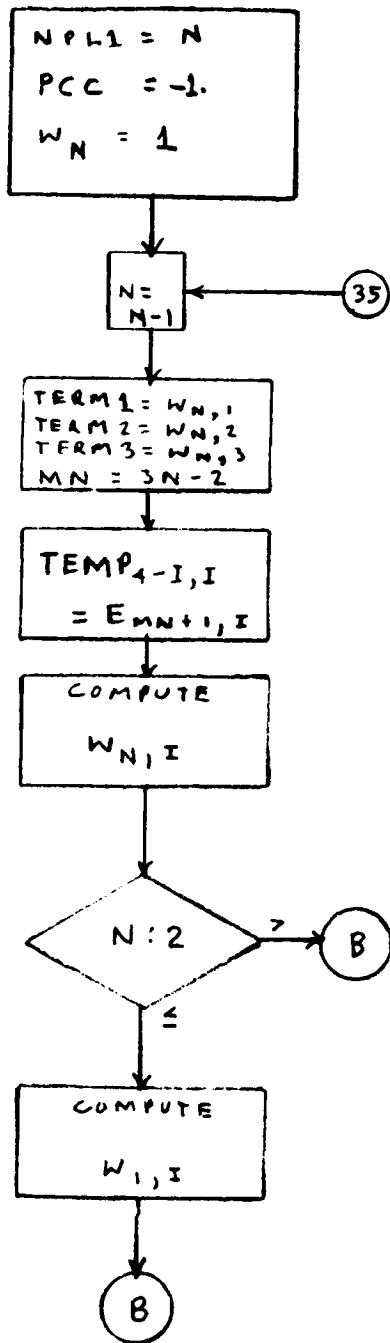
SUBROUTINE ABCD



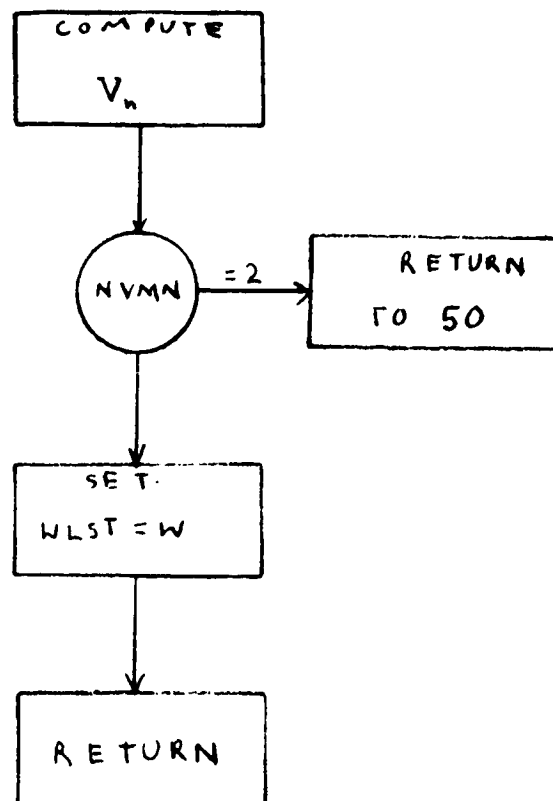
SUBROUTINE EKP



SUBROUTINE WNSUB



SUBROUTINE VMNSUB




```
COMMON/COM1/BK,EM,EC,C1,PI,AKO,R,Y(1000),TE,DUM(10),TW,EKSI, EKSI  
1,DUM1(7),MEDGE,EKSI  
  
COMMON/COM3/SMLHH(3),V(1000),WLST(1000,3),W(1000,3),TEEKSI(10)  
  
COMMON/COM5/N,NPL1,PCC,NWRIT,KK,NK,CONST,NRTST,NTIMES,DUM3(9),NVMN  
  
C RETURN HERE FOR START OF NEXT CASE  
  
10 MEDGE=1  
  
NRTST = 1  
  
NTIMES = 0  
  
NK = 1  
  
BK = 1.38E-23  
  
EM = 9.107E-31  
  
EC = 1.602E-19  
  
C1 = 2.42E21  
  
PI = 3.1416  
  
AKO = 8.854E-12  
  
Y(1) = 0.  
  
R = 8.317E3  
  
CALL READIN  
  
40 CALL EDGE1  
  
SMLHH(2) = TW/TEEKSI(MEDGE)  
  
50 N = 0  
  
CALL NXTLST  
  
60 N = 1  
  
CALL NXTLST  
  
70 N = N+1  
  
CALL ABCD  
  
CALL EKPK  
  
IF (NRTST-N) 80,80,90  
  
80 CALL TEST
```

```

      NRTST = N
      IF (CONST) 90,200,200
90  IF (N-999) 70,110,110
C    CONVERGENCE NOT ATTAINED, PRINT AND GO TO NEXT CASE
110 WRITE (6,903)
      NWRIT = NPL1
      CALL WOSUB
      GO TO 10
C    CONVERGENCE ATTAINED, GO TO NEXT PROFILE
200 CALL WNSUB
      IF (PCC) 201,202,202
201 NK = KK
202 IF (KK-NK) 220,220,210
C    ITERATE UP TO (K-1) TIMES
210 NVMN = 2
      NK = NK+1
      CALL VMNSUB($50)
C    INITIALIZE FOR NEXT PROFILE
220 NK = 1
      NVMN = 1
      NWRIT = NPL1
      CALL VMNSUB($50)
      IF (EKSIM-EKSI) 260,260,40
260 WRITE (6,902)
      N=NWRIT-1
      PUNCH 900,((W(I,J),I=1,N),J=1,3)
      PUNCH 900,(V(I),I=1,N)
      PUNCH 901,(N)
      GO TO 10
900 FORMAT (4E18.8)

```

901 FORMAT (7H NWRIT=,I4)

902 FORMAT (16H THATS ALL FOLKS)

903 FORMAT (36H CONVERGENCE NOT ATTAINED, TRY AGAIN)

END

CHEADIN

```

SUBROUTINE READIN
  DIMENSION ARAKSI(10)
  COMMON/COM1/DUM1(1018),TW,EKSI,EKSI,DKSI,DUM2(3),DETA,TSQSI,DELTA,
  1A,MEGE,EKSI
  COMMON/COM2/EDGE(10,11),TEMPRA(50),QEAT(50),QECST(50)
  COMMON/COM3/SMLHH(3),V(1000),WLST(1000,3),W(1000,3),TEEKSI(10)
  COMMON/COM5/N,NPL1,PCC,NWRIT,KK,NK,CONST,NRTST,NTIMES,EP1,EP2,EP3,
  1ERR,EPP1,EPP2,EPP3,NPRINT,NTAB,NVMN
  COMMON/COM6/DUM3(25),C2,PER,QIN,CP,ROMR,CM,TIW,TIWC,PIZ,SM,BZ
  DIMENSION FF(12)
  NAMELIST/NAME1/DELTA,EKSI,EKSI,DKSI,DETA,QIN,CM,SM,TIWC,CP,PER,P
  1I,C2,BZ,ERR,EPP1,EPP2,EPP3,EP1,EP2,EP3
  NAMELIST/NAME2/TEMPRA,QEAT,QECST,EDGE,SMLHH,TEEKSI,NWRIT
  NAMELIST/NAME3/KK,NTAB
  READ (5,911)(FF(I),I = 1,12)
  CALL SPGHDR(FF)
  READ (5,NAME1)
  READ (5,NAME2)
  7 READ (5,NAME3)
  IF (NWRIT .EQ. 0) GO TO 8
  READ (5,899)((W(I,J),I=1,NWRIT),J=1,3)
  READ (5,899)(V(I),I=1,NWRIT)
899 FORMAT (4E18.8)
  GO TO 9
  8 NWRIT = N
  9 CONTINUE
  ROMR=3.1E-7*EDGE(1,7)*EDGE(1,2)**.75
  WRITE (6,900)EKSI,EKSI,DKSI,DETA,QIN
900 FORMAT (7HDEKSI=E16.8,3X,6HEKSI=E16.8,3X,5HDKSI=E16.8,3X,5HDETA=
  1E16.8,3X,4HQIN=E16.8//)
  WRITE (6,901)DELTA,ROMR,CM,SM,CP
901 FORMAT (7HDELTA=E16.8,3X,6HROMR =E16.8,3X,5HCM =E16.8,3X,5HSM =
  1E16.8,3X,4HCP =E16.8//)
  WRITE (6,902)TIW,PER,PIZ,C2,BZ
902 FORMAT (7HTIW =E16.8,3X,6HPER =E16.8,3X,5HPIZ =E16.8,3X,5HC2 =
  1E16.8,3X,4HBZ =E16.8//)
  CALL INITIL
  CALL WOSUB
  WRITE (6,905)
905 FORMAT (1H1/14X6HTEMPRA20X4HQEAT21X5HQECST/)
  WRITE (6,906)(TEMPRA(I),QEAT(I),QECST(I),I = 1,NTAB)
906 FORMAT (1H 3E25.8)
  NN = (EKSI-EKSI)/DKSI+1.5
  WRITE (6,907)
907 FORMAT (1H1/10X4HEKSI17X2HDE18X2HTE18X3HEIF17X3HDE17X3HDE/)
  ARAKSI(1) = EKSI
  DO 10 I = 2,NN
  10 ARAKSI(I) = ARAKSI(I-1)+DKSI
  WRITE (6,908)(ARAKSI(I),(EDGE(I,J),J = 1,5),I = 1,NN)
908 FORMAT (1H 6E20.8)
  WRITE (6,909)
909 FORMAT (1H1/7X4HEKSI13X4HDETE13X4HRRHOE13X5HRRHOE12X4HAJYE14X3HEXE1
  3X4HPRFS/)
  WRITE (6,910)(ARAKSI(I),(EDGE(I,J),J = 6,11),I = 1,NN)
910 FORMAT (1H 7E17.8)
911 FORMAT (12A6)
9999 RETURN
END

```

```

SUBROUTINE INITIL
  COM 10N/COM1/DUM1(1007),TE,DUM2(10),TW,DUM3(3),TDA,TDDA,DETA2,DETA,
1DUM4(4)
  COMMON/COM3/SMLHH(3),V(1000),WLST(1000,3),W(1000,3),TEEKSI(10)
  COMMON/COM5/N,NPL1,PCC,NWRIT,DUM5(15)
  DO 10 I = 1,NWRIT
    DO 11 J = 1,3
11  WLST(I,J) = W(I,J)
10  CONTINUE
    IF (NWRIT-1000) 9,14,14
C    EXTEND PROFILES
9    NPL1 = NWRIT+1
    DO 12 I = NPL1,1000
      V(I) = V(I-1)-DETA
    DO 13 J = 1,3
      WLST(I,J) = 1.
13  W(I,J) = 1.
12  CONTINUE
14  TW = SMLHH(2)*TEEKSI(1)
    TDA = 2.*DETA
    TDDA = 2./DETA
    DETA2 = DETA**2
9999 RETURN
  END

```

CEDGE1

SUBROUTINE EDGE1

COMMON/COM1/DUM1(1007),TE,ETE,PRES,AJYE,UE,DUE,DTE,DETE,RHOE,DRHOE
1,EXE,TW,EKSIS,EKSI,DKSI,DUM2(4),TSQSI,DELTA,MEDGE,EKSI

COMMON/COM2/EDGE(10,11),DUM3(150)

COMMON/COM6/DUM4(29),ROMR,CM,TIW,TIWC,DUM5(2),BZ

UE = EDGE(MEDGE,1)

TE = EDGE(MEDGE,2)

ETE = EDGE(MEDGE,3)

DUE = EDGE(MEDGE,4)

DTE = EDGE(MEDGE,5)

DETE = EDGE(MEDGE,6)

RHOE = EDGE(MEDGE,7)

DRHOE = EDGE(MEDGE,8)

AJYE = EDGE(MEDGE,9)

EXE = EDGE(MEDGE,10)

PRES = EDGE(MEDGE,11)

ROMR=RHOE*3.1E-7*TE**.75

IF (AJYE) 1, 2, 2

1 TIW= TIWC

GO TO 3

2 TIW= 0.

3 AA = MEDGE-1

EKSI = EKSIS+AA*DKSI

MEDGE = MEDGE+1

TSQSI = SQRT(2.*EKSI)

9999 RETURN

END

CNXTLST

```
SUBROUTINE NXTLST
COMMON/COM1/BK,EM,EC,C1,PI,AKO,R,Y(1000),TE,ETE,PRES,AJYE,UE,DUM(5
1),EXE,DUM1(7),DETA,TSQS1,DUM2(3)
COMMON/COM2/EDGE(10,11),TEMPRA(50),QEAT(50),QECST(50)
COMMON/COM3/SMLHH(3),V(1000),WLST(1000,3),W(1000,3),TEEKSI(10)
COMMON/COM4/DUM4(12000),H(3,3),EF(3,3),DUM5(60)
COMMON/COM5/N,NPL1,DUM6(15),NTAB,NVMN
COMMON/COM6/ELLS,EL,ELNX,YAMLS,YAM,YAMNX,PRNLS,PRN,PRNNX,ALF1LS,AL
1F1,ALF1NX,ALF2LS,ALF2,ALF2NX,S,GNX,THENX,ENX,CONX,SXM,BETAX,QEI,QE
2A,QECS,C2,PER,QIN,CP,ROMR,CM,TIW,TIWC,PIZ,SM,BZ
QEAQAA = .1
NPL1 = N+1
ELLS = EL
EL = ELNX
YAMLS = YAM
YAM = YAMNX
PRNLS = PRN
PRN = PRNNX
ALF1LS = ALF1
ALF1 = ALF1NX
ALF2LS = ALF2
ALF2 = ALF2NX
GNX = .5*(W(NPL1,2)+WLST(NPL1,2))
THENX = .5*(W(NPL1,3)+WLST(NPL1,3))
ET = ETE*THENX
PRNNX = 2./3.
ELNX = GNX**(-.25)
S=C1*(ET)**1.5*EXP(-C2/ET)
GRP = 4.*PER/(BK*S)*PRES/TE/GNX
IF (.01-GRP) 2,1,1
```

```

1 ENX = GRP/4.*(1.-GRP/4.)*S
   GO TO 3
2 ENX = S/2.*(SQRT(1.+GRP)-1.)
3 ENUIN = (QIN/BK)*(PRES/GNX/TE)*SQRT((8.*BK*TE*GNX)/(PI*EM))
   CALL TABLE(TEMPRA,QEAT,QECST,ET,NTAB,N,QEA,QECS)
   QEI = PI*((EC/AKO)*(EC/(16.*BK*ETE*THENX))),**2
   QEI = QEI*ALOG(32.*(BK*ETE)**1.5/EC/EC*AKO**1.5/(EC*ENX**0.5)
1*(THENX**1.5))
   ENUE = PRES*QEA/(BK*GNX*TE)+(PER*PRES/BK/TE/GNX-ENX)*QECS+ENX*QEI
   SQT = SQRT(8.*BK/EM*ETE*THENX/PI)
   ENUE = ENUE*SQT
   CONX = EC/EM*EC*ENX/ENUE
   BETAX = BZ*EC/ENUE/EM
   BETA1 = BZ*EC/ENUIN/CM
   SXM = 1.+BETAX*BETA1
   A1 = 1.24E7*ET**1.5/ENX**0.5
   A2 = 1.8E5*ET/ENX**(1./3.)
   GAM = ENX*(BK*TE/PRES)*GNX
   BKSKA = 3.E-6*ET**2.5/(TE*GNX)**0.75/ALOG(55.+A1**4+A2**4)
   BKEKA = BKSKA/(1.+BETAX**2)/(1.+1.414*(1.-GAM)/GAM*BKSKA*
1(QEAQAA)*SQRT(EM/CM*GNX*TE/ET))
   YAMNX = ELNX/PRNNX*BKEKA
   ALF1NX = 1./SXM
   ALF2NX = CONX*BETA1/SXM
   IF (NPL1-1) 5,5,9999
5 GRP = YAMNX*CP*ROMR*UE*(EC/BK)/TSQSI/DETA
   AJEYW = ALF1NX*AJYE+ALF2NX*EXE
   SCRB = (AJYE+TIW)/EC/ENX*SQRT(2.*PI*EM/(BK*ETE*THENX))+SQRT((2.*PI
1*EM)/SM)
   B2 = 2.*GRP/((2.-ALOG(SCRB))*(AJYE+EC*ENX*SQRT(BK*ETE*THENX/SM
1)))+1.5*GRP-2.5*AJEYW+2.*TIW)

```



```

      B3 = -.25*B2
      DO 10 J = 1,3
      DO 11 I = 1,3
      H(I,J) = 0.
11 EF(I,J) = 0.
10 CONTINUE
      H(3,3) = B2
      EF(3,3) = B3
      SMLHH(3)=B2*WLST(2,3)+B3*WLST(3,3)-WLST(1,3)+4.*TE*GNX*TIW/ETE
      1/(2.*GRP/B2)
9999 WRITE(6,100) YAM, BETAX, ENX, BETAI, CONX, SCRB, BKEKA
100 FORMAT (7E17.4)
      RETURN
      END

```

CTABLE

```

SUBROUTINE TABLE(TEMP,QEA,QECS,ARG5,KTAB,N,XQEA,XQECS)
  DIMENSION TEMP(50),QEA(50),QECS(50)
  XTEMP = ARG5
  9 IF (N) 10,101,10
  10 IF (XTEMP-XTEMPL) 101,11,11
101 J = 1
  NTAB = KTAB
  11 NTAB1 = NTAB+1
  K = J-1
  CALL TLU1(XTEMP,NTAB,TEMP(J),J,IERR)
  IF (IERR) 13,14,13
  13 WRITE (6,901)XTEMP
  GO TO 9999
  14 NTAB = NTAB1-J
  J = J+K
  IF (NTAB) 9999,9999,15
  15 XQEA = TNT1(XTEMP,NTAB,TEMP(J),QEA(J),2,IERR)
  XQECS = TNT1(XTEMP,NTAB,TEMP(J),QECS(J),2,IERR)
  16 XTEMPL = XTEMP
  901 FORMAT (34H THIS TEMPERATURE IS NOT IN TABLE-,E16.8)
9999 RETURN
  END

```

CABCD

SUBROUTINE ABCD

COMMON/COM1/BK,EM,EC,C1,PI,AKO,R,Y(1000),TE,ETE,PRES,AJYE,UE,DUE,D

ITE,DETE,RHOE,DRHOE,EXE,TW,EKSIS,EKSIM,DKSI,TDA,TDDA,DETA2,DETA,TSQ

ISI,DELTA,MEDGE,EKSI

COMMON/COM3/SMLHH(3),V(1000),WLST(1000,3),W(1000,3),TEEKSI(10)

COMMON/COM4/E(3000,3),PHI(1000,3),H(3,3),EF(3,3),TEMP(3,3),AA(3,3)

1,B(3,3),C(3,3),D(3),A(3,3),CKMAT(3,3),TEMPP(3)

COMMON/COM5/N,NPL1,DUM(15),NTAB,NVMN

COMMON/COM6/ELLS,EL,ELNX,YAMLS,YAM,YAMNX,PRNLS,PRN,PRNNX,ALF1LS,AL

1F1,ALF1NX,ALF2LS,ALF2,ALF2NX,S,GNX,THENX,ENX,CONX,SXM,BETAX,QEI,QE

2A,QECS,C2,PER,QIN,CP,ROMR,CM,TIW,TIWC,PIZ,SM,BZ

FP = .5*(W(N,1)+WLST(N,1))

G = GNX

THETA = THENX

BETAE = BETAX

COND = CONX

ENE = ENX

SUM = SXM

DO 10 I=1,3

10 D(I) = 0.

DO 11 I=1,3

DO 11 J=1,3

AA(I,J)=0.

B(I,J)=0.

11 C(I,J)=0.

SNUS = (PRES/BK*QEA)/TE/G/CM+(QECS/SM)*(PER*PRES/TE/BK/G-ENE)+(EN
1E*QE1)/CM

SNUS = SNUS*DELTA*SQRT(8.*BK*ETE*THETA/PI/EM)

GRP = PRES*PER/BK/TE/G

S1 = S*(1.5/ETE/THETA+C2/(ETE*THETA)**2)*(-.5+(S/2.+GRP)/S/SQRT(1.
1+4.*GRP/S))

H11

$S2 = .8 * (CM / BK) * GRP / TE / G / \sqrt{1. + 4. * GRP / S}$
 $S3 = 2. * GRP / PRES / \sqrt{1. + 4. * GRP / S}$
 $FPA = (WLST(N+1,1) - WLST(N-1,1)) / TDA$
 $FPAA = (WLST(N+1,1) - 2. * WLST(N,1) + WLST(N-1,1)) / DELTA2$
 $GA = (WLST(N+1,2) - WLST(N-1,2)) / TDA$
 $GAA = (WLST(N+1,2) - 2. * WLST(N,2) + WLST(N-1,2)) / DELTA2$
 $THA = (WLST(N+1,3) - WLST(N-1,3)) / TDA$
 $THAA = (WLST(N+1,3) - 2. * WLST(N,3) + WLST(N-1,3)) / DELTA2$
 $RHOS = R / PRES / 40. * TE * (WLST(N,2) + WLST(N-1,2))$
 $Y(N) = Y(N-1) + TSQSI * RHOS * .5 * DELTA / UE$
 CALL NXTLST
 $ELA = (ELNX - ELLS) / TDA$
 $YAMA = (YAMNX - YAMLS) / TDA$
 $PRA = (PRNNX - PRNLS) / TDA$
 $ALF1A = (ALF1NX - ALF1LS) / TDA$
 $ALF2A = (ALF2NX - ALF2LS) / TDA$
 $V1 = V(N)$
 $Q1 = DKSI / (4. * Eksi * FP * TDA)$
 $Q2 = 2.5 * BK * ETE / EC * TSQSI / (ROMR * UE * CP * TE)$
 $Q3 = DKSI * DTE$
 $Q4 = PIZ / (RHOE * CP * TE)$
 $Q5 = 1.5 * BK * ETE * THETA + PIZ$
 $Q6 = 2.5 * BK * ETE * THETA + PIZ$
 $Q7 = 5. * BK / EC * RHOE * ETE * UE / TSQSI / G$
 $Q9 = ROMR * UE ** 2$
 $Q0 = RHOE * CP * ETE * Q9$
 $Q8 = RHOE * CP * TE * Q9$
 $Q10 = 1.5 * BK * ENE$
 $F1 = FP$
 $Q = G$
 $FP = WLST(N,1)$
 $G = WLST(N,2)$

```

THETA = WLST(N,3)

AA(1,1) = Q1*(V1-2.*EL/DETA-ELA)

AA(1,2) = 0.

AA(1,3) = 0.

B(1,1) = 1.+DKSI*DUE/2./UE+4.*Q1*EL/DETA

B(1,2) = -DKSI*DUE/(2.*UE*F1)

B(1,3) = 0.

C(1,1) = Q1*(-V1-2.*EL/DETA+ELA)

C(1,2) = 0.

C(1,3) = 0.

D(1) = FP*(1.-DKSI*DUE/2./UE)+(DKSI/4./EKS1/F1)*(-FPA*V1+2.*EKS1*G
1*DUE/UE+ELA*FPA+EL*FPAA)

AA(2,1) = -2.*Q1*UE**2/CP/TE*EL*FPA

AA(2,2) = Q1*(V1-2.*EL/PRN/DETA-ELA/PRN+Q4*ENE*V1-PIZ*S2*V1*G/RHOE
1)

AA(2,3) = Q1*(-2.*ETE*YAM/DETA/TE-ETE*YAMA/TE-Q2*(ALF1*AJYE+ALF2*E
1XE)+Q4*ETE*V1*S1*G)

B(2,1) = 0

B(2,2) = 1.+DKSI*UE*DUE/(2.*CP*TE)*(1.-PIZ*S3)+4.*Q1*EL/PRN/DETA+Q
13/2./TE+(Q4*S1)*THETA*Q3/2.-PIZ*S2*G/RHOE-PIZ*CP*Q3*S2*G/RHOE/UE

B(2,2) = B(2,2)+DKSI/2.*UE*DUE*(ENE*Q4)+(PIZ*ENE)/CP/RHOE/TE+(Q4*
1ENE)/2./TE*Q3-DKSI*COND*EXE**2/Q8/2./F1/SUM-DKSI*AJYE**2*(SUM**2+
2BETAE**2)/(2.*COND*F1*Q8*SUM)+DKSI*AJYE*BZ*(1.-PIZ*S3)/2.*UE/Q8-
3DKSI*(PIZ*ENE)*BZ/2./PRES*UE/Q8*AJYE

B(2,3) = 4.*Q1*ETE*YAM/DETA/TE-Q2*DKSI/8./F1/EKS1*(AJYE*ALF1A+EXE*
1ALF2A)+Q4*ETE*S1*G+Q4*S1*G*Q3/2.

C(2,1) = -AA(2,1)

C(2,2) = Q1*(-V1-2.*EL/DETA/PRN+ELA/PRN-Q4*ENE*V1+PIZ*S2*V1*G/RHOE
1)

C(2,3) = Q1*(ETE/TE*(-2.*YAM/DETA+YAMA)+Q2*(AJYE*ALF1+EXE*ALF2)-Q4
1*S1*ETE*V1*G)

```

$$D(2) = G - Q3 * G / 2. / TE - (1. - PIZ * S3) * UE * DKS I * G / (2. * CP * TE) * DUE + 2. * DETA * Q$$

$$11 * (EL / PRN * GAA + GA * (ELA / PRN - V1) + ETE / TE * (YAM * THAA + THA * YAMA) + Q2 * (THA * ($$

$$2AJYE * ALF1 + EXE * ALF2) + THETA * (AJYE * ALF1A + EXE * ALF2A)) - Q4 * ETE * S1 * G * THA *$$

$$3V1 - Q4 * ENE * GA * V1 + PIZ * S2 * V1 * G * GA / RHOE + 2. * G * EKS I / SUM * (COND * EXE ** 2 + AJY$$

$$4E ** 2 / COND * (SUM ** 2 + BETAE ** 2)) / Q8) + Q4 * S1 * ETE * G * THETA - PIZ * S2 * G ** 2 / RHO$$

$$5E - DKS I * UE * RHOE * (Q4 * ENE) * G / 2. / PRES * DUE + Q4 * ENE * G + DKS I * AJYE * BZ / 2. * UE$$

$$6 / Q8 * (G * (1. - PIZ * S3) + G * PIZ * ENE / PRES) - Q4 * ENE * Q3 * G / 2. / TE$$

AA(3,1) = 0.

AA(3,2) = (ENE/Q*Q6-S2*Q5*CP*TE)*Q9*V1/8./EKS I/DETA

$$AA(3,3) = Q9 * ETE / 4. / EKS I / DETA * (V1 / 2. * (Q10 + S1 * Q5) - CP * RHOE / Q * (YAM / DE$$

$$1TA + YAMA / 2.)) - Q7 / 8. / DETA * (ALF1 * AJYE + ALF2 * EXE)$$

$$B(3,1) = THETA * (Q9 * DETA / 2. * (Q10 + S1 * Q5) - .75 * ETE * BK * S3 * UE * (-AJYE * BZ +$$

$$1Q9 * RHOE * DUE)) - (ENE * Q6) * Q9 * DRHOE / 2. / RHOE - S2 * Q5 * Q9 / 2. * CP * DTE * G - PIZ$$

$$2 * S3 / 2. * (Q9 * UE * RHOE * DUE - UE * AJYE * BZ)$$

$$B(3,2) = Q9 * FP * ((ENE * Q6) / Q / DKS I - (Q5 * S2) * CP * (TE / DKS I + DTE / 2.)) - Q10 *$$

$$1TE * (EM * SNUS)$$

$$B(3,3) = (Q10 + S1 * Q5) * Q9 * (TE * F1 / DKS I + .5 * DETA * FP) - .75 * BK * ETE * S3 * FP * Q$$

$$19 * RHOE * UE * DUE + Q0 * YAM / 2. / (EKS I * DETA * .2 * Q) - .25 * Q7 * (ALF1A * AJYE + ALF2A *$$

$$2EXE) + Q10 * ETE * (EM * SNUS) + .75 * ETE * UE * S3 * AJYE * BZ * FP * BK$$

C(3,1) = 0.

C(3,2) = -(ENE/Q*Q6-S2*Q5*CP*TE)*Q9*V1/8./EKS I/DETA

$$C(3,3) = -(Q10 + Q5 * S1) * Q9 * ETE * V1 / 8. / EKS I / DETA - Q0 * (YAM / DETA - YAMA / 2.)$$

$$1 / 4. / EKS I / DETA / Q + Q7 / DETA * (ALF1 * AJYE + ALF2 * EXE) / 8.$$

$$D(3) = Q9 * ETE * (Q10 + Q5 * S1) * (+F1 / DKS I * THETA - V1 * THA / 4. / EKS I) + Q9 * (ENE /$$

$$1G * Q6 - S2 * Q5 * CP * TE) * (FP * G / DKS I - V1 * GA / 4. / EKS I) + ENE * Q6 * Q9 * .5 / RHOE * DRHO$$

$$2E * FP$$

$$D(3) = D(3) + PIZ * S3 / 2. * FP * (Q9 * RHOE * UE * DUE - UE * AJYE * BZ) + Q0 * (YAM * THAA +$$

$$1YAMA * THA) / 4. / EKS I / Q + .25 * Q7 * (THA * (ALF1 * AJYE + ALF2 * EXE) + THETA * (ALF1A *$$

$$2AJYE + ALF2A * EXE)) + COND * EXE ** 2 / SUM ** 2 + AJYE ** 2 / COND * (SUM ** 2 + BETAE ** 2)$$

$$3 / SUM ** 2 + Q10 * TE * G * (EM * SNUS) - Q10 * ETE * THETA * (EM * SNUS)$$

CEKPK

SUBROUTINE EKPK

COMMON/COM3/SMLHH(3),DUM1(7010)

COMMON/COM4/E(3000,3),PHI(1000,3),H(3,3),EF(3,3),TEMP(3,3),AA(3,3)

1,B(3,3),C(3,3),D(3),A(3,3),CKMAT(3,3),TEMPP(3)

COMMON/COM5/N,NPL1,DUM(17)

DIMENSION SCRACH(3,3)

IF (N-2) 10,10,140

10 DO 40 I = 1,3

DO 30 J = 1,3

A(I,J) = B(I,J)

TEMP(I,J) = AA(I,J)

DO 20 K = 1,3

A(I,J) = C(I,K)*H(K,J)+A(I,J)

20 TEMP(I,J) = C(I,K)*EF(K,J)+TEMP(I,J)

30 CKMAT(I,J) = A(I,J)

40 CONTINUE

50 CALL MXINV

DO 80 I = 1,3

DO 70 J = 1,3

AA(I,J) = 0.

DO 60 K = 1,3

60 AA(I,J) = A(I,K)*TEMP(K,J)+AA(I,J)

70 CONTINUE

80 CONTINUE

DO 110 I = 1,3

E(6,I) = -AA(3,I)

E(4,I) = -AA(1,I)

TEMPP(I) = 0.

DO 100 J = 1,3

100 TEMPP(I) = C(I,J)*SMLHH(J)+TEMPP(I)

110 D(I) = D(I)-TEMPP(I)

H15

```

DO 130 I = 1,3

PHI(2,I) = 0.

DO 120 J = 1,3
120 PHI(2,I) = A(I,J)*D(J)+PHI(2,I)
130 CONTINUE

GO TO 9999

140 MN = (N-1)*3-2

DO 160 J = 1,3

TEMP(3,J) = E(MN+2,J)

A(3,J) = B(3,J)

TEMP(2,J) = E(MN+1,J)

A(2,J) = B(2,J)

TEMP(1,J) = E(MN,J)

160 A(1,J) = B(1,J)

DO 190 I = 1,3

DO 180 J = 1,3

DO 170 K = 1,3

170 A(I,J) = C(I,K)*TEMP(K,J)+A(I,J)

180 CONTINUE

190 CONTINUE

200 CALL MXINV

DO 230 I = 1,3

DO 220 J = 1,3

TEMP(I,J) = 0.

DO 210 K = 1,3

210 TEMP(I,J) = A(I,K)*AA(K,J)+TEMP(I,J)

220 CONTINUE

230 CONTINUE

M = 3*N-2

DO 250 I = 1,3

E(M+2,I) = -TEMP(3,I)

E(M+1,I) = -TEMP(2,I)

250 E(M,I) = -TEMP(1,I)

```



```

      DO 270 I = 1,3
      TEMPP(I) = 0.
      PHI(N,I) = 0.
      DO 260 J = 1,3
260  TEMPP(I) = C(I,J)*PHI(N-1,J)+TEMPP(I)
270  D(I) = D(I)-TEMPP(I)
      DO 290 I = 1,3
      DO 280 J = 1,3
280  PHI(N,I) = A(I,J)*D(J)+PHI(N,I)
290  CONTINUE
      P1=PHI(N,1)
      P2=PHI(N,2)
      P3=PHI(N,3)
9999 RETURN
      END

```

CTEST

SUBROUTINE TEST

COMMON/COM3/SMLHH(3),DUM1(7010)

COMMON/COM4/E(3000,3),PHI(1000,3),DUM2(78)

COMMON/COM5/N,DUM3(5),CONST,DUM4(2),EP1,EP2,EP3,DUM5(7)

M = 3*N-2

TERM1 = ABS(1.-E(M,1)-E(M,2)-E(M,3)-PHI(N,1))

TERM2 = ABS(1.-E(M+1,1)-E(M+1,2)-E(M+1,3)-PHI(N,2))

TERM3 = ABS(1.-E(M+2,1)-E(M+2,2)-E(M+2,3)-PHI(N,3))

IF (TERM1-EP1) 1,100,10

1 IF (TERM2-EP2) 2,100,10

2 IF (TERM3-EP3) 3,100,10

100 CONST = -1.

GO TO 9999

3 CONST = 0.

9999 RETURN

END

SUBROUTINE WNSUB

DIMENSION AAA(3),BBB(3)

COMMON/COM3/SMLHH(3),V(1000),WLST(1000,3),W(1000,3),TEEKSI(10)

COMMON/COM4/E(3000,3),PHI(1000,3),H(3,3),EF(3,3),TEMP(3,3),XH(51)

COMMON/COM5/N,NPL1,PCC,DUM2(10),EPP1,EPP2,EPP3,DUM3(3)

NPL1=N

DO 10 I = 1,3

10 W(N,I) = 1.

PCC = -1.

35 N = N-1

TERM1 = W(N,1)

TERM2 = W(N,2)

TERM3 = W(N,3)

MN = 3*N-2

DO 50 I = 1,3

TEMP(3,I) = E(MN+2,I)

TEMP(2,I) = E(MN+1,I)

50 TEMP(1,I) = E(MN,I)

DO 70 I = 1,3

W(N,I) = 0.

DO 60 J = 1,3

60 W(N,I) = TEMP(I,J)*W(N+1,J)+W(N,I)

70 W(N,I) = W(N,I)+PHI(N,I)

IF (N-2) 75,75,20

20 IF (PCC) 30,30,3

30 IF (ABS(TERM1-W(N,1))-EPP1) 1,1,100

1 IF (ABS(TERM2-W(N,2))-EPP2) 2,2,100

2 IF (ABS(TERM3-W(N,3))-EPP3) 3,3,100

100 PCC = +1.

3 IF (N-2) 9999,9999,35

75 DO 90 I = 1,3

AAA(I) = 0.

BBB(I) = 0.

DO 80 J = 1,3

AAA(I) = H(I,J)*W(2,J)+AAA(I)

80 BBB(I) = EF(I,J)*W(3,J)+BBB(I)

90 W(1,I) = BBB(I)+AAA(I)+SMLHH(I)

GO TO 20

9999 RETURN

END

CVMNSUB

```
      SUBROUTINE VMNSUB(*)  
      COMMON/COM1/DUM1(1019),EKSIS,EKSIM,DKSI,TDA,TDDA,DETA2,DETA,DUM2(3  
1),E<SI  
      COMMON/COM3/SMLHH(3),V(1000),WLST(1000,3),W(1000,3),TEEKSI(10)  
      COMMON/COM5/DUM3(18),NVMN  
      TERM1 = EKSI*DETA/DKSI  
      TERM2 = DETA/4.  
      DO 10 I = 2,1000  
10  V(I) = V(I-1)-(TERM1+TERM2)*(W(I,1)+W(I-1,1))+(TERM1-TERM2)*(WLST(  
      11,1)+WLST(I-1,1))  
      GO TO (29,99),NVMN  
29  DO 11 I = 1,1000  
      DO 12 J = 1,3  
12  WLST(I,J) = W(I,J)  
11  CONTINUE  
      CALL WOSUB  
      GO TO 9999  
99  RETURN 1  
9999 RETURN  
      END
```

```
SUBROUTINE WOSUB  
COMMON/COM1/DUM(7),Y(1000),DUM1(12),EKSIS,EKSIM,DKSI,DUM2(6),MEDGE  
1,EKSI  
COMMON/COM3/SMLHH(3),V(1000),WLST(1000,3),W(1000,3),TEEKSI(10)  
COMMON/COM5/N,NPL1,PCC,NWRIT,DUM3(15)  
IF (1-MEDGE) 1,2,1  
2 EKSI = EKSI-.5*DKSI  
DO 10 I = 2,NWRIT  
10 Y(I) = Y(I-1)+1.  
GO TO 3  
1 EKSI = EKSI+.5*DKSI  
3 WRITE (6,902)(EKSI)  
902 FORMAT (1H1/5HEKSI=E16.8/  
WRITE (6,903)  
903 FORMAT (1H011X2HFP19X1HG16X5HTHETA18X1HV19X1HY/  
WRITE (6,904)((W(I,J),J = 1,3),V(I),Y(I),I = 1,NWRIT)  
904 FORMAT (1H 5E20.8)  
9999 RETURN  
END
```

CMXINV

SUBROUTINE MXINV

COMMON/COM4/DUM1(12057),A(3,3),DUM2(12)

DIMENSION S(3,3)

S(1,1)= (A(2,2)*A(3,3)-A(2,3)*A(3,2))

S(2,1)=- (A(2,1)*A(3,3)-A(2,3)*A(3,1))

S(3,1)= (A(2,1)*A(3,2)-A(2,2)*A(3,1))

S(1,2)=- (A(1,2)*A(3,3)-A(1,3)*A(3,2))

S(2,2)= (A(1,1)*A(3,3)-A(1,3)*A(3,1))

S(3,2)=- (A(1,1)*A(2,3)-A(1,2)*A(3,1))

S(1,3)= (A(1,2)*A(2,3)-A(1,3)*A(2,2))

S(2,3)=- (A(1,1)*A(2,3)-A(1,3)*A(2,1))

S(3,3)= (A(1,1)*A(2,2)-A(1,2)*A(2,1))

DETER=A(1,1)*S(1,1)+A(1,2)*S(2,1)+A(1,3)*S(3,1)

DO 11 I=1,3

DO 10 J=1,3

10 A(I,J)=S(I,J)/DETER

11 CONTINUE

9999 RETURN

END